TECHNICAL AND ECONOMIC EVALUATION OF THE UTILISATION OF SOLAR ENERGY AT SOUTH AFRICA'S SANAE IV BASE IN ANTARCTICA

Jürgen Richter Olivier

Thesis presented in partial fulfilment of the requirements for the degree of

MScEng in Mechanical Engineering

Stellenbosch University

Thesis supervisor:

Professor T.M. Harms

Department of Mechanical Engineering

DECEMBER 2005

Pectora roborant cultus recti

Declaration

I, the undersigned, hereby declare that the work contained in this thesis is my own original work and that I have not previously, in its entirety or in part, submitted it at any university for a degree.

Signature: _____ Date: _____

Jürgen R. Olivier

Abstract

There are numerous challenges that have to be overcome in order to generate the electrical and thermal energy required to power Antarctic research stations in a technically, economically and environmentally suitable manner. Consequently the costs associated with generating energy at these latitudes are high, and ways are constantly being sought to improve energy generation methods and protect the pristine environment. These endeavours are strongly encouraged by the Antarctic Treaty.

This thesis aims to investigate the technical and economic feasibility of using solar energy at South Africa's SANAE IV (South African National Antarctic Expedition IV) station in Antarctica. The idea of using solar energy in Antarctica is not novel, and as is shown a number of stations have already capitalised on opportunities to generate savings in this manner. Similarly, at SANAE IV, there exists the opportunity to alleviate an increased summer energy load on the station and reduce diesel consumption through the proper implementation of such a system. There is also ample scope to use wind energy, which would have a marked positive impact on the base's operation.

The data used in this thesis was obtained mainly during the 2004/2005 takeover expedition to South Africa's SANAE IV station in Antarctica. Included are measurements of total and diffuse radiation that were measured during the months of January and February 2005, and which form an important part of the investigation. Since there are currently no radiation sensors, or any historical record of measured radiation at the station, the only measured data available from SANAE IV was the data recorded during the 2004/2005 takeover expedition. By further collecting archived values of fuel consumption, electricity generation and load profiles, an energy audit of the station was also completed during the 2004/2005 takeover expedition.

The expected savings that could be generated by solar systems were calculated by considering the use of both photovoltaic and solar thermal devices at the South African station. The 40 kW photovoltaic system that was investigated was able to significantly reduce the load on the diesel-electric generators, however it was only possible to fully recover the initial costs sunk into commissioning the system after 21 years. The installation of such a system would equate to a Net Present Value of 302 915 Rand at the end of the 25 year system lifetime (assuming a real hurdle rate of 8 % and fuel price escalation rate of 5 %), saving 9 958 litres of diesel annually and

generating energy at a cost of 3.20 Rand/kWh. It should be noted, however, that under more ideal conditions (i.e. less attractive alternative investment opportunities, higher fuel price escalation rates and a stronger emphasis on environmental concerns) investment into a photovoltaic system could potentially breakeven after approximately 10-15 years, while simultaneously significantly improving base operation.

Furthermore, it was found that a flat-plate solar thermal collector utilised with the snow smelter at SANAE IV is better suited to generating savings than photovoltaic devices. The average cost of generating electricity after commissioning such a system with a 143 m^2 collector field would be approximately 3.13 Rand/kWh, as opposed to the 3.21 Rand/kWh of the current diesel-only system, and would realise an annual fuel saving of approximately 12 245 litres. The system would arrive at a breakeven point after approximately 6 years, and represent a Net Present Value of 2 148 811 Rand after 25 years. By further considering environmental factors such as the cost of removing soiled snow from Antarctica and diesel fuel emissions the magnitude of the net present savings would increase by approximately 500 000 Rand over the expected 25 year project lifetime.

The opportunity to install a solar energy system at SANAE IV therefore warrants action. There is potential not only to generate savings over the operational lifetime but also to preserve the environment in accordance with the desires of the Antarctic Treaty. It is firmly believed that with careful planning and implementation such a project can and should be successfully undertaken.

Opsomming

‘n Aantal unieke uitdagings moet oorkom word om die elektriese en termiese energie wat by navorsingstasies in Antarktika benodig word in ‘n toepaslike tegniese, ekonomiese en omgewingsbewuste manier op te wek. Die kostes verbonde aan die gebruik van energie by hierdie breedtegrade is om hierdie rede hoog. Daar is dus ook geen einde nie aan die soektog vir beter maniere van energieopewekking en omgewingsbeskerming, pogings wat deur die Antarktiese Traktaat ondersteun word.

In hierdie tesis word daarna gemik om die tegniese en ekonomiese lewensvatbaarheid van die gebruik van sonenergie by Suid Afrika se SANAE IV (Suid Afrikaanse Nasionale Antarktiese Ekspedisie IV) basis in Antarktika te ondersoek. Die aanwending van sonenergie in Antarktika is geensins ‘n nuwe idee nie, en soos hier gewys word het ‘n aantal navorsings stasies alreeds van sulke bespaaringsgeleenthede gebruik gemaak. In dieselfde manier bestaan daar die geleentheid by SANAE IV om die verhoogde somerenergielas op die basis se energiestelsels, en diesel verbruik te verminder. Die aanwending van windenergie kan ook ‘n merkbare positiewe verskil maak.

Hierdie tesis gebruik ook hoofsaaklik inligting wat versamel was gedurende die 2004/2005 ekspedisie na Suid Afrika se SANAE IV stasie in Antarktika. Ingesluit is lesings van totale en diffuse sonstralingsenergie gemeet gedurende die maande van Januarie en Februarie 2005, wat ‘n belangrike rol speel in die opeenvolgende ondersoek. Tans is daar geen sensors wat sonstralingsenergie by SANAE IV meet nie, en ook geen historiese sonstralingsenergiedata nie, en dus is die data wat gedurende die 2004/2005 ekspedisie versamel was die enigste huidige lesings van SANAE IV. Deur inligting te versamel gedurende die ekspedisie oor brandstofverbruik, elektrisiteitsopwekking en lasprofiele is ‘n energie oudit van die stasie ook voltooi.

Moontlike besparings wat deur die gebruik van sonenergiestelsels by Suid Afrika se basis gerealiseer kan word was bepaal deur die gebruik van beide fotovoltaaise en termiese stelsels te oorweeg. Verbeterde werkverrigting van dieselopwekkers is verkry met die gebruik van ‘n 40 kW fotovoltaaise sisteem, alhoewel projekkostes slegs na21 jaar herwin kan word. Die gebruik van so ‘n stelsel sal ‘n huidige waarde van 302 915 Rand verteeneewordig na die projekleeftyd van 25 jaar (gestel dat die *regte* hekkiekoers 8 % en brandstofstygingskoers 5 % is), jaarliks

omtrent 9 958 liter diesel bespaar en energie opwek teen ‘n koste van 3.20 Rand/kWh. Onder meer voordelige omstandgihede (m.a.w ‘n hoë tempo van brandstof kosteverhogings, min aantreklike alternatiewe bellegings en ‘n hoë klem op omgewingsake) sal ‘n fotovoltaaise sisteem heel waarskynlik na 10-15 jaar kan gelykbreek, terwyl dit terselfdetyd ‘n merkbare positiewe verskil sou maak aan die werksverrigting van die basis.

Daar is vasgestel dat ‘n platplaat termiese sonkollektor by SANAE IV vir gebruik met die stasie se sneeusmelter die hoogste bespaaringspotensiaal het. Die gemiddelde energiekostes na die instalering van ‘n platplaat termiese sonkollektorsisteem met 143 m^2 versamelveld sal ongeveer 3.13 Rand/kWh wees, in teenstelling met die 3.21 Rand /kWh van die huidige dieselstelsel. Daar sal ook jaarliks omtrent 12 245 liter diesel bespaar word. Die projekkostes hoort na 6 jaar gelyk te breek, en sal na 25 jaar ‘n Netto Huidige Waarde van 2 148 811 Rand verteenwoordig. Deur verder te kyk na kostes verbonde aan die verwydering van dieselbesmette sneeu en eselopwekker uitlaatgasse word die Netto Huidige Waarde met ongeveer 500 000 Rand vermeerder.

Die geleentheid om ‘n sonenergiestelsel by die SANAE IV basis in gebruik te neem vereis daarom dringende aandag. In ooreenstemming met die inhoud van die Antarktiese Traktaat bestaan daar besliste besparingspotensiaal, tesame met die geleentheid tot omgewingsbeskeming. Met omsigte beplanning en uitvoering sou so ‘n projek onderneem kon word en dit word gestel dat daarom ook behoort onderneem te word.

"From whose womb comes the ice?
Who gives birth to the frost from the heavens,
When the waters become hard as stone,
When the surface of the deep is frozen?
Can you bind the beautiful Pleiades?
Can you loose the cords of Orion?
Can you bring forth the constellations in their seasons
Or lead out the Bear with its cubs?"

- Job 38:29-32

Lorentzenpiggen, a mountain peak located directly south of SANAE IV (Olivier, 2005)

Acknowledgements

I would like to thank the following people and institutions for providing valuable assistance during the course of this study:

- Professor Thomas M. Harms, as thesis supervisor, for his encouragement, guidance and insight that has added greatly to this project.

- Mr. Franz Hoffman, co-ordinator of the 2004/2005 SANAE IV takeover expedition, for his administrative assistance that made it possible for me to join the 2004/2005 takeover expedition to SANAE IV and obtain much of the data required for this study.

- Mr. Daniël J. Esterhuyse, from the South African Weather Services, for his advice regarding the measurement of solar radiation, and his assistance in obtaining the pyranometers that were used to measure solar radiation at SANAE IV during the 2004/2005 takeover expedition.

- Mr. Cobus J. Zietsman, from the University of Stellenbosch, for his assistance in obtaining many of the accessories required for measuring solar radiation at SANAE IV, and for his endless patience and keen insights offered during the preparations for the SANAE IV 2004/2005 takeover expedition.

- The South African Department of Environmental Affairs and Tourism, Subdirectorate Antarctica and Islands, for funding and logistical support, as well as the South African Department of Science and Technology who through the South African National Research Foundation also contributed in funding.

- To those, including friends and colleagues, but especially my parents, who gave of their time to listen, discuss, or just reflect over some of the difficulties that this project presented.

Table of Contents

List of Figures

List of Tables

Nomenclature

Engineering Symbols:

A	= Area	[m^2]
A_o	= Area on the outside of heat exchanger	[m^2]
Al	= Altitude	[km]
C_p	= Thermal heat capacity	[kJ/kg. K]
E	= Available energy	[J]
FC	= Fuel Consumption	[Litres]
G	= Global radiation incident on a horizontal surface	[W/m^2]
G_{cnb}	= Clear-Sky normal beam radiation	[W/m^2]
G_d	= Diffuse radiation on a horizontal surface	[W/m^2]
G_o	= Top of atmosphere radiation on a horizontal surface	[W/m^2]
G_{on}	= Top of atmosphere radiation on a surface normal to the incoming rays	[W/m^2]
$\overline{H}$	= Monthly-average daily insolation on a horizontal surface	[kWh/m^2]
$\overline{H}_O$	= Monthly-average daily top of atmosphere insolation on a horizontal surface	[kWh/m^2]
$\overline{K}_T$	= Monthly-average clearness index	[ ]
K_T	= Daily-average clearness index	[ ]
k_T	= Hourly-average clearness index	[ ]
$\dot{m}$	= Mass flow-rate	[kg/s]
$NOCT$	= Nominal Operating Cell Temperature	[°C]
P	= Power	[W]
PP	= Power Production	[kWh]
Q	= Heat transfer	[J]
$\dot{Q}$	= Rate of heat transfer	[J/s]
R_T	= Thermal resistance	[$K/(W/m^2)$]
T	= Temperature	[K]
U_o	= Overall outside heat transfer coefficient	[W/m^2K]

Greek Engineering Symbols:

ΔT	= Temperature difference	[K]
ρ	= Reflectivity	[ ]
β	= Tilt of collecting surface away from horizontal (i.e. for a wall $\beta = 90°$)	[°]
β_p	= Temperature coefficient of module efficiency	[%/°C]
r	= Climate coefficient	[ ]
τ	= Radiation transmissivity	[ ]
θ_Z	= Angle between incoming rays and zenith (i.e. at sunset $\theta_Z = 90°$)	[°]
η	= Efficiency	[ ]
μ_T	= Percentage decrease in efficiency with increase in temperature	[%/°C]
λ	= Energy losses	[%]

Economic Symbols:

BC	= Benefit Cost ratio	[ ]
C	= Capital investment	[Rand]
F	= Fuel costs	[Rand]
i	= Interest rate	[%]
IRR	= Internal Rate of Return	[%]
L	= Labour costs	[Rand]
M	= Maintenance costs	[Rand]
MARR	= Minimum Attractive Rate of Return	[%]
R	= Rand (i.e. South African currency)	[Rand]
n	= Time	[Years]
NAW	= Net Annual Worth	[Rand]
NPV	= Net Present Value	[Rand]
LCC	= Life Cycle Costs	[Rand]
O & M	= Operation and Maintenance costs	[Rand]
PW	= Present Worth	[Rand]
PWF	= Present Worth Factor	[ ]
US$	= American dollars	[Dollars]
X	= Externalities	[Rand]

Abbreviations

AAD	Australian Antarctic Division
AC	Alternating Current
AHU	Air Handling Unit
ASHRAE	American Society of Heating, Refrigerating and Air-Conditioning Engineers
ATSCM	Antarctic Treaty Special Consultative Meeting
AUD	Australian Dollar
BC Ratio	Benefit to Cost Ratio
BSRN	Baseline Surface Radiation Network
CEP	Committee for Environmental Protection
CO	Carbon Monoxide
CO_2	Carbon Dioxide
COMNAP	Council of Managers of National Antarctic Programs
DC	Direct Current
DEAT	South African Department of Environmental Affairs and Tourism
FCU	Fan Coil Unit
FRA	France
GEF	Global Environment Facility
GER	Germany
H&V	Heating and Ventilation System
HIT	Heterojunction with Intrinsic Thin layer
Hz	Hertz (i.e. cycles per second)
IEA	International Energy Agency
IGY	International Geophysical Year
IND	India
IRR	Internal Rate of Return
JAP	Japan
L	Litre
LCC	Life Cycle Costs
LPG	Liquid Petroleum Gas
MPPT	Maximum Power Point Tracker
NASA	National Aeronautic and Space Agency
NAW	Net Annual Worth

NOR	Norway
No_x	Oxides of Nitrogen
NPV	Net Present Value
O&M	Operation and Maintenance
PLC	Programmable Logic Controller
PM	Particulate Matter
PV	Photovoltaic
PW	Present Worth
PWF	Present Worth Factor
R	South African Rand (i.e. South African currency)
ROW	Rest Of World
RUS	Russia
SAB	Special Antarctic Blend (i.e. special freeze resistant diesel)
SANAE IV	South African National Antarctic Expedition IV, or South Africa's fourth base in Antarctica. The Roman numeral is in reference to a base.
SANAE 4	South African National Antarctic Expedition 4, or the fourth South African team to have overwintered on Antarctica (in 2005 SANAE 44 overwintered at SANAE IV). The ordinary numeral is in reference to a team of people.
SANAP	South African National Antarctic Programme (which administrates activities on South African controlled Southern Ocean islands as well as at SANAE IV)
SAWS	South African Weather Services
SCAR	Scientific Committee on Antarctic Research
SO_2	Sulphur Dioxide
SRB	Surface Radiation Budget dataset collated by NASA
SSE	Surface meteorology and Solar Energy dataset collated by NASA
STC	Standard Testing Conditions
SWE	Sweden
TOA	Top Of Atmosphere
UNEP	United Nations Environment Programme
US$	American Dollars (i.e. American currency)
VLF	Very Low Frequency
VOC	Volatile Organic Compounds

Pectora roborant cultus recti

Chapter 1 – Introduction

1.1 Background

South Africa's current Antarctic station, named the South African National Antarctic Expedition IV (SANAE IV), is positioned at 70° 40' 25" South and 2° 49' 44" West, approximately 4 500 km from Cape Town in South Africa and 3 000 km from the geographical South Pole. The base is one of seven overwintering stations (viz. Maitri [IND], Molodezhnaya [RUS], Neumeyer [GER], Novolazarevskaya [RUS], Syowa [JAP], SANAE IV [SA] and Troll [NOR]) operational in Queen Maud Land during the winter and one of fifteen stations to run programmes in Queen Maud Land during the summer (SCAR, 2005). The German Neumeyer and Norwegian Troll stations are SANAE IV's closest neighbours (located approximately 300 km to the northwest and 360 km to the east respectively) and in conjunction with SANAE IV are three of forty-seven overwintering stations that currently operate in Antarctica and the surrounding islands (an area collectively referred to as the Antarctic) all year round.

Figure 1.1: SANAE IV located in Queen Maud Land (Perry-Castañeda, 2005)

All of these countries administrating stations in the Antarctic do so under the terms of the Antarctic Treaty. Established in Washington on 1 of December 1959, this treaty was one outcome of the 1st International Geophysical Year (IGY), the first scientific research effort to undertake concurrent scientific activities that spanned the globe. Forty-five countries have since ratified the Antarctic Treaty, although originally only twelve had signed the agreement in 1959. South Africa was one of the original twelve signatories. South Africa is currently also: one of

twenty-seven consultative parties to the Antarctic Treaty, a member of the Council of Managers of National Antarctic Programmes (COMNAP), a member of the Committee for Environmental Protection in Antarctica (CEP) and a national member of the Scientific Committee on Antarctic Research (SCAR). Furthermore, since the first South African overwintering team was dispatched to the SANAE I station in 1961, forty-four expeditions have overwintered on the continent, and carried out numerous scientific and logistical activities.

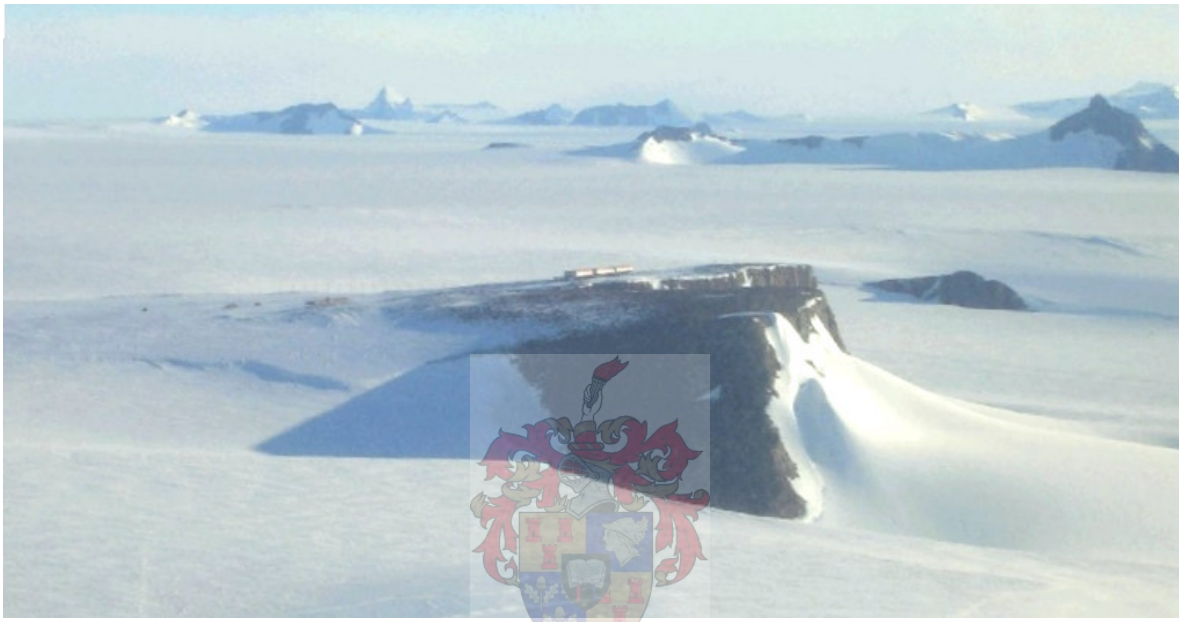

Figure 1.2: South Africa's SANAE IV base atop Vesleskarvet, a rocky outcrop (Olivier, 2005)

Currently expeditions to SANAE IV allow South Africa the opportunity to participate in a number of projects requiring not only proximity to the magnetic South Pole but also a high level of scientific expertise. In conjunction with Britain and Japan, for example, South Africa is a partner in the internationally collaborative SHARE project. SHARE contributes to the larger worldwide Super Dual Auroral Radar Network (SuperDARN) used to study electric fields, velocities and irregularities of the Earth's upper atmosphere by investigating data obtained from fifteen radar stations around the globe (nine in the Northern Hemisphere and six in the Southern Hemisphere). Ultimately this information is used to study changes in the Earth's biosphere that shields life from harmful cosmic rays.

South Africa also participates in the Solar Terrestrial Energy Programme (STEP), which investigates energy-transfer processes in the Earth's magnetosphere and ionosphere. By using magnetometers, auroral imaging devices, Very Low Frequency (VLF) direction finding systems

and a host of other instrumentation, the processes that are known to *"…disrupt radio communications, cause damage to satellites, disrupt or destroy large networks of electric power lines and on occasion threaten astronauts and Concorde passengers with harmful levels of proton fluxes"* (SANAP, 2005) can be studied.

Neutron count-rates are also recorded and forwarded to global data-centres, assisting research into ground-based solar events initiated by changes on the sun's surface. Total ozone column and UV-fluxes are monitored to supplement satellite measurements, making it possible to calculate the size of the Earth's ozone hole. The Southern Hemisphere telemetry for Sweden's Astrid-2 satellite is operated from the station, and can be used in a joint Swedish, Danish and South African collaboration by incorporating the Oersted satellite. This has allowed South Africa access to all data and software on the satellite in return for simultaneous ground-based aurora, magnetometer and VLF radio-wave measurements. Through SANAE IV South Africa also contributes to the IGS Programme (International GPS for Geodynamics Programme, involving 140 other partners), undertakes geological studies, serves as a weather station for the SAWS (South African Weather Services), is the centre for casualty evacuations in Queen Maud Land and is a partner with Germany in joint logistical operations.

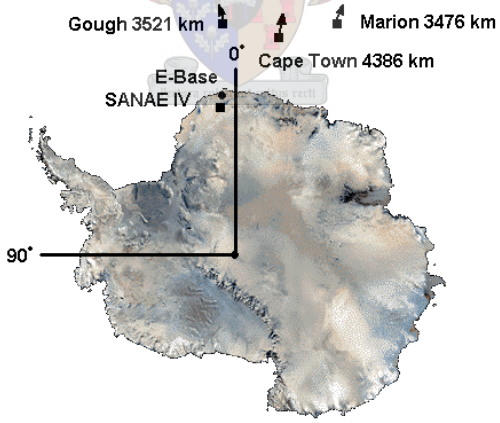

Figure 1.3: Map of SANAP operations in Antarctica (Theodora Maps, 2005)

Yet SANAE IV is not the only South African station in the Antarctic (refer to figure 1.3). South African Southern Ocean research stations also include: Marion Island (located 3 476 km from SANAE IV), Gough Island (3 521 km from SANAE IV) and E-Base (which exists purely in case of emergencies at SANAE IV and has no personnel that reside there). The necessary provisions are supplied to these stations by South Africa's well-known ice-reinforced relief vessel, the SA-

Agulhas, collectively administrated by SANAP (the South African National Antarctic Programme). SANAP in turn is a subdirectorate of South Africa's Department of Environmental Affairs and Tourism (DEAT).

Every 12 months the SANAP stations in Antarctica (i.e. SANAE IV and E-Base) are visited during what is referred to as the summer takeover period. Fresh food, diesel fuel, a temporary maintenance crew and a new overwintering team are transported to the station. SANAE IV comfortably houses the entire takeover crew, which may number up to 80 people, yet only the overwintering team, totalling approximately 10 people, will remain behind after the takeover is complete. The station is constructed from three main blocks (viz. the A-, B- and C-Blocks) and two smaller interconnecting passages or "links", with the laboratories, living-quarters and heavy machinery distributed in the A, B and C sections respectively. Notably, SANAE IV is a South African design and construction (completed in 1997).

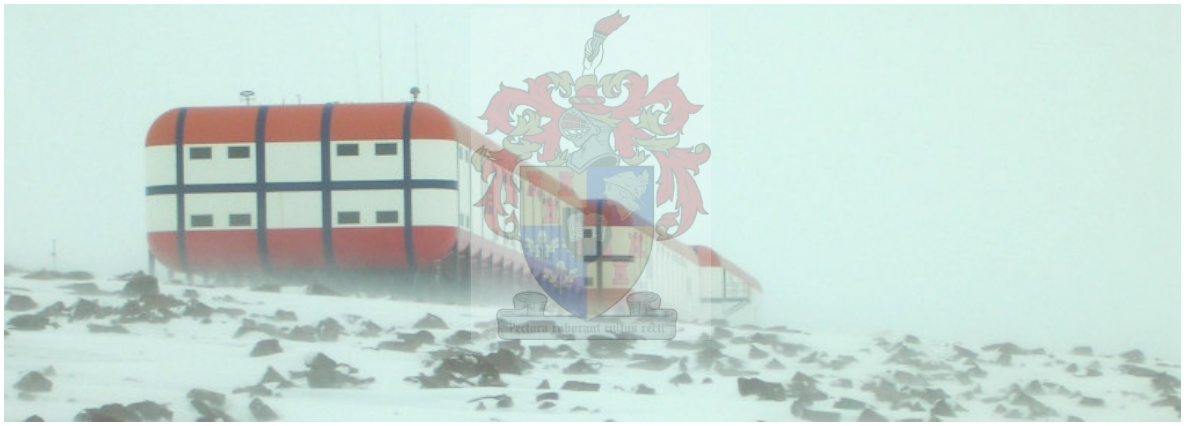

Figure 1.4: South Africa's SANAE IV station, completed in 1997 (Olivier, 2005)

1.2 Objectives

The efforts required to operate SANAE IV and other SANAP stations are intensive. Thus, in view of the associated costs of running South Africa's Antarctic stations as well as an increasing global awareness of alternative energy-generation methods this study aims to investigate the feasibility, and sensibility, of harnessing solar energy incident at SANAE IV.

Utilising solar energy in Antarctica is not a novel idea. America, Australia, Japan, Spain and Sweden have all commissioned solar energy systems at their stations, while Australia, Germany and Sweden are further investigating the possibility of installing hybrid solar- and wind-powered hydrogen fuel-cell systems. Teetz (2002) has already investigated the feasibility of installing a

wind turbine at SANAE IV and concluded that it would be advantageous to do so, although to date no device has yet been installed at the station. The American, Argentinean, Australian, German, Indian, Japanese, Spanish and Swedish stations on the other hand are all currently utilising wind energy. In fact, the Australian Mawson base has achieved the target of generating an unprecedented 80 % of its energy demand from wind power.

Such efforts by countries to install renewable energy systems at their Antarctic stations are strongly encouraged by the Antarctic Treaty. For instance, in 1991 during the XIth Antarctic Treaty Special Consultative Meeting (ATSCM) a noteworthy decision was made to adopt the Madrid Protocol (Madrid Protocol, 1991) to the Antarctic Treaty. Essentially this protocol states that signatories to the Treaty are *"…convinced of the need to enhance the protection of the Antarctic environment and dependent and associated ecosystems"*. Furthermore it is stated in the Protocol that, *"The Parties commit themselves to the comprehensive protection of the Antarctic environment and dependent and associated ecosystems and hereby designate Antarctica as a natural reserve, devoted to peace and science."* As a result it was established during the XIth ATSCM that *"…the use of alternative energies, such as solar and wind power in the Antarctic Treaty Area, and the study of a systematic way of implementing energy saving methods with the aim of reducing the use of fuels to the maximum extent possible* [should be investigated]*"* (Steel, 1993). This project aims to proceed with the mandate issued at the XIth ATSCM, and to determine the potential benefits that might arise from the suggested changes to SANAP operations in Antarctica.

Figure 1.5: Where the Antarctic ice-shelf, suspended in the ocean, breaks off into icebergs (Olivier, 2005)

1.3 Layout of Thesis

This thesis has been divided into six chapters. Chapters 2-4 essentially pose questions intended to assist in determining the feasibility of utilising solar energy at SANAE IV. These questions address: the amount of incident solar radiation at SANAE IV, the amount of energy consumed by the station, a consideration of what one could use to capture solar energy at SANAE IV, and an evaluation of expected lifecycle costs. The information obtained from each of these sections was collated, and an answer on the technical and economic feasibility of utilising solar energy at South Africa's Antarctic station and the recommended course of action are provided in the final chapter (Chapter 6).

To summarise, this thesis contains the following six chapters:

- Chapter 1 – Background
- Chapter 2 – Available Solar Energy at SANAE IV in Antarctica
- Chapter 3 – SANAE IV Energy Demand
- Chapter 4 – Solar Energy Capturing Solutions
- Chapter 5 – Economic Analysis
- Chapter 6 – Conclusion

The investigation described in chapter 2 has been limited by the size of a relatively small set of actual measured data obtainable from SANAE IV. Nonetheless, suggested values are well supported by an examination of three alternative resources and accuracy estimates have been made. Predicted values of radiation at various tilt angles are also presented. The end of the chapter includes a comparison of the expected radiation at SANAE IV with data from three other Antarctic stations (viz. the Dumont d'Urville [FRA], WASA [SWE] and Neumeyer [GER] bases).

Chapter 3 includes a review of work previously undertaken at SANAE IV by Cencelli (2002) and Teetz (2002). It is considered important for understanding how much energy is consumed at the station. Energy loads found suitable for utilising solar energy are identified and observations regarding potential efficiency improvements at the station are made. It is also shown how the entire energy system of SANAE IV can be divided into an electrical and a thermal energy demand, the same two categories that define solar energy systems.

Chapter 4 investigates the alternative methods of capturing solar energy, and describes which of these are optimal for the conditions at SANAE IV. Some of the difficulties encountered due to the low ambient temperatures and strong winds are highlighted, and the expected collector efficiencies of various available products are calculated. Each of the recommended solutions has been described in terms of its expected energy savings, as well as by way of examining the associated prices of each product.

Chapter 5 presents an economic analysis based on the *"Integrated Environmental Management Information Series"* published for the Department of Environmental Affairs and Tourism (DEAT, 2005). Payback periods, energy generation costs and externalities are calculated and then discussed.

Finally, conclusions are given in chapter 6. Here an answer is given regarding the feasibility of utilising solar energy at South Africa's SANAE IV station in Antarctica. Included are recommendations and the suggested future course of action.

Figure 1.6: Joint German and South African logistics on the ice-shelf (Olivier, 2005)

Chapter 2 – Available Solar Energy at SANAE IV in Antarctica

2.1 Introduction

Investigating the feasibility of using solar energy at South Africa's SANAE IV base in Antarctica necessitates a careful study of the insolation received throughout the year. This chapter aims to provide an answer to the question of how much solar energy is available for the displacement of diesel at the base and under what conditions this insolation will be available.

Section 2.2 of this chapter endeavours to provide a first approximation of the expected average insolation rates at SANAE IV. To this end the databases maintained by the National Aeronautic and Space Agency (NASA) have been investigated for the locations of the South African (SANAE IV) and German (Neumeyer) stations located approximately 300 km from each other. These databases, created using satellite imagery and ground-based measurements from around the world, currently represent the most modern method of mapping meteorological information on a global scale. The section therefore also aids in understanding how solar radiation conditions at SANAE IV compare to other locations around the world.

Next a theoretical analysis of solar radiation at SANAE IV is presented. Here various correlations are investigated and compared with the values suggested by NASA, helping to further establish what the most probable amounts of radiation at the South African station are. A small amount of data measured at SANAE IV during 2005 is also analysed in these comparisons and the results from correlations that most adequately describe the radiation conditions in Antarctica are identified. Subsequently these results are used to estimate the performance of solar energy devices in chapters 4 and 5.

Finally, a short summary of the investigation and some conclusions are provided. Accuracy estimates are presented and the areas that would most benefit from future study are highlighted.

2.2 Global Databases – A First Estimate

The NASA database utilised in this section was established in 1986 after competition amongst various international agencies resulted in an effort to collate measurements of solar radiation from around the world. Ultimately NASA became the benefactor of this information and has made it available in the Surface Radiation Budget (SRB) and Surface meteorology and Solar Energy (SSE) datasets (SSE, 2005).

Figure 2.1 is compiled with data from NASA's SSE dataset and illustrates estimates of annual average insolation everywhere on Earth for flat surfaces (i.e. horizontal insolation). According to this image (which accounts for local weather, or *all-sky* conditions) the high latitudes receive less global horizontal insolation on average over a year than the more central equatorial regions, due mainly to the *cosine effect* or low average zenith angle at high latitudes.

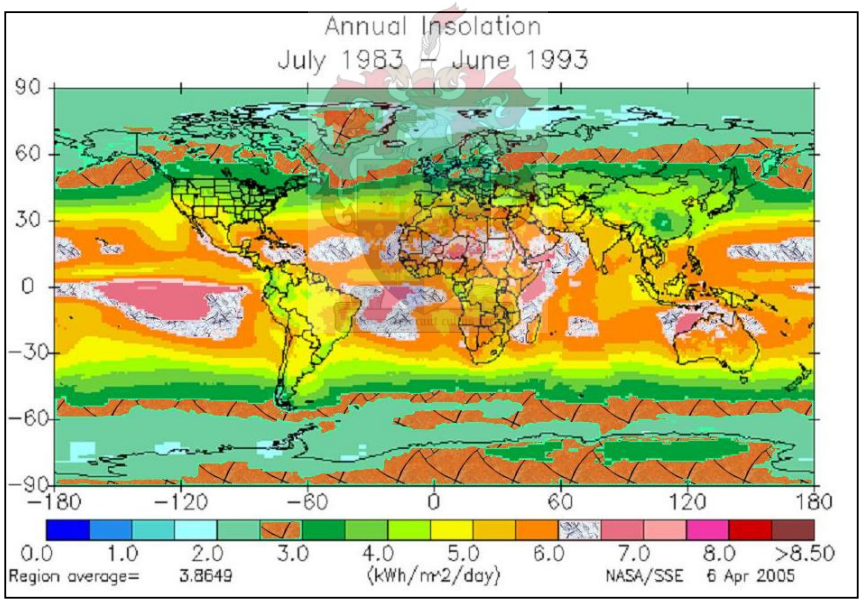

Figure 2.1: Estimated average total all-sky global horizontal insolation (SSE, 2005)

It is possible, however, to tilt collector surfaces at higher latitudes towards the sun and mitigate the disadvantages of the obliquely received sunlight. In fact, calculating the annual insolation on two-axis tracking surfaces reveals that every location on the planet would, not considering the effect of the Earth's atmosphere, receive equal amounts of energy from the sun. Consequently two significant criteria in the current investigation are the added cost of installing tracking mechanisms, and the local weather conditions at SANAE IV. Unfortunately, latitude also has

bearing on the received insolation for another reason. Even on clear days there are absorptive and reflective losses of radiation associated with the distance sunlight travels through the atmosphere, which is a maximum at the poles. This effect is summarised in a parameter referred to as *air-mass.*

Therefore, as shown in figure 2.1 it is evident that the more central and sun facing equatorial latitudes are better disposed to harnessing solar energy than the polar-regions. There is less need for tracking surfaces, a lower air-mass and not as much seasonal variation of radiation. According to figure 2.1 these latitudes receive on average approximately 3 kWh/m^2, or 200 % more horizontal radiation than Antarctica and other polar-regions annually.

Figure 2.2 illustrates the southern-hemisphere summer radiation conditions. Antarctica receives very high insolation during the summer mainly because the sun remains above the horizon throughout the day. Even when considering all-sky conditions it is evident that Antarctica has extremely high flat-plate insolation rates during this short period. In fact, together with western parts of Australia and South Africa's Northern Cape, they are the highest in the world during the southern-hemisphere summer months.

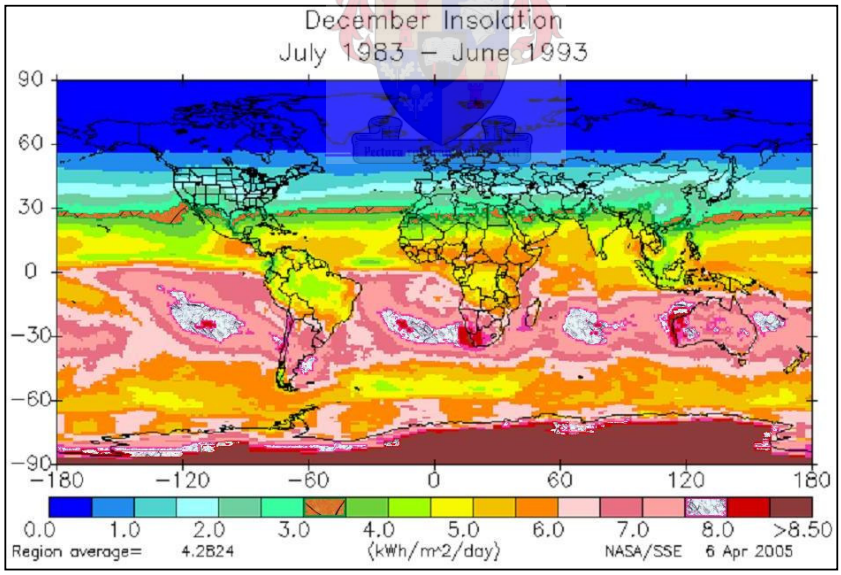

Figure 2.2: Estimated average December total horizontal insolation (SSE, 2005)

A plot of the estimated daily-total horizontal insolation (in kWh/m^2) incident at SANAE IV over the five-year period from 1988 until 1992 is given in figure 2.3. From the figure it is evident that surface insolation is a maximum from late November to early January (coincident with the summer solstice on the 21st of December), and that minima are encountered during winter when

zero sunlight is present. It can be seen that Top Of Atmosphere (TOA) radiation remains constant throughout annual cycles, and it is estimated from figure 2.3 that on a clear summer's day 9 kWh/m^2 of insolation should be received at ground level.

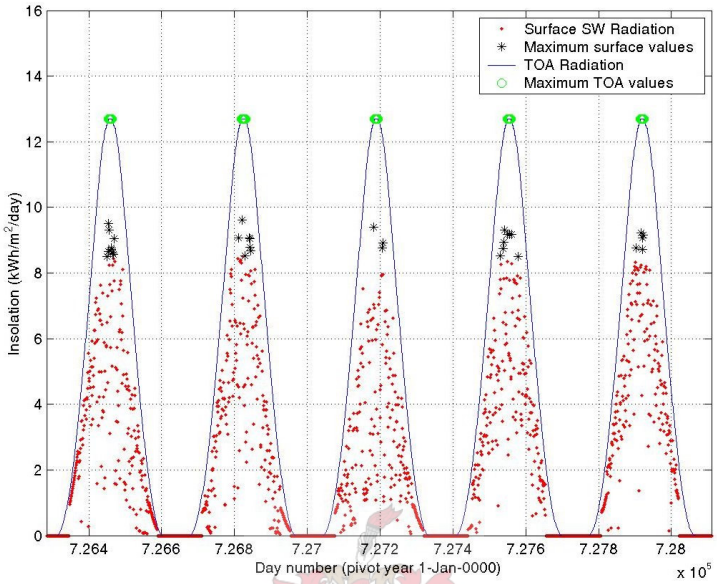

Figure 2.3: Surface and TOA horizontal insolation at SANAE IV, 1988 to 1992 (SSE, 2005)

Also derived from the SSE database is figure 2.4. Here the annual average radiation at SANAE IV is shown in greater detail and it can be seen, for instance, that during December at noon approximately 650 W of radiation will fall on a horizontal surface. A more detailed investigation of the solar radiation expected at SANAE IV, which studies the theory of clear-sky and all-sky conditions, follows in section 2.3.

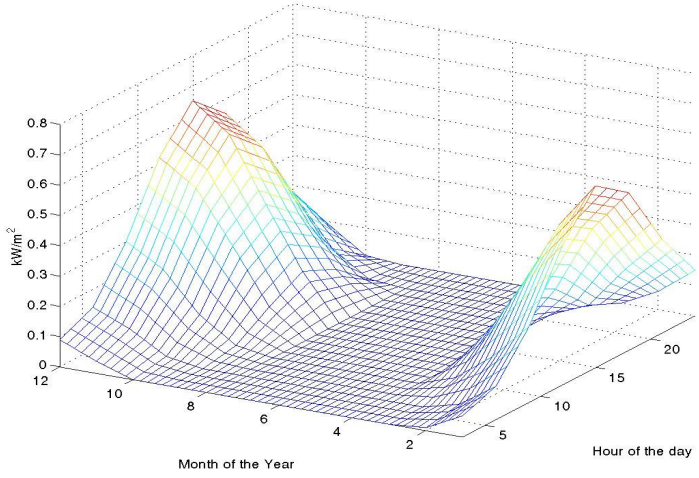

Figure 2.4: Monthly-average daily global horizontal radiation at SANAE IV (SSE, 2005)

2.3 Solar Radiation at SANAE IV – A Theoretical Study

2.3.1 Data Capture Instrumentation and Procedures

All references in this thesis to measurements of radiation recorded at SANAE IV pertain to data obtained by the author during the 2004/2005 takeover. Instrumentation used included: one Kipp & Zonen SP-*Light* pyranometer, two Kipp & Zonen CM5 pyranometers, a Hewlett-Packard 34970A data logger, shielded low-temperature resistant cable, a 5-Watt Liselo-Solar photovoltaic (PV) module, thermocouples, and a shade-ring that was designed by the author and manufactured locally. Measurements were recorded to a personal computer each second for eighteen days (10^{th} till 27^{th} January 2005), however the data presented here are one-minute averages of the original set. The photovoltaic (PV) module was used to determine PV energy output and cell temperatures, and simultaneous temperature measurements of all instrumentation were taken using the thermocouples which enabled corrections to be made for thermal effects.

2.3.2 Clear-Sky Radiation

Clear-sky correlations model the surface radiation conditions without considering the influence of clouds. Of these Hottel (1967) has presented a method for estimating the clear-sky global radiation that accounts for four different climate types, and Liu and Jordan (1960) have presented methods for estimating global clear-sky diffuse radiation from these values. Figure 2.5 utilises these correlations to plot curves of the January global clear-sky horizontal and diffuse radiation alongside data measured at SANAE IV (the details of which are given in section 2.3.1). Also plotted in figure 2.5 for comparison are the ASHRAE standard atmosphere (an average atmosphere for every location on Earth) and a Hottel curve with coefficients that have been adjusted in order to replicate measured data more accurately (the details of which are given at the end of section 2.3.2).

From figure 2.5 it is evident that all of the unadjusted correlations underestimate the global radiation at SANAE IV. This underestimation has been attributed to the relatively clear skies of Antarctica since the suggested equations are measured averages that account for the haziness of other sites. From figure 2.5 it has also been calculated that on a clear-sky day in January at SANAE IV a total of 9.1 kWh will be available per square metre of horizontal surface. That is, 379 W/m^2 for a 24-hour period. The diffuse radiation plotted in figure 2.5 is predicted acceptably

well by Liu and Jordan (1960) and is the suggested correlation for future use, however, it is not advisable to use the simple ASHRAE standard atmosphere model.

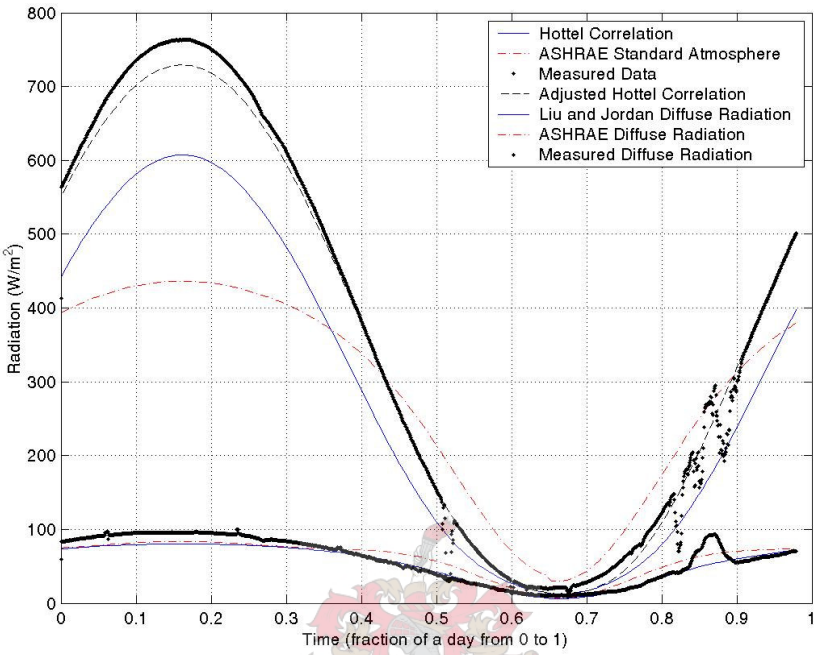

Figure 2.5: Clear-sky curves of daily radiation at SANAE IV

Both the Hottel and the Liu and Jordan correlations mentioned above (which were used to predict clear-sky global radiation and clear-sky diffuse radiation respectively) are presented below. Here the subscripts *"cnb"* refer to clear-sky normal beam radiation, *"on"* to TOA normal beam radiation and *"b"* to beam radiation. The effect of clear-sky atmospheric effects can then be approximated by:

$$G_{cnb} = G_{on} \cdot \tau_b \qquad 2.1$$

Where G_{on} (W/m^2) in equation 2.1 is easily calculated from equations provided by Duffie and Beckman (1991), and τ represents the atmospheric transmissivity at SANAE IV suggested by Hottel (1967). If *Al* is the altitude of the location in kilometres, τ is approximated as:

$$\tau_b = a_0 + a_1 \cdot e^{\left(\frac{-k}{\cos\theta_Z}\right)} \qquad 2.2$$

Where,

$$a_0 = r_0 \cdot a_0' \qquad a_0' = 0.4237 - 0.00821 \cdot (6 - Al)^2$$

$$a_1 = r_1 \cdot a_1' \qquad a_1' = 0.5055 + 0.00595 \cdot (6.5 - Al)^2$$

$$k = r_k \cdot k' \qquad k' = 0.2711 + 0.01858 \cdot (2.5 - Al)^2$$

Table 2.1: Hottel climate coefficients

CLIMATE TYPE	r_0	r_1	r_k
Tropical	0.95	0.98	1.02
Midlatitude summer	0.97	0.99	1.02
Subarctic summer	0.99	0.99	1.01
Midlatitude winter	1.03	1.01	1.00

From Hottel (1976)

The fitted or adjusted Hottel curve shown in figure 2.5 uses:

$$r_0 = 0.99 \qquad r_1 = 0.99 \qquad r_k = 0.45$$

The correlation proposed by Liu and Jordan for estimating the amount of diffuse radiation is:

$$\tau_d = \frac{G_d}{G_o} \qquad \text{Where,} \qquad \tau_d = 0.271 - 0.294 \cdot \tau_b \qquad 2.3$$

2.3.3 All-Sky Conditions

The interaction of clouds with incoming solar radiation makes it very difficult to accurately predict the actual surface insolation throughout the year. *All-sky* correlations must surpass modelling only the effects of water vapour, ozone and particulate matter in the atmosphere (i.e. transmissivity), and for this reason are normally derived empirically. To predict actual values of surface insolation analytically is very difficult, and in fact Norris (1968) concludes that, *"The foregoing discussion… indicate*[s]*… it is probably impossible to use cloud information to predict solar radiation."* Therefore, since recorded data will automatically reflect the effect of cloud conditions specific to a location and provide acceptable averages for further investigation, there is little that can replace a database of previously measured radiation.

Unfortunately values of solar insolation are not currently being recorded at SANAE IV even though the base is classified as a first class weather station. Thus, instead of seeking correlations

that relate cloud cover data (available at SANAE IV) to insolation, a number of methods collated by Duffie and Beckman (1991) will form the basis of further investigation.

HORIZONTAL SURFACES – ANALYSIS FOR JANUARY

An important parameter used often in the correlations presented by Duffie and Beckman (1991) is the *clearness index*, and is simply the ratio of global horizontal radiation on the Earth's surface to that at the TOA. TOA insolation is easily calculated for any location on Earth, and global horizontal radiation is a standard measurement that forms part of any solar radiation dataset. Thus, knowing the global horizontal insolation the clearness index can easily be derived from:

$$\overline{K}_T = \frac{\overline{H}}{\overline{H}_O} \qquad 2.4$$

Where $\overline{K}_T$ is the monthly average clearness index (dimensionless), $\overline{H}$ is the monthly average daily radiation on a horizontal surface (kWh/m^2) and $\overline{H}_O$ is the monthly average daily TOA radiation on a horizontal surface (kWh/m^2). There are also analogous equations for daily and hourly clearness indices defined by K_T and k_T respectively.

From clearness indices Erbs et al. (1982) have suggested a well-known and widely used method to predict the values of *diffuse* radiation. The correlation was created using data from one Australian and four American weather stations, yet referring to figure 2.6 (Neumeyer, 2005), it can be seen that this method underestimates the amount of diffuse radiation for conditions in Antarctica. The recorded data shown in figure 2.6 was measured at Neumeyer by instrumentation endorsed by the Baseline Surface Radiation Network (BSRN), of which the German base is a member. This is a significant observation since concentrating solar energy systems utilise only the beam portion of incoming solar radiation, and consequently the correlations suggested by Erbs et al. (1982) are regarded as inappropriate for further investigation at SANAE IV.

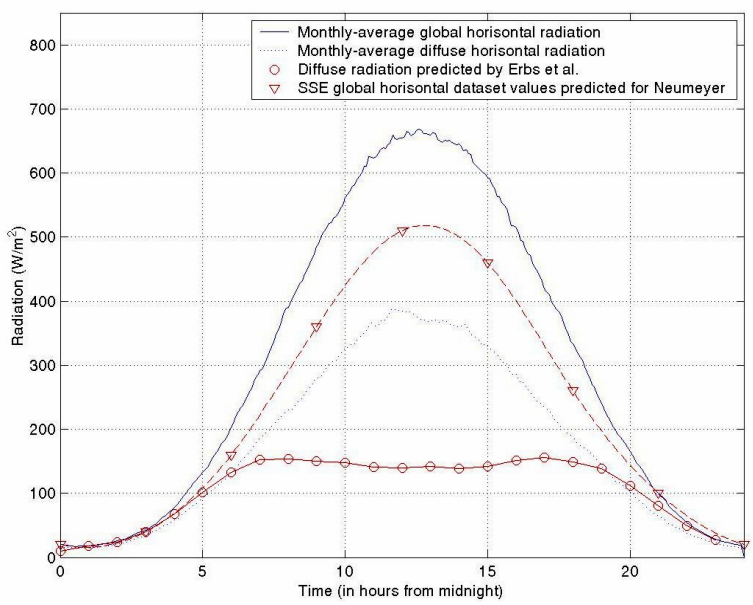

Figure 2.6: Five-year average January daily radiation at Neumeyer station (1994 to 1998)

From figure 2.6 it is also evident that SSE values tend to underestimate the global horizontal radiation for locations in Antarctica. The underestimation has been calculated as 24 % of the daily peak value and just over 20 % of the total daily horizontal insolation. Yearly weather conditions, however, may vary by this much (SSE suggests seasonal average variations of 17 % in January), thus it can be said that for the location of Neumeyer the SSE database presents useful estimates of worst-case conditions.

SSE also provides estimates of average cloud cover, and a quick consideration of other available meteorological data is in order. Cloud cover observations taken at Neumeyer station suggest an average January cloud cover of 7/10ths (or 70 %), and compares well to the amount given in SSE of 67.6 %. Comparatively, visual observations recorded at SANAE IV suggest a cloud cover of 4/10ths at the South African station while the value presented by NASA's database is 51.7 %. It is reasonable, therefore, to assume that SANAE IV is expected to experience less cloud cover than Neumeyer during January. The direct implication of this is that SANAE IV will also experience higher values of global horizontal radiation and lower relative amounts of diffuse radiation than Neumeyer.

Note that although reference was made earlier to the statement by Norris (1968) that, *"The foregoing discussion… indicate*[s]*… it is probably impossible to use cloud information to predict solar radiation"* this does not imply that higher amounts of cloud cover are not analogous with

lower amounts of global radiation for adjacent locations. Rather, it only states that one cannot conclude by exactly how much the levels of radiation at these locations will differ.

The most accurate averages of expected insolation are still derived from recorded data however, and in figure 2.7 measurements of radiation logged at SANAE IV over an eighteen-day period during January 2005 (10^{th} till 27^{th} January 2005) are presented (as specified in section 2.3.1). The average clearness index of the period is 51.2 % (refer to equation 2.4), and plotted alongside is SSE global radiation data. Considering that the five-year clearness index of Neumeyer is 63.7 % (from the data in figure 2.6) and is a location known to have higher amounts of cloud cover than SANAE IV, it is evident that the data presented in figure 2.7 represents a particularly cloudy January period. It is again apparent that SSE values are conservative approximations of the actual conditions in Antarctica.

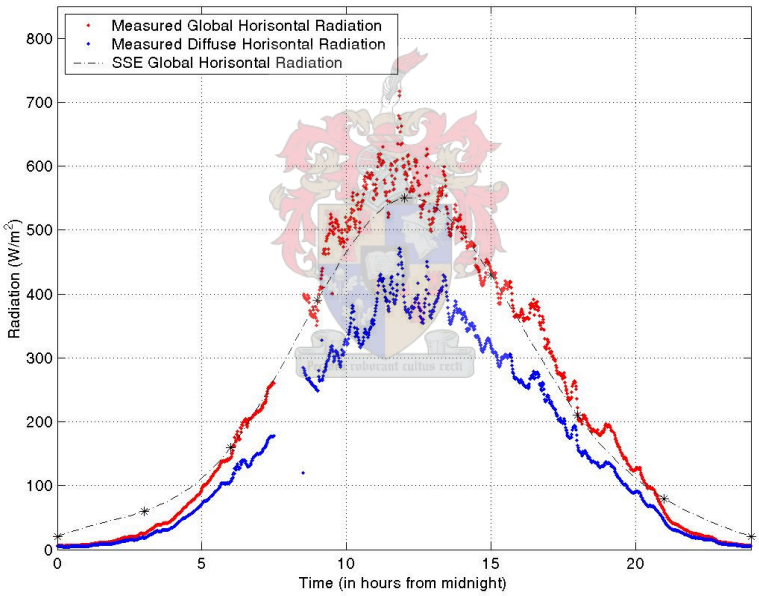

Figure 2.7: Comparison of SANAE IV data with values predicted by the SSE dataset

The suggested equations for calculating the January radiation at SANAE IV are presented in equations 2.5 and 2.6. They were created by incrementing SSE dataset values by 20 %, and are essentially equal to the average radiation conditions at Neumeyer (refer to figure 2.12). As stated above this is known to be a conservative estimate. The diffuse radiation was calculated by determining the relative fraction of diffuse to global radiation at Neumeyer, and applying this condition to the global radiation at SANAE IV. For a list of the equations pertaining to other months please turn to appendix B.1.

Monthly-average instantaneous global horizontal radiation (W/m^2) where x is a number in hours from 0 to 24 is given by equation 2.5.

$$G = -0.0003187x^6 + 0.024072x^5 - 0.64063x^4 + 6.8013x^3 - 22.662x^2 + 33.863x + 6.5175 \qquad 2.5$$

Monthly-average instantaneous diffuse horizontal radiation (W/m^2) where x is a number in hours from 0 to 24 is given by equation 2.6.

$$G_d = -0.0001608x^6 + 0.012169x^5 - 0.32434x^4 + 3.4278x^3 - 11.02x^2 + 16.759x + 11.998 \qquad 2.6$$

Table 2.2: Estimated January radiation averages for the conditions at SANAE IV

PARAMETER	VALUE
January-average global horizontal insolation (kWh/m^2)	7.3
January-average midday global horizontal radiation (W/m^2)	663
January-average mean global horizontal radiation over 24 hours (W/m^2)	304

THE EFFECT OF SURFACE TILT

The importance of surface tilt was alluded to earlier in section 2 of this chapter where it was noted that valuable gains may be realised by proper management of the *cosine effect*. Analysing these gains, however, poses certain problems. Although tilting a collecting surface towards the sun will increase the beam radiation in a manner simply proportional to the cosine of the zenith angle, the diffuse radiation changes independently according to the tilt angle, reflectivity of the ground and view factor with the sky. Consequently it is necessary to know both the diffuse and beam radiation before it is possible to determine available tilted insolation.

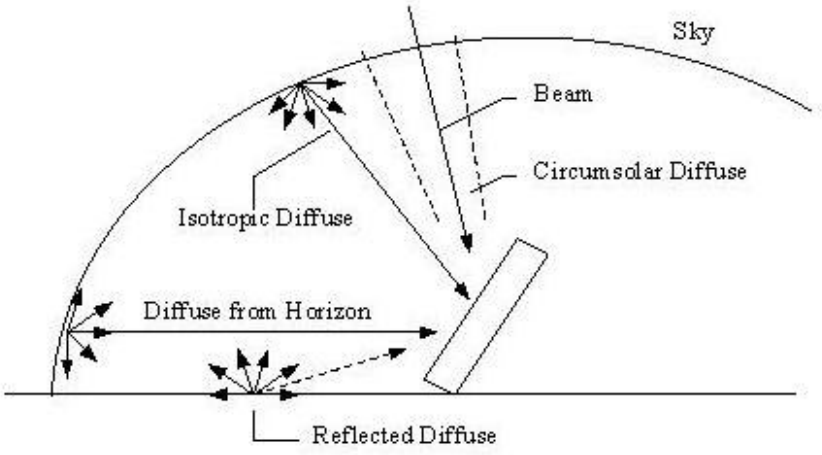

Figure 2.8: Components of beam and diffuse radiation (Duffie et al., 1991)

A further complication is the modelling of the individual responses to tilt of various components of diffuse radiation (refer to figure 2.8). Included are the components of horizon brightening (a band of higher intensity diffuse radiation at the horizon), circumsolar radiation (high intensity diffuse radiation in the vicinity of the sun), isotropic, and reflected ground components. For the purposes of this study it will be assumed that the diffuse reflective surface of snow reflects 70 % of the incident radiation (Duffie and Beckman, 1991), although Schmidt et al. (1994) have suggested a value of 84 %.

Determining global tilted radiation allows the use of any or all of the above-mentioned factors, depending on the accuracy desired. Perez et al. (1988) have considered all of these factors in their correlation (the utilisation of which has led to the creation of figures 2.9 and 2.10) while Liu and Jordan (1963) assume that the intensity of diffuse radiation is equal at any orientation. These two approximations, which will be referred to again, are known as the anisotropic and isotropic conditions respectively.

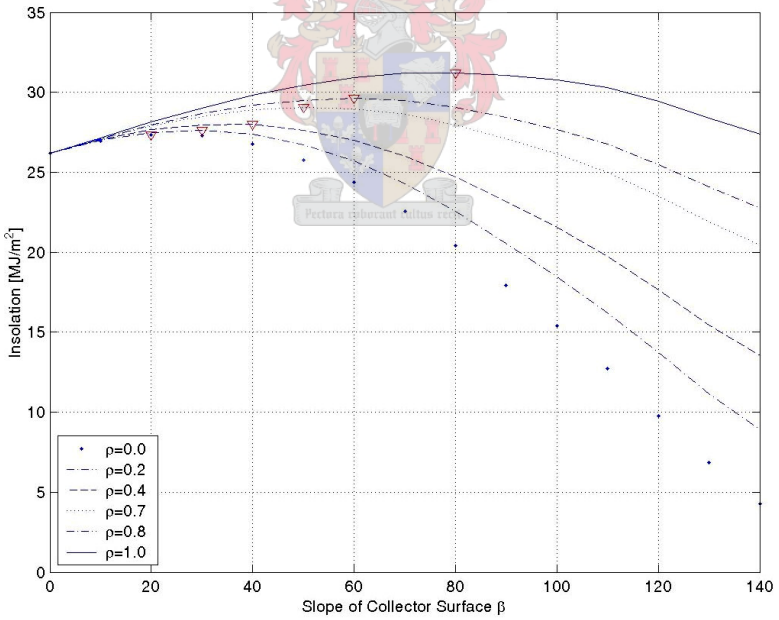

Figure 2.9: January daily insolation rates on a tilted surface with different ground reflectivity

From studying figure 2.9 (refer to appendix B.2 for computational details) it is evident that the optimum tilt angle for global radiation at SANAE IV during January is 52° from the horizontal. At this angle an increase of 11 % in daily insolation is expected.

Available beam radiation at various tilt angles is shown in figure 2.10. In this instance ground reflectivity is of no significance since beam radiation reflected from the snow is scattered diffusely, and there exists only a single curve as opposed to the various lines visible in figure 2.9. The optimum tilt for a collector that utilises only beam radiation is 39°, and is associated with a 21 % increase in incident radiation compared to the insolation received on a horizontal surface.

Figure 2.10: Expected daily beam insolation on a tilted surface with different ground reflectivity

Using the Perez et al. (1988) correlation expected average daily totals for each month of the year have been derived at their optimum tilt angles and are presented in table 2.3. As can be seen the seasonal variations are considerable, and surface tilting may increase the available global radiation on average by 37 %. Attention is drawn to the fact that the equations used to calculate these values of *insolation* (in kWh) on tilted surfaces are also valid for determining *radiation* (in kW) at any time during the day. While the Perez et al. (1988) method uses statistical coefficients derived for hourly horizontal insolation measurements (and is therefore not suggested for this purpose) the isotropic correlation suggested by Liu and Jordan (1963) is well suited to the task of determining daily profiles from horizontal data at various surface angles (see figure 2.11 below). The measured data presented in figure 2.11 is part of the dataset recorded by the author.

The data shown in table 2.3 summarises the investigation undertaken in this chapter so far. This data represents the best estimates of radiation that could be attained, and will subsequently also be used to estimate the diesel savings that can be realised by utilising solar-energy devices. As

described above the values have been derived from both the Perez et al. correlation and the average monthly radiation profiles developed at the end of section 2.3.3 in equations 2.5 et al.

Table 2.3: Expected monthly-average daily totals of insolation at SANAE IV

MONTH	GLOBAL HORIZONTAL INSOLATION (kWh/m^2.day)	OPTIMUM TILT (°) – GLOBAL	TILTED GLOBAL INSOLATION (kWh/m^2.day)	PERCENTAGE INCREASE AT TILT (%) – GLOBAL	HORIZONTAL BEAM INSOLATION	OPTIMUM TILT (°) – BEAM	TITLED BEAM INSOLATION (kWh/m^2.day)	PERCENTAGE INCREASE AT TILT (%) – BEAM	AVERAGE TEMP (°C)
Jan	7.26	52	8.05	11	2.92	39	3.54	21	-6.6
Feb	4.78	63	6.11	28	1.88	53	2.99	59	-10.3
Mar	2.13	74	3.51	65	0.74	68	1.99	169	-14.9
Apr	0.72	84	2.54	253	0.26	83	2.12	715	-18.2
May	0.01	90	0.01	0	0.01	90	0.01	0	-19.5
Jun	0.00	00	0.00	0	0.00	00	0.00	0	-20.1
Jul	0.00	00	0.00	0	0.00	00	0.00	0	-23.1
Aug	0.17	88	1.24	629	0.06	87	1.13	1783	-22.9
Sep	1.53	78	3.23	111	0.59	75	2.21	275	-22.9
Oct	3.93	69	6.86	75	1.49	68	3.78	154	-18.2
Nov	6.23	52	7.14	15	2.47	44	3.18	29	-12.8
Dec	7.63	48	8.30	9	3.09	35	3.55	15	-7.1
Avg	*2.87*	*70*	*3.92*	*37*	*1.13*	*64*	*2.04*	*81*	*-16.4*

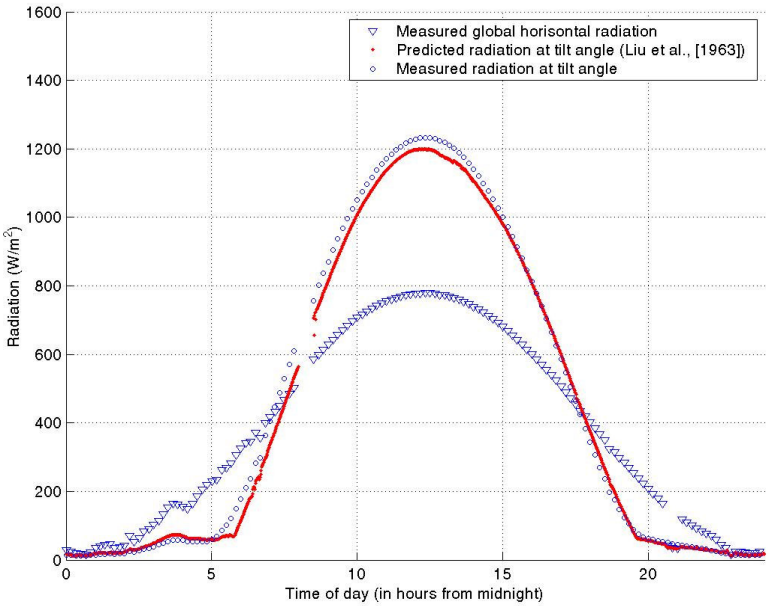

Figure 2.11: Typical measured and predicted values of radiation for a surface tilted at 40°

Considering figure 2.11, the accuracy of predicting the solar radiation incident on a tilted surface has to be questioned for conditions where the ground is uneven or undulating. Investigation revealed that all predicted daily totals on tilted surfaces derived using the Liu and Jordan isotropic sky method (1963) were on average within 7 % of the actual measured values (that included facing the pyranometer towards hills and snow mounds at various bearings). The largest error was an inaccuracy of 13 %, and all predictions were underestimates. Hence Liu and Jordan (1963) give a reasonable conservative estimate of the expected *radiation* (kW) at various tilt angles for conditions at SANAE IV.

Figure 2.12 gives comparative results of average global horizontal radiation at four Antarctic stations (viz. France's Dumont d'Urville, Sweden's WASA station, Germany's Neumeyer station and South Africa's SANAE IV base) with their respective latitudes indicated in the legend (Henryson et al. [2004], Steel [1993] and Schmidt et al. [1994]). Comparing the estimated radiation with the values suggested for WASA, Dumont d'Urville and Neumeyer it seems that the predicted values of radiation at SANAE IV are reasonable, and an estimate of their accuracy is provided in section 2.4.

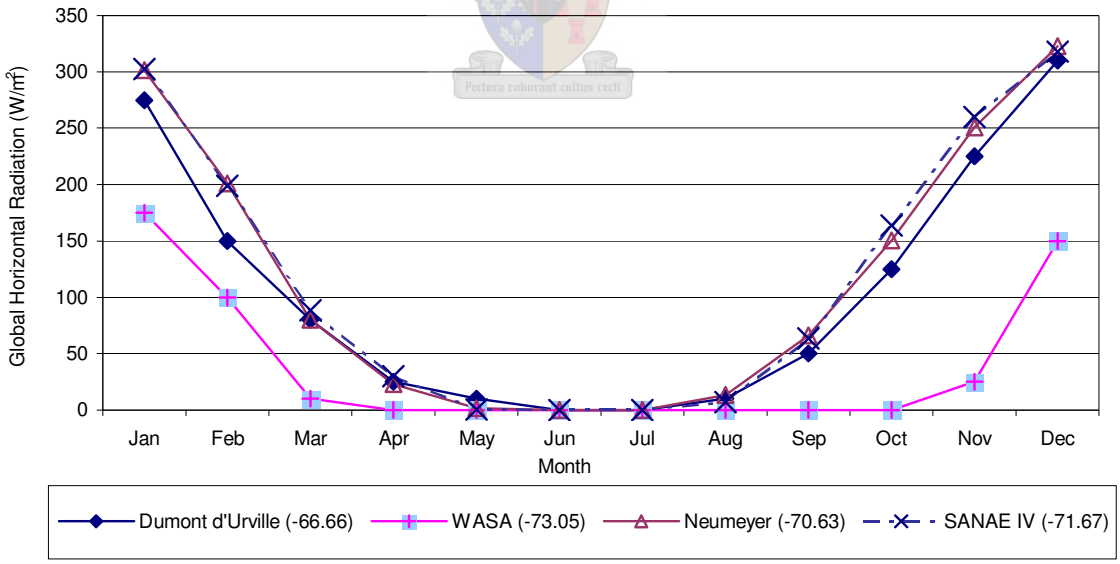

Figure 2.12: Monthly-average global horizontal radiation at four Antarctic stations

2.4 Summary

Available solar energy in Antarctica is characterised, much like many other attributes of the continent, by extremes. During the summer there are exceedingly large amounts of radiation at hand, however, long winter months have the effect of reducing annual averages to such an extent that SANAE IV is classified as a low insolation site.

Estimates of annual insolation have been summarised in table 2.3, and will be used in chapters 4 and 5 to estimate the expected fuel savings from solar energy devices. These values are conservative estimates of the annual radiation at SANAE IV including approximations at the optimal collector tilt angles. As shown in figure 2.12 these radiation values are essentially equal to the conditions at Neumeyer, yet an estimate of the data accuracy for the month of January can be made by noting that actual monthly averages of insolation must be less than clear-sky values. Because it is known that the suggested averages are conservative estimates (c.f. section 2.3.3), and that this data is within 20 % of the clear-sky value (c.f. section 2.3.2), the suggested averages must lie well within 20 % of the actual average. This is especially true considering that only two clear-sky days are expected in January (SSE, 2005).

From table 2.3 it also evident that diffuse radiation forms a significant portion of global radiation (estimated at 1.74 kWh/m^2.day, or 60 % of the average global radiation in table 2.3). Furthermore, figures 2.9 and 2.10 show that collectors will require relatively high tilt angles, starting at 50° in the summer and increasing up to 90° in the winter. This will make it difficult to design compact collector fields since the high tilt angles will not allow placing collectors behind each other.

It is suggested that the potential benefits to the SAWS and BSRN of permanently installing instruments at SANAE IV are investigated. Solar radiation measurements are a fundamental component of any meteorological dataset, significant in view of the fact that although SANAE IV is classified as first class weather station there are currently no instruments at the base measuring solar radiation. This is understandable, however, in view of the associated economic and environmental related difficulties. Measurements of solar radiation at SANAE IV would allow meaningful contributions to be made towards global research projects such as the BSRN.

Chapter 3 – SANAE IV Energy Demand

3.1 Introduction

Diesel is bunkered at SANAE IV in a raised structure located approximately 400 meters from the station. Designed to stockpile almost two year's worth of fuel at once (viz. 600 000 litres) diesel from this bunker is used only for the purposes of refuelling vehicles and supplying the day-tank located in the base. The day-tank in turn supplies diesel to three diesel-electric generators, and these convert the fuel into the two entities of electricity and heat. Together, electricity and heat can be used to classify every single energy load at SANAE IV.

In this chapter the station's energy systems are audited in order to establish which loads are suitable for use with solar electric and solar thermal devices. Utilising these renewable energy devices would be desirable not only for reducing diesel consumption but also for providing the station with greater energy autonomy. Currently 100 % of the electrical and thermal load at the base is met by diesel. Annual diesel demand at SANAE IV amounts to approximately 347 222 litres, of which 297 872 litres are used by the generators for generating electricity, and the remainder is used for re-fuelling the fleet of diesel-powered vehicles. Small amounts of petrol and jet-fuel are also required to power Skidoos and aircraft respectively, yet amount to approximately only 5 % of the overall fuel consumption at the station. Along with diesel the small amounts of petrol and jet-fuel (and negligible amounts of Liquid Petroleum Gas [LPG]) define the complete array of fuels currently utilised at SANAE IV.

There is no obvious replacement for diesel in Antarctica. Internal combustion engines are reliable, safe and easily maintained, used in spite of the difficulties involved with getting fuel to the continent. Heat created by the generators while making electricity is recovered to warm the base and internal combustion engines display an affinity to the cold ambient conditions of Antarctica. It is not surprising that so much time, energy and money are spent on maintaining the current operating systems. Moreover, important machinery such as the diesel-powered vehicles are indispensable to SANAP, and will always require the current diesel infrastructure. It is important to appreciate, however, that on this scale small savings can make a large difference. This is especially true since 81 % of all fuel consumed at SANAE IV is used to generate electricity and heat for the station, two entities very easily displaced by solar alternatives.

3.2 Base Operating Systems

In this chapter a basic layout of the operating systems at SANAE IV is first presented, aimed at providing background to the discussions that follow. Next, quantitative as well as qualitative analyses are undertaken in an attempt to find values of “how much” and “at what times" energy is demanded. This identification of temporal load patterns is particularly important for load-matching renewable resources. Although illustrations that aid in understanding the text have been provided the reader is also directed to appendix C for more information, in which all data presented was collected at the station during the 2004/2005 SANAE IV takeover.

Both Cencelli (2002) and Teetz (2000, 2002) have given descriptions of the SANAE IV station operating systems. Cencelli has mainly classified and explained in some detail how each system operates while Teetz was most interested in quantifying loads. Essentially this chapter draws on their work and is meant to include the changes that have taken place at South Africa’s station since their reports were published.

3.2.1 SANAE’s Five-fold Operating System

For the purposes of auditing the energy systems at SANAE IV the structure suggested by Cencelli (2002) has been followed. Therefore, all machinery at the station will be classified under one of the following five categories. These are:

1. The Water System,
2. The Heating and Ventilation System,
3. The Power Generation and Electricity Transmission System,
4. The Control or PLC System, and
5. The Sewage System.

Refer to figure 3.1 for an illustration of the above classification system.

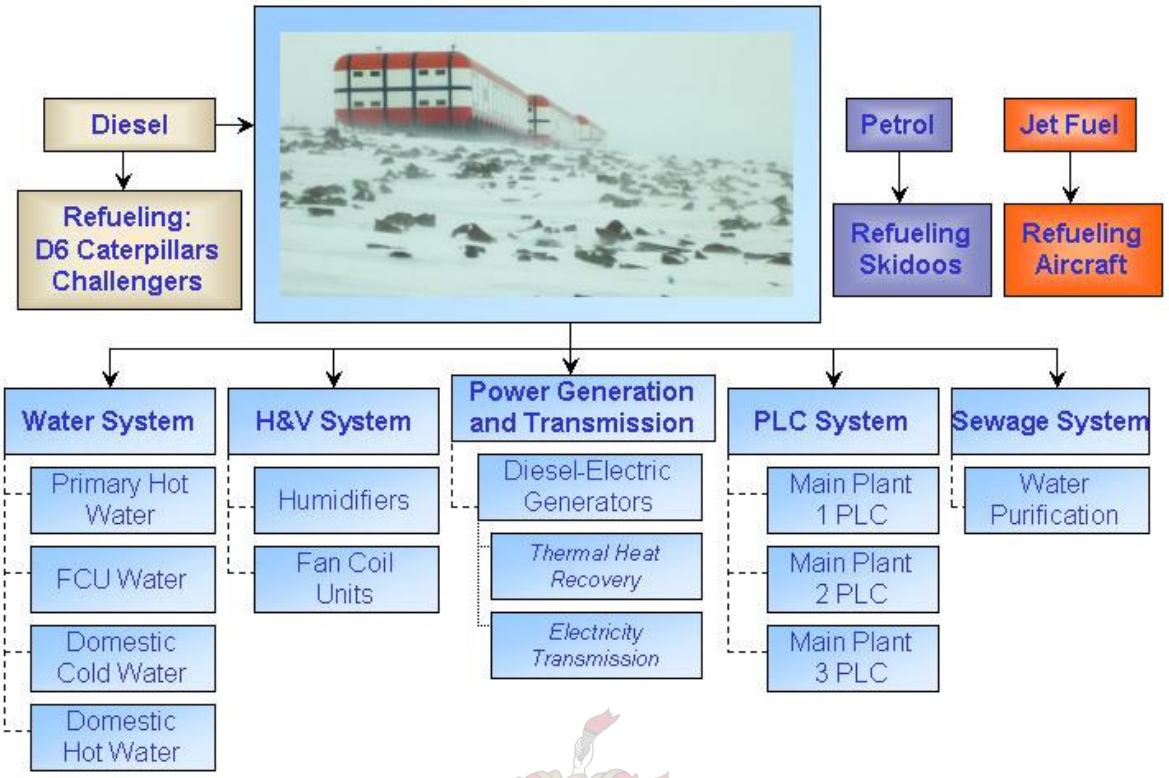

Figure 3.1: Energy systems at SANAE IV use only electricity and generator waste heat

3.2.2 Water Systems

Apart from its more obvious properties water is also very useful as an energy transporter. Consequently, the water systems at SANAE IV are responsible not only for supplying the domestic needs of the base (drinking, cooking, cleaning, etc.) but also for transporting heat.

The Primary Hot Water System (refer to figure 3.1) exists as a closed loop within the confines of the plant room. This system is responsible for transporting waste heat from the diesel-electric generators (obtained from the generator coolant fluid as well as the exhaust gasses) to the Fan Coil Unit Water (FCU Water) and Domestic Hot Water Systems and supplements their thermal loads. Typically this method of waste-heat recovery results in exceptional engine efficiencies in the order of around 70 %. Unfortunately, even though the electrical efficiencies of the generators are known (36.4 %, refer to section 3.2.4), the combined or total efficiency cannot currently be calculated. Knowing the inlet and outlet temperatures of the air-conditioning heat exchangers in each block alone (that are recorded daily) is insufficient information to determine this value since the energy transferred at these units includes a significant contribution from inline heating elements that are not recorded. It would be possible to use the temperature difference across the

Primary Hot Water heat exchanger and estimate a flow rate, losses and efficiencies between this heat exchanger and the loads, unfortunately the temperature difference across the Primary Hot Water System is not currently being recorded either.

Next the FCU Water System transports the energy to FCUs located in each block (refer again to figure 3.1). These FCUs in turn heat the outside air (utilising 100 % fresh air with no re-circulation) in order to keep inside temperatures of the base at comfortable levels. The waste-heat recovered from the generators therefore replaces heat lost from the base, which total about 39 kW in summer and 72 kW in winter (Cencelli, 2002).

There are, however, a number of heat sources within the base (computers, lights, people, etc.) that require consideration. Net summer and winter losses (the losses to the environment noted above minus heat given off from internal sources) have been estimated as –10.75 kW (a net heat gain) and 28.5 kW (a net heat loss) respectively, and imply that during summer the station requires cooling. Therefore there is a mismatch between the space-heating demands of the base and the available solar energy throughout the year. Furthermore, this observation begins to explain why summer takeover months are characterised by generator overheating. Since the station requires cooling during summer months the FCU Water Loop cannot use and will not accept generator waste heat. Since the heat-dump designed for these situations is undersized (Cencelli, 2002) heat is trapped inside the Primary Hot Water Loop. As a result the generators begin overheating. A solution sometimes employed by the Engineers is to force the generator heat into the FCU Water Loop (requires overriding normal automatic control), and mix it with more cold outside air by running the FCU fans at higher speeds.

The remaining two water systems, the Domestic Hot and Cold Water (refer to figure 3.1), supply the domestic water needs of the base occupants for cooking, cleaning and sanitation. The demand for fresh water at SANAE IV during the summer takeover period is, however, a source of much distress due to an insufficient water supply from the snow smelter. The snow smelter, a solar thermal and/or solar electrical load is critically important to station functionality, and presents an immediate opportunity for employing solar energy devices.

Lastly, all the water systems operational at SANAE IV are supplemented with water from the twelve storage tanks located along both sides of the hangar in the C-Block. These tanks are capable of storing up to 46 000 litres at a time with the option of isolating tanks from each other.

In this way water can be held in reserve to ensure that a small amount will always be available for keeping the Water Systems operational. There are also a number of unmentioned pumps, controls and in-line heaters associated with these systems that consume energy, and although it is not necessary for the purposes of this discussion to present all detail a more thorough description of each of these systems is provided by Cencelli (2002).

SNOW SMELTER

Antarctica is home to approximately seventy-percent of all the world's fresh water. This reserve, in the form of snow and ice, is consequently also the source of water for the base. In its original form of snow it is of little use, yet the snow smelter (one of biggest energy consumers at the station [refer to figure 3.3]) is able to melt the snow into its liquid form. It is situated approximately 200 meters from the base and is filled by shovelling snow into a chute that leads to one of the two storage tanks located below ground level, known as the "cold" side (refer to figure 3.2). Heating elements within the tanks melt the snow and heat the water while a circulation pump circulates the fluid between the two tanks. Eventually the main pump will pump the water up to the base and into the storage tanks located in the hangar. Together the smelter's two tanks can store 4 600 litres of water though only about half of this volume is normally produced during each smelting session (mainly because of the difficulties involved in compressing the snow as one shovels it into the tank). As a rule there are three snow smelter filling sessions per day during the takeover season.

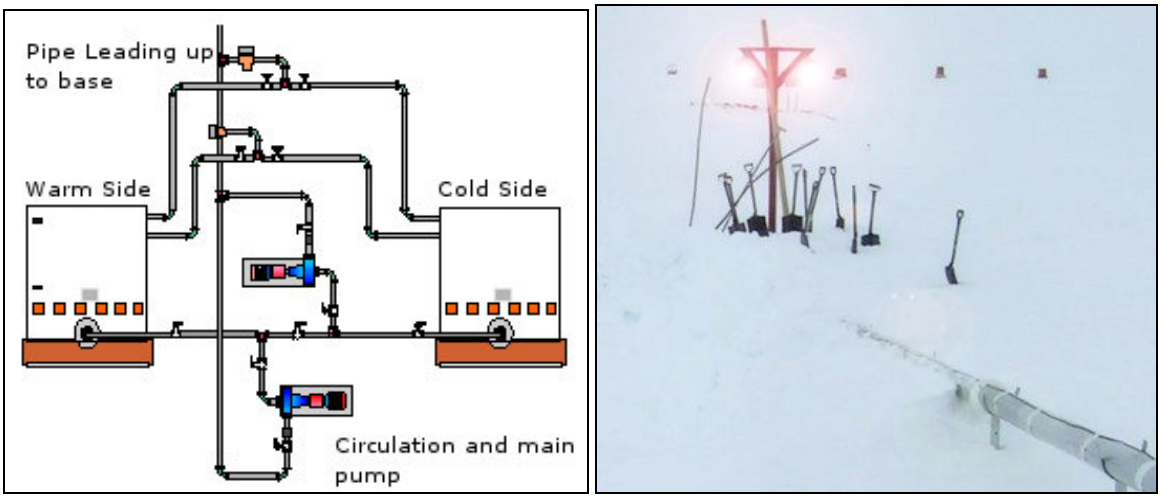

Figure 3.2: The snow smelter (SANAE IV database, 2005)

In comparison to the minimum human water requirement estimated by Gleick (2005) of 50 litres per person per day for the activities of drinking, cooking, washing and sanitation the consumption at SANAE IV is more than 160 % higher. Calculated at 80 litres per person per day this figure is derived from documentation at the base suggesting that peak total daily takeover consumption amounts to 8000 litres (for the entire base of 80 people) while yearly averages of daily consumption range between 600 and 1000, or sometimes 2000 litres per day (for the overwintering team of 10).

Historically there has never been sufficient water available during the takeover periods. From the start of the takeover occupants are limited to showering every alternate day, with periods of total bans and other restrictions often implemented. Although attending continuously to the snow smelter would ensure a sufficient supply of water for all occupants and their activities this commodity does not come without a price. Part of the cost of producing this water is a considerable 95 kW spike in the electricity load at a time when the generators are experiencing difficulty in shedding heat and should ideally be producing less (Cencelli, 2002). An indication of the minimum amount of energy required to meet the average domestic takeover water demand is provided in table 3.1.

Table 3.1: Energy requirements of takeover water demand

PARAMETER	VALUE
Initial snow temperature (°C)	0
Final water temperature (°C)	30
Latent heat of fusion for snow (kJ/kg)	335
Cp of water (kJ/kg. K)	4.190
Average water requirement per person per day (litres)	80
Number of people	80
Minimum amount of energy required to melt the snow (kWh)	819
Equivalent minimum average daily electricity demand (kW)	34

The snow smelter is an energy intensive load where it makes sense to supplement the current demand with solar alternatives. This opportunity for use with solar energy devices is brought about mainly by the size of the load and its match with the availability of sunshine. It is also a thermal load, presenting the possible advantage of capturing energy at higher collector efficiencies than solar electric devices can deliver.

3.2.3 Heating and Ventilation System

A more thorough study of the Heating and Ventilation System (H&V System) is provided in appendix C.1. As explained in section 3.2.2, however, it is evident that the H&V System is 180 degrees "out of phase" with the availability of sunshine. During the summer there is ample heat available from the generators to keep the base warm (in fact it is necessary to cool the base) while conversely the winter periods are characterised by cold inside temperatures. With the obvious lack of sunshine during the winter periods it is evident that the Heating and Ventilation System is not an ideal application for the utilisation of solar energy. Nonetheless, as discussed in the appendix improving the current computer simulation programme of the station could indirectly result in significant savings.

3.2.4 Power Generation System

Central to all the operating systems are three ADE diesel-electric generators (viz. two turbo-charged ADE 442T with a rated power of 260 kW and one turbo-charged inter-cooled 442Ti rated at 320 kW) that output energy to the station's electrical mini-grid at 3-phase, 380 VAC and 50 Hz. These generators are used on a rotational and load-sharing basis with only a single master generator operational while the electricity demand remains below 162 kW. A stand-by generator is always primed and ready for use should the load exceed this limit at which time load sharing occurs between the master and slave generators while the third generator is always left out of operation. This slave generator will only be switched off again when the demand drops to below 140 kW.

A number of corresponding electricity-production and diesel-consumption data points were collected for analysis (see appendix C.6). Consequently, it was found that the electrical efficiency of the generators is 36.4 %, although it is still uncertain what the combined thermal and electrical efficiency is. A useful and improved (from Teetz [2002]) linear regression correlation for the production of energy is given in equation 3.1, where total electrical energy production is calculated from generator diesel consumption using:

$$PP = 3.5652 \cdot FC - 2.5683 \qquad 3.1$$

In this equation PP is power production in kWh, FC is diesel consumption in litres and the regression coefficient for the correlation is 0.99. Using equation 3.1, data from Teetz (2002) and

the fuel consumption data presented in section 3.3, some important parameters are derived and presented in table 3.2.

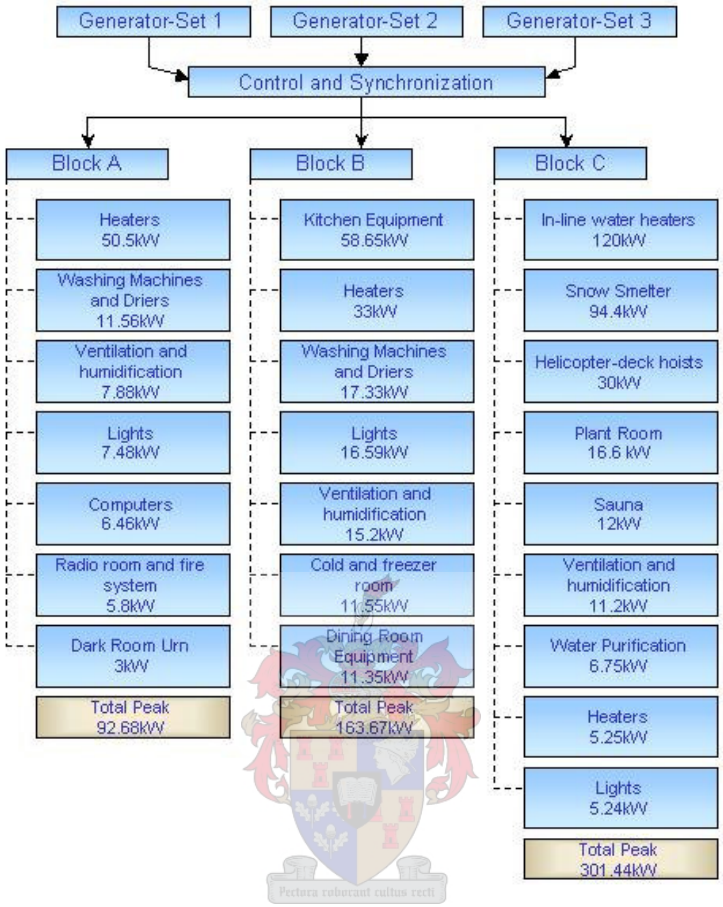

Figure 3.3: Peak power demand breakdown of energy consumers (updated from Teetz, 2002)

Table 3.2: Electricity consumption data, 2005

PARAMETER	TOTAL
Four-Year Average Annual Electricity Consumption (kWh)	1 061 971
Expected Maximum Daily Electricity Consumption (kWh)[Ψ]	5 160
Expected Minimum Daily Electricity Consumption (kWh)[Ψ]	1 440
Average Daily Electricity Consumption (kWh)	2 910
Average Daily Electricity Load (kW)	121.2

[Ψ]Teetz (2002)

Two design aspects of the plant room (which houses the diesel-electric generators) merit further discussion. Firstly, even though one of the three generators is an inter-cooled combustion engine, the fluid used in the intercooler is taken from the Primary Hot Water System (with temperatures often in the region of 90°C). Water supplied from the Domestic Cold Water System would in all

likelihood result in higher engine efficiencies. Secondly, although the station Engineers currently funnel air from a ventilation fan in the plant room (i.e. cold outside air) to the air-intake of the generators, the plant room itself is normally perilously close to its maximum allowable temperature during takeover (Cencelli, 2002). It is suggested that one window in the plant room be replaced with a fan and some flexible tubing so that more cold air can be used where desired during the summer.

Adding renewable electrical energy to the mini-grid of SANAE IV is a feasible option for using solar energy devices. The base energy demand is able to accept large contributions from renewable energy devices without requiring energy storage (refer to figure 3.3), and there exists the associated benefit of reducing the problematic amount of waste heat generated by the diesel-electric generators during the summer months (as discussed in section 3.2.2).

3.2.5 PLC System

The PLC Systems essentially carry control information to and from machinery all around the station. Cencelli (2002) noted that improved operation could be achieved if these PLCs communicated amongst themselves and were not isolated from each other as is currently the case. In particular Cencelli gave the following example. High temperatures inside the station will cause the FCU fans to turn faster (and in so doing blow more cold air into the base) on command of the FCU PLCs. This in turn will result in FCU Water Loop temperatures dropping away from their set-point values. Consequently heat will be added to the FCU Water System (on command of the Main Plant 1 PLC) through in-line heaters that maintain the temperature of the FCU Water System at a pre-determined temperature. This ultimately results in greater diesel consumption, when, in fact, it is not at all necessary. Linking PLCs as recommended could prove to be beneficial. Currently the engineers turn all heating elements off during the takeover period to circumvent many of the difficulties normally encountered during this period.

The electricity consumption of the PLC System is known to be negligibly low. Thus, feeding renewable energy into the power grid is most likely the best method to support this system.

3.2.6 Sewage System

SANAE IV processes all of its own waste. While solid waste is transported back to South Africa the fluids are purified and disposed of locally. Initially the effluent is stored temporarily in two

tanks located inside the links, after which it is pumped to the water purification plant. In total this system draws only about 6.75 kW of electricity, and ss with the PLC System a very flexible solution to supplementing this system's energy needs would be to simply supply the electrical mini-grid with renewable energy.

3.3 Fuel Consumption and Energy Demand

Temperatures at SANAE IV may reach -40°C in the middle of winter. Under these conditions ordinary diesel would freeze, so consequently a Special Antarctic Blend (SAB) is used for powering the energy systems. Table 3.3 below lists some of the properties of this fuel.

Table 3.3: Properties of SAB

PROPERTY	VALUE
Specific Viscosity (N.s/m^2)	1.4
Density (kg/m^3)	800
Sulphur Content (% m/m max)	0.1
Freezing Point (°C)	-65
Lower Heating Value (kWh/L)	9.8

Figure 3.4: Diesel bunker located 400 m from the base (Olivier, 2005)

Details of the annual fuel consumption at SANAE IV are presented below in tables 3.4 and 3.5. The generator diesel consumption is calculated on a four-year average using records from the base (see end of appendix C.5) while the report by Taylor et al. (2002) has been used to obtain the values for the Challenger and Caterpillar D6 Dozer consumption listed in table 3.5. The Skidoo and aeroplane consumption values are rough estimates, and negligibly small amounts of LPG Gas have been omitted from the analysis.

Table 3.4: Average annual fuel consumption by type

SOURCE	AVERAGE ANNUAL FUEL CONSUMPTION (LITRES)
Diesel	347 222
Petrol¥	5 000
Jet-Fuel¥	15 000

¥Estimated values

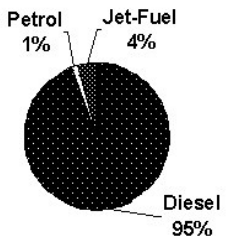

Table 3.5: Average annual fuel consumption by user

SOURCE	AVERAGE ANNUAL FUEL CONSUMPTION (LITRES)
Diesel Generators	297 872
CAT Dozers[Ħ]	21 600
Challengers[Ħ]	27 750
Skidoos[¥]	5 000
Aeroplanes[¥]	15 000

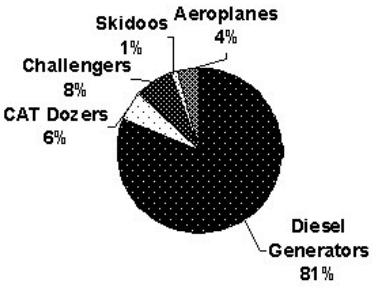

[Ħ]Taylor et al. (2002); [¥]Estimated values

It is evident from table 3.5 that due to the large component of diesel in the breakdown of total fuel consumption any time and effort spent optimising the systems that utilise diesel, specifically the diesel generator system, should result in good returns on investment.

Figure 3.5 is a plot of the average monthly generator diesel consumption at SANAE IV that essentially represents the data illustrated in tables 3.4 and 3.5 temporally. An explanation for the three outlying data points of the year 2004 is provided in the discussion below where some important consumption related issues are also investigated.

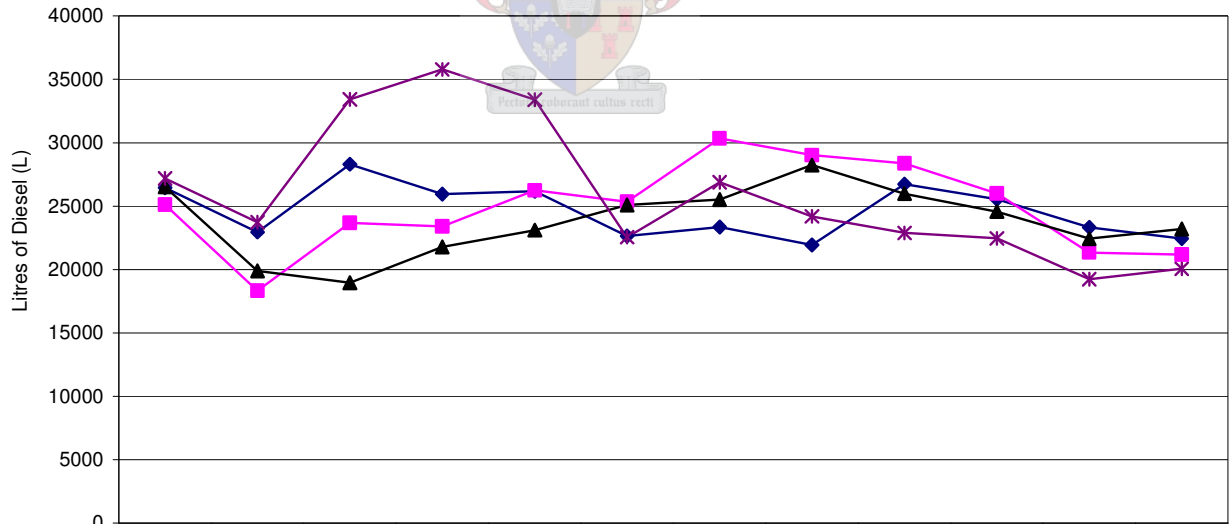

	Jan	Feb	Mar	Apr	May	Jun	Jul	Aug	Sep	Oct	Nov	Dec
2000	26460	22960	28311	25956	26180	22652	23352	21938	26740	25550	23324	22450
2001	25119	18332	23680	23394	26250	25354	30338	29019	28378	26012	21350	21190
2002	26538	19894	18956	21784	23114	25102	25528	28238	25984	24570	22442	23204
2004	27198	23731	33423	35793	33397	22559	26887	24199	22891	22461	19246	20060

Figure 3.5: Generator diesel usage from the years 2000, 2001, 2002 and 2004

Over the last four years of data collection the average generator diesel consumption has amounted to 24 822 litres per month or 297 872 litres annually. The total monthly consumption remains reasonably constant throughout the year even though the number of people inhabiting the base is reduced from approximately 80 to 10 when comparing takeover to overwintering periods. This energy-demand "inertia" is almost certainly due to the fact that sections of the base are not decommissioned as the number of people residing at SANAE IV changes. Consequently the space of the station that requires heating and ventilation essentially remains the same. From figure 3.3 it is conceivable that decommissioning one Block of the base could result in as much as a 20 % reduction in average generator load, and using equation 3.1 it is found that these energy savings would translate into an annual diesel saving of 18 %. This is a reduction in yearly diesel consumption of 61 595 litres. Unfortunately such changes are not possible to implement since, amongst other problems, the hospital, kitchen and plant room are all located in separate blocks. Infrastructure such as pipes and cabling for instance have also not been designed for this purpose.

It is reasoned that the unprecedented fuel demand shown in figure 3.5 during March, April and May of 2004 was due to an increased heating load in the base caused essentially by ambient conditions. As temperatures drop the base "shrinks", an effect of colder weather that can cause cracks to open around windows and where the links join onto the main Blocks for instance. Warm air will now escape and locally temperatures inside these areas of the base will plummet. If these cracks are attended to the smaller ones can be sealed with pliable materials such as silicon and remain closed for a number of seasons. The effort undertaken by the overwintering team during June 2004 to find and seal these holes, but especially to minimise the use of heaters, most likely resulted in a reduced consumption from June 2004 onwards. Teetz (2000) estimates that during very cold weather as much as 32 kW of heat is lost through leakages around doors and other seals, which is over a quarter of the annual average electricity demand. Thus, any measures that can be taken to reduce this type of heat loss are encouraged.

3.3.1 Temporal Variations of Energy Demand

An average profile of the monthly generator diesel consumption is plotted in figure 3.6 not including the three outlying data points of March, April and May 2004. According to this figure the effect of seasonal temperature and weather changes are moderate and probably account for a maximum difference of 5100 litres of diesel consumed per month. This is almost equivalent to

the effect of population variations (that is, comparing the summer months with and without takeover crew), which appear to translate into monthly differences of 5700 litres.

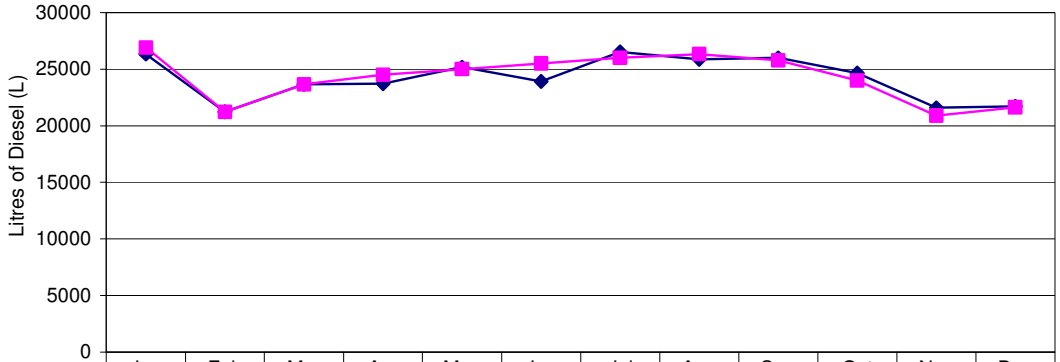

	Jan	Feb	Mar	Apr	May	Jun	Jul	Aug	Sep	Oct	Nov	Dec
4-Year Avg	26329	21229	23649	23711	25181	23917	26526	25849	25998	24648	21591	21726
Suggested Avg	26922.2	21217	23649	24500	25000	25500	26000	26326.4	25790.4	23994.2	20884.4	21634

Figure 3.6: Monthly variations of diesel consumption

Comparatively, daily electricity consumption during the summer takeover period is very erratic. Odd maintenance jobs and other projects are carried out around the base at irregular intervals since the long hours of sunlight allow people to work till late at "night" on tasks that would otherwise be postponed to the following day. The result is a load profile that is prone to large daily variations. Using mean values would therefore result in significant mismatches between the demanded energy and that supplied by renewable resources.

A graph of daily station electrical load during the summer takeover period is presented in figure 3.7 (further details are supplied in appendix C.4). The figure shows a load average of 134.7 kW, which is a value that corresponds well with data in table 3.2 and implies that the measurements used to create this graph was not exceedingly far from normal operating conditions. Note, however, that when comparing the 19-day average profile in this figure to a single day's worth of measurement there is a marked reduction of variability. On average the peaks and troughs of the data used were 28 % above and below their respective means, displaying a significant reduction in load swings.

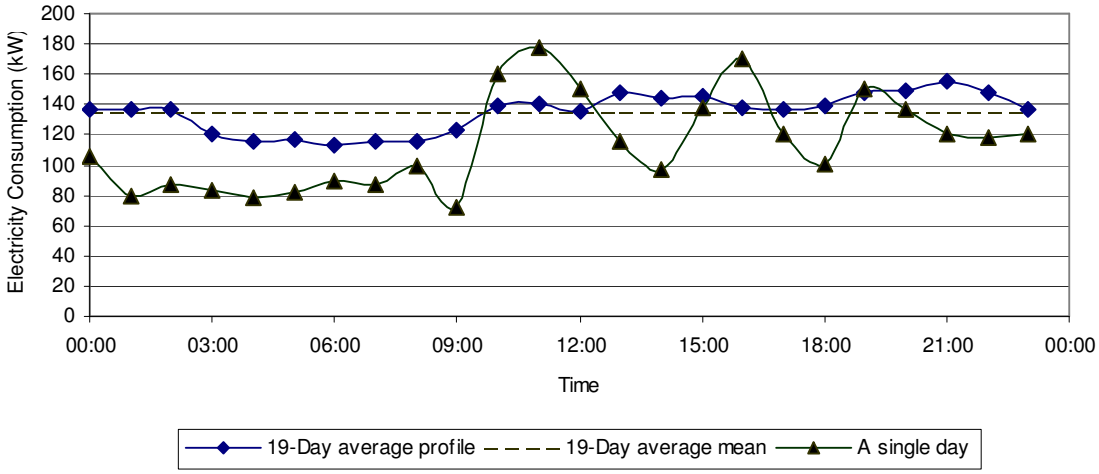

Figure 3.7: Average load profiles

For the purposes of this project the base-load of the station will be used for further investigation (refer to figure 3.8). The implication is that any solar energy supplied to the station will always be met with the expected demand (since this demand should always exceed the base load). Due to the magnitude of the base electrical load at SANAE IV (approximately 60 kW) it is highly unlikely that a renewable energy system will supply beyond this minimum. However, any design that does aim to supply energy somewhere between this minimum and the average value will have to account for those times that available energy will not be utilised.

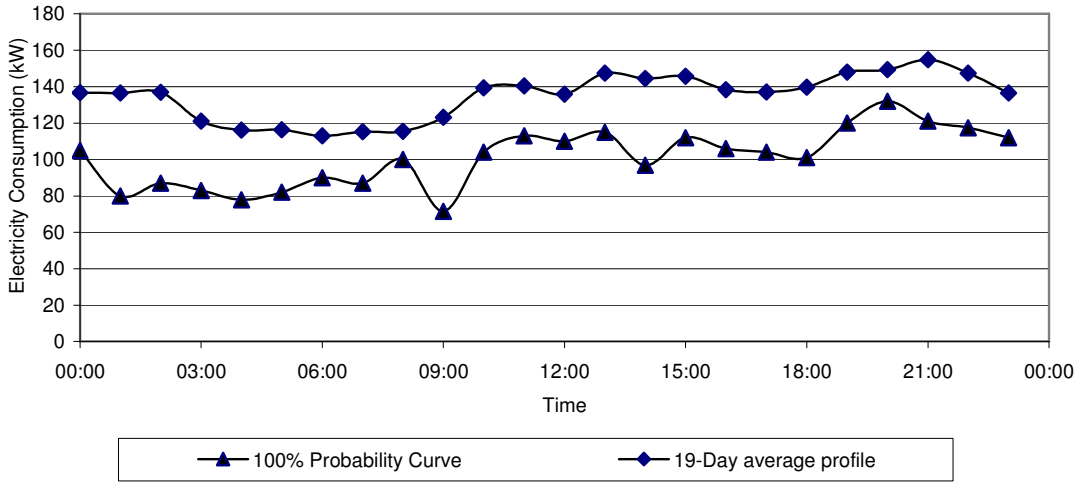

Figure 3.8: Minimum and average generator load profile at SANAE IV

3.4 Summary

The energy systems at SANAE IV have been investigated in chapter 3 by classifying and studying the individual components in detail (refer to figure 3.1). There exists the potential not only to reduce diesel consumption by implementing a solar energy system, but also to increase the station's independence from this fuel source since currently the generators provide 100 % of the station's electrical and thermal needs. The loads best suited to solar energy applications were identified as the SANAE IV electrical mini-grid and snow smelter

Suggestions for possible improvements to some of the station's energy systems were made throughout the chapter. Notably, some of the difficulties with PLC control (c.f. section 3.2.5), plant room temperatures during the summer takeover period (c.f. section 3.2.4), heat losses to the environment (c.f. section 3.3) and the potential for improvements through updating the existing station simulation programme (c.f. section 3.2.3) were discussed.

It is further suggested that an effort is made to implement the changes discussed above before undertaking to install a solar or other renewable energy device. The large amounts of capital and effort that will go into commissioning a renewable energy system at SANAE IV could best be justified if firstly, the station is not wasting or poorly utilising energy, and secondly, all of the most significant shortcomings have already been addressed (i.e. Pareto's Principle).

Chapter 4 – Solar Energy Capturing Solutions

4.1 Introduction

Figure 4.1 below illustrates some of the processes that solar radiation will undergo before it can be used at the station. Since the available solar insolation throughout the year has already been estimated in chapter 2, and the energy demand of South Africa's base was studied in chapter 3, it remains in this chapter only to investigate the characteristics of the individual solar energy devices.

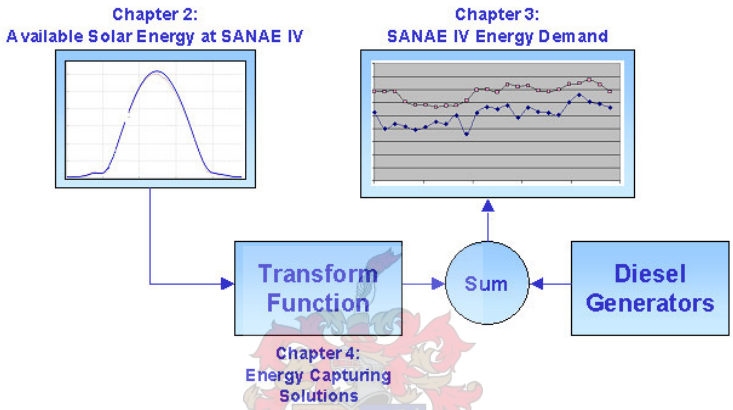

Figure 4.1: SANAE IV solar energy system

Solar-energy devices may be classified as either electrical or thermal collectors. Ordinarily electrical collectors (i.e. photovoltaic or PV panels) are easier to commission, however they also have significantly lower system efficiencies traditionally in the order of 10 %. Conversely solar thermal devices may collect as much as 75 % of the available solar radiation, yet this value is highly dependent on ambient temperatures and radiation levels. The final product of hot water or steam produced by solar thermal devices may also be of little use if there are no thermal loads. In this instance it is therefore necessary to compare the various alternatives of capturing solar energy by considering more carefully the conditions relevant to SANAE IV.

Chapter 4 calculates expected performance characteristics of various solar energy systems at SANAE IV. It begins with a brief overview of the solar energy industry, and then investigates PV and solar thermal systems respectively for the given conditions. The expected efficiencies of recommended photovoltaic and solar thermal collectors have been calculated in sections 4.2.3 and 4.3.1, and the relevant energy savings summarised in tables 4.6 and 4.9. The reader is also referred to appendix D for supplementary information.

4.2 Solar Electric Collectors

4.2.1 Background

Solar electric technology has developed tremendously since its inception in 1954 when it was first used in the space industry yet has never become a large-scale contributor of global energy demand (Yates, 2003). Even though certain photovoltaic cells can harness up to 36 % of the available insolation (produced by Spectrolab, a subsidiary of Boeing) this top-end technology is not currently economically feasible and traditional efficiencies of 11 to 15 % are more common. There is a general misconception concerning solar panels and wind turbines, which suggests that it requires more energy to manufacture these devices than what they will produce in their lifetime (Corkish, 1997). The *energy payback* periods for solar PV panels are normally six years, while their average lifetimes may exceed twenty-five years.

Conventional PV systems are ideally suited for low wattage electrical loads at isolated locations where the cost of laying power-lines far exceeds the cost of newly installed panels. In these instances (e.g. radio repeater stations, borehole water-pumping, ocean buoy lights etc.) the benefits of utilising solar energy far outweigh the associated costs, yet the growing PV market is also being fuelled by installations meant as a means of generating large-scale energy supplies (refer to figure 4.2). Such photovoltaic deployment remains expensive, however, even when considering environmental costs. The PV marker in figure 4.3 for instance is not shown, lying at a distant [0.88 US$/kWh, 22 000 US$/kW] according to Broniki (2001) (also consult Helm [2005]).

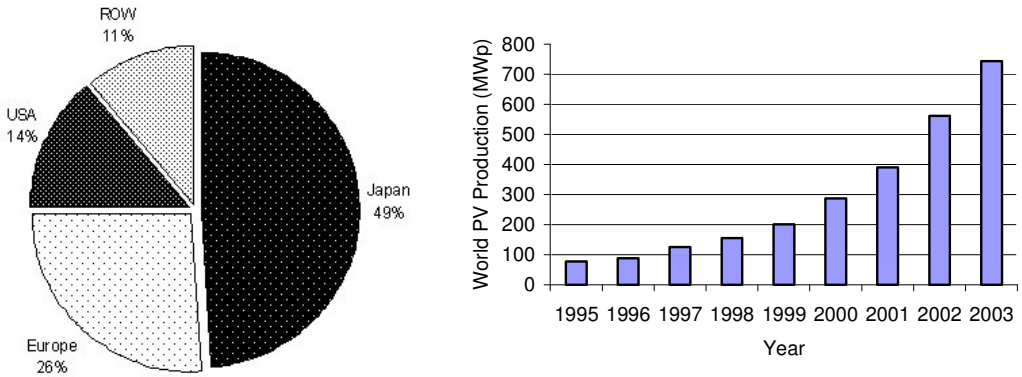

Figure 4.2: Apportioned photovoltaic production in 2003, and historical trend (EPIA, 2005)

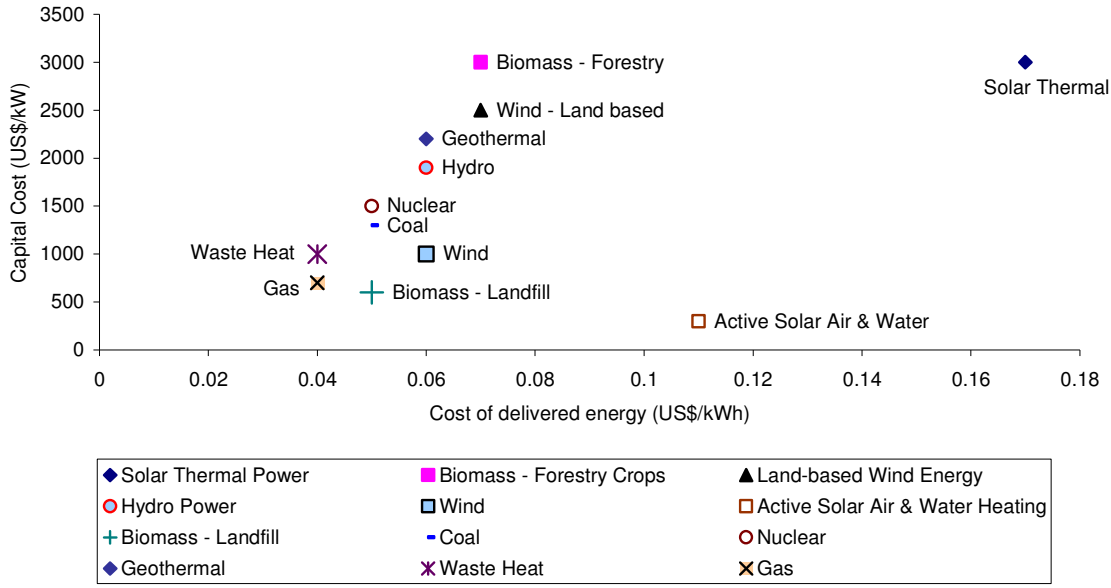

Figure 4.3: Costs of renewable and other energy generation methods (Broniki, 2001)

Nonetheless, photovoltaic panels will play an increasingly important role in power generation. This should occur as greater emphasis is placed on environmental concerns, increased global demand for oil hinders the *availability* of conventional fossil fuels (and not initially the total reserves remaining [Helm, 2005]) and possibly as the costs of PV panels are further reduced by the economy of scale and technological advances as shown in figure 4.4. PV systems offer a clean, reliable and sustainable source of energy that is bound to establish itself in various niches of the energy market.

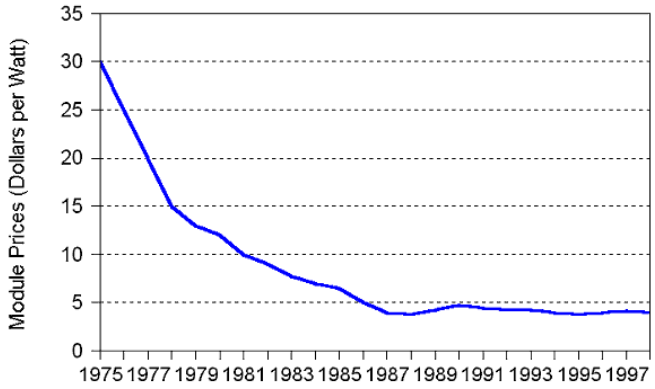

Figure 4.4: Photovoltaic prices from 1975 to 1998 (Maycock, 1999)

4.2.2 Implementing Photovoltaics at SANAE IV

The relatively large 60 kW base-load at SANAE IV (refer to section 3.3.1) allows substantial contributions to be made by a photovoltaic system without incorporating the use of storage devices. Any electrical supply larger than this base-load would require the use of batteries, allowing for greater energy contributions but also increasing the energy generation costs in R/kWh. In view of the economic results given in section 5.8.1 this would make a photovoltaic system completely economically unfeasible for use at SANAE IV. Consequently energy storage devices have not been included in the ensuing investigation of PV systems and consideration has only been given to the solar panels, Maximum Point Power Trackers or MPPTs (that maximise the photovoltaic output at all light conditions) and inverters (that convert direct current [DC] to alternating current [AC]).

A more detailed representation of the suggested photovoltaic system for use at SANAE IV is presented in figure 4.5. It is acceptable to assume that the inverter and MPPT have transform functions that can be modelled by simple constants (efficiencies of above 90 %) and will allow estimates of panel efficiencies to be obtained in section 4.2.3.

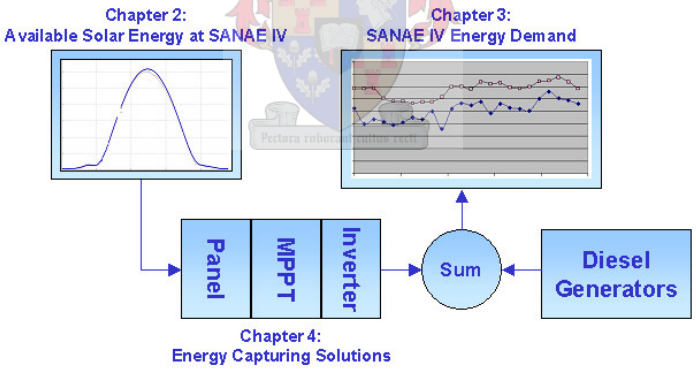

Figure 4.5: SANAE IV solar energy system implementing photovoltaic panels

4.2.3 Expected Efficiencies of Photovoltaic Panels at SANAE IV

South Africa does not currently manufacture any of its own solar panels. All photovoltaic cells are purchased from overseas' manufacturers as either ready for re-sale in the module form, or ready for final assembly. For the purpose of this investigation three local South African companies that stock photovoltaic panels were sourced, the results of which are presented below.

Table 4.1: Local South African suppliers of photovoltaic panels

	KYOSERA	SANYO	SHELL	TOTAL ENERGY
Solardome	✓	✓	✓	×
Solar Power Products	×	×	✓	✓
SINETECH	×	✓	✓	×
Nominal Efficiency	15 %	15 %	13 %	11 %

Commercially available photovoltaic panels are categorised according to the atomic structure of the photovoltaic material, viz. mono-crystalline, poly-crystalline, thin-film etc. (refer to figure 4.6 below). The atomic structure in turn is determined by the manufacturing process of the panel and is consequently very closely related to the final cost. Panel efficiency will generally increase with an increasing order in the atomic structure; yet it will also become harder to manufacture the panel and thus the more expensive it will be to purchase.

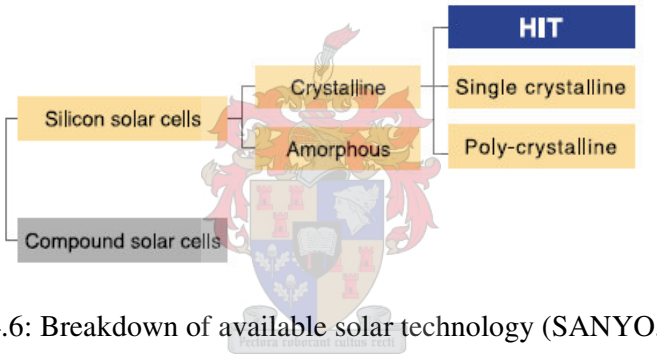

Figure 4.6: Breakdown of available solar technology (SANYO, 2005)

Mono-crystalline photovoltaic cells are generally slightly more efficient than their poly-crystalline counterparts (15-18 % and 10-14 % respectively), while amorphous cell efficiencies range between 6-7 % and exhibit shorter lifetimes (Yates, 2003). Amorphous cells are much cheaper to manufacture, yet for the reasons given above they are not commonly utilised in large systems except when initial cost is an inhibiting factor. In figure 4.6 the relatively new technology of Heterojunction with Intrinsic Thin layer (HIT) SANYO panels is also specified which show efficiencies and costs very similar to the mono-crystalline cells.

JANUARY EFFICIENCY ESTIMATES USING MANUFACTURER SPECIFICATIONS

Nominal efficiencies are often provided for photovoltaic panels by manufacturers, specified at the Standard Testing Conditions (STC) of 1000 W/m^2 illumination and a cell temperature 25°C. Using the widely accepted temperature dependence of 0.5 %/°C (Yates, 2003) for photovoltaic

panels and the average measured PV cell temperature at SANAE IV during January of 1°C (refer to section 2.3.1) the expected efficiency of a photovoltaic panel at SANAE IV can be calculated using:

$$\eta_{total} = \left(\frac{P_o (1 + \eta_{temp} \times [T_{STC} - T_{cell}])}{P_i} \right) \times \eta_{losses} \qquad 4.1$$

Where P_i is the available solar radiation (W), P_o is the output power at the nominal maximum power point (W), η_{temp} is specified as 0.5 %/°C, T is temperature (at STC and actual cell operating conditions respectively, in °C) and η_{losses} is the combined efficiency of the ancillary equipment (estimated as 93 % for a MPPT and 96 % for an inverter). Some results for the standard PV collectors defined in section 4.2.3 have been presented in table 4.2.

Table 4.2: Expected January efficiencies at ambient SANAE IV conditions

PV TYPE	CELL TEMP (°C)	NOMINAL EFFICIENCY (%)	TOTAL EFFICENCY (%)	TILTED YIELD (kWh/m^2.day)
Mono-crystalline	1	15	15.12	1.22
Poly-crystalline	1	11-14	11.08-14.11	0.85-1.14
Thin film	1	6-7	6.04-7.06	0.49-0.57

JANUARY EFFICIENCY ESTIMATES USING HEAT TRANSFER CALCULATIONS

A second method of estimating the efficiencies at a given set of ambient conditions is presented by Yates (2003). Here a heat transfer analysis is carried out on a solar panel assuming that the thermal characteristics of the panel are known (such as thermal resistance). Although this method is rigorous the values used in this investigation are broad averages and, consequently, calculated answers will differ somewhat from values of specific PV panels. The process is most useful if the true properties (that are measurable although unfortunately not often specified by manufacturers) of the panel in question are known. The equation used is:

$$P_c = \frac{P_I (1-\alpha)(1 - \mu_T R_T (1-\alpha) P_I)}{1/\eta_N - \mu_T R_T (1-\alpha) P_I} - P_{losses} \qquad 4.2$$

Where P_c is the collected radiation (W/m^2), P_I is the incident radiation (W/m^2), α is the reflectivity of the collector cover, μ_T is the percentage decrease in efficiency with increased temperature (%/°C), η_N is the nominal efficiency and R_T is the thermal resistance (K.m^2/W). The power losses P_{losses} are assumed to be due to a charge controller (viz. a MPPT and inverter combined) operating at an average efficiency of 90 %. Hence, using standard values of α = 0.06, μ_T = 0.004, R_T = 1.95 and η_N given individually in table 4.3 total efficiencies and estimated yields can be provided. The results are also shown in table 4.3.

Table 4.3: Heat transfer analysis of photovoltaic panels

PV TYPE	NOMINAL EFFICIENCY (%)	TOTAL EFFICIENCY (%)	TILTED YIELD (kWh/m^2.day)
Mono-crystalline	15	12.69	1.02
Poly-crystalline	11-14	9.30-11.84	0.75-0.96
Thin film	6-7	5.07-5.92	0.41-0.48

JANUARY EFFICIENCY ESTIMATES USING RETSCREEN

A third technique used to compare the efficiencies of photovoltaic panels is the methodology presented by RETScreen (RETScreen, 2005). This organisation, which is supported by the United Nations Environment Programme (UNEP), NASA and the Global Environment Facility (GEF), *"…seeks to build the capacity of planners, decision-makers and industry to implement renewable energy and energy efficiency projects"*, and suggests that the procedure shown in figure 4.7 be used to determine efficiencies of PV systems at non-standard conditions.

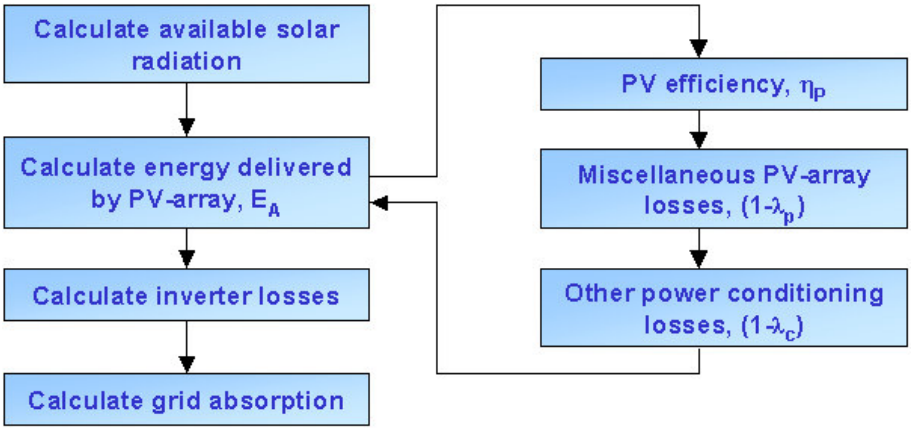

Figure 4.7: RETScreen On-Grid Energy Model flowchart

Referring to figure 4.7 the following associated equations and information are provided by RETScreen:

$$\eta_p = \eta_r \cdot (1 - \beta_p (T_c - T_r)) \qquad 4.3$$

$$T_c = T_a + (219 + 832 \cdot K_t)\left(\frac{NOCT - 20}{800}\right) \qquad 4.4$$

$$E_A = E_p \cdot (1 - \lambda_p)(1 - \lambda_c) \qquad 4.5$$

$$E_p = A \cdot \eta_p \cdot H_t \qquad 4.6$$

$$\eta_A = \frac{E_A}{A \cdot H_t} \qquad 4.7$$

Here η_A is the total array efficiency and η_p is the efficiency of a single panel. The symbol A is the surface area of the array (m^2), H_t is the solar insolation at the specified location (kWh/m^2), E_A is the array energy available for use (kWh/m^2), E_p is the energy delivered by the PV array (kWh), λ_p are the *"miscellaneous PV array losses"* (in this instance equal to 0), λ_c are the *"other power conditioning losses"* (estimated at 0.07 for the MPPT), K_t is the clearness index (estimated as 0.65 for January [refer to section 2.3.3]), $NOCT$ is the Nominal Operating Cell Temperature (°C), T_a is the ambient temperature (°C), T_c is the average module temperature (°C), T_r is the reference temperature (25°C), β_p is the temperature coefficient of module efficiency (%/°C), and η_r is the PV module efficiency at reference room temperature. In this instance the inverter losses are assumed to be 4 % and the electrical mini-grid absorption losses are taken to be equal to 0 %.

Table 4.4: PV module characteristics for standard technologies (RETScreen, 2005)

PV MODULE TYPE	η_r (%)	$NOCT$ (°C)	β_p (%/°C)
Mono-Si	13.0	45	0.40
Poly-Si	11.0	45	0.40
a-Si	5.0	50	0.11
CdTe	7.0	46	0.24
CIS	7.5	47	0.46

Table 4.5: RETScreen analysis of PV panels (using equations 4.3 – 4.7 and inverter efficiencies)

PHOTOVOLTAIC CELL	NOMINAL EFFICIENCY (%)	TOTAL EFFICIENCY (%)	TILTED YIELD (kWh/m^2.day)
Mono-crystalline	15	13.81	1.11
Poly-crystalline	11-14	10.13-12.89	0.82-1.04
Thin film	6-7	5.53-6.45	0.45-0.52

COMPARISON OF EFFICIENCY ESTIMATES

The methodology presented by RETScreen will be used as the benchmark of further investigation. Using equations 4.3 to 4.7 the annual averages of the expected amounts of energy that could be captured with solar electric devices have been calculated, and are presented in table 4.6.

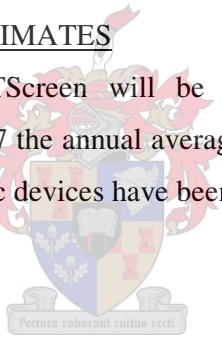

Table 4.6: Expected efficiencies and daily energy capture from different PV materials

			MONO-CRYSTALLINE		POLY-CRYSTALLINE		THIN FILM	
	Average Temp	***kWh/m²***	*Average*	*kWh/m²*	*Average*	*kWh/m²*	*Average*	*kWh/m²*
	(°C)	***Available***	*Efficiency*	*Captured*	*Efficiency*	*Captured*	*Efficiency*	*Captured*
January	*-6.60*	*8.05*	13.81	1.11	11.51	0.93	5.99	0.48
February	*-10.30*	*6.11*	14.01	0.86	11.68	0.71	6.07	0.37
March	*-14.90*	*3.51*	14.26	0.50	11.88	0.42	6.18	0.22
April	*-18.20*	*2.54*	14.43	0.37	12.03	0.31	6.25	0.16
May	*-19.50*	*0.01*	14.50	0.00	12.09	0.00	6.29	0.00
June	*-20.10*	*0.00*	14.54	0.00	12.11	0.00	6.30	0.00
July	*-23.10*	*0.00*	14.70	0.00	12.25	0.00	6.37	0.00
August	*-22.90*	*1.24*	14.69	0.18	12.24	0.15	6.36	0.08
September	*-22.90*	*3.23*	14.69	0.47	12.24	0.40	6.36	0.21
October	*-18.20*	*6.86*	14.43	0.99	12.03	0.83	6.25	0.43
November	*-12.80*	*7.14*	14.14	1.01	11.79	0.84	6.13	0.44
December	*-7.10*	*8.30*	13.84	1.15	11.53	0.96	6.00	0.50
Average	***-16.40***	***3.92***	***14.34***	***0.56***	***11.95***	***0.47***	***6.21***	***0.24***

It should be noted that research conducted by the AAD (which has installed two solar energy systems at stations on the continent) established that tilted collectors, as opposed to tracking collectors, are the most economical solution for harnessing solar energy in Antarctica (AAD, 2005). The AAD determined that collectors tilted towards the sun collected greater amounts of solar energy justifiable in view of the added cost, however the same was not true for tracking collectors.

4.3 Solar Thermal Collectors

The types of solar thermal systems that could potentially be implemented at SANAE IV range from the standard flat-plate collectors to high-temperature concentrating devices. As an instructive tool for evaluating which solar thermal collector might best be suited to the conditions at the South African station a list of all the energy systems currently in use at the various stations in Antarctica has been given in table 4.7 (COMNAP, 2005). This table will be considered shortly below.

Table 4.7: Currently installed renewable energy systems in Antarctica (COMNAP, 2005)

NATION	STATION	TYPE	SIZE	kWh/YEAR
Argentina	Belagrano I	Wind	Not known	Not known
Argentina	Esperanza	Wind	Not known	Not known
Argentina	Primavera	Wind	Not known	Not known
Argentina	San Martin	Wind	Not known	Not known
Australia	***Davis***	***Flat Plate Collector***	***12m²***	***Not known***
Australia	*Law Base*	*Photovoltaics*	*0.4m²*	*Not known*
Australia	Casey	Wind	Not known	10780 kWh
Australia	Mawson	Wind	2	1288342 kWh
Germany	Neumeyer	Wind	1	Not known
India	Maitri	Wind	Not known	Not known
Japan	*Syowa*	*Photovoltaics*	*323m²*	*40060 kWh*
Japan	Syowa	Wind	Not known	22400 kWh
Spain	*Juan Carlos I*	*Photovoltaics*	*27m²*	*Not known*
Spain	Juan Carlos I	Wind	3	3641 kWh
Sweden	*Wasa*	*Photovoltaics*	*20.6m²*	*Not known*
USA	*McMurdo*	*Photovoltaics*	*236m²*	*2390 kWh*
USA	McMurdo	Wind	Not known	8930 kWh

From table 4.7 it is evident that by far the most popular renewable energy systems currently installed are wind turbines since eleven out of the seventeen stations cited above are currently using this resource (viz. Argentina, Australia, Germany, India, Japan, Spain and the USA). Next to wind the solar-electric devices are the second most popular energy devices, with Japan and America both having commissioned large photovoltaic plants (in excess of 300 and 200 square-meters respectively). The solar energy systems of Australia, Spain and Sweden are much more moderately sized however. There is also a single flat-plate solar collector installed at Australia's Davis station which *"…perform*[ed] *very satisfactorily"*, and could produce hot water at a cost *"…comparable to, if not lower than diesel"*, (Antarctic Renewable Energy, 2005).

Since Antarctica is widely known as the windiest place on Earth it is not surprising that a fair number of wind turbines have been installed on the continent. These devices can sometimes operate competitively with local and conventional electricity generation methods (refer to figure 4.3), while comparatively electricity generation in Antarctica is subject to the added difficulty of transporting fuel to remote stations. Wind is also available throughout the year and not subject to

large seasonal variations of availability providing this resource with a fair competitive edge over solar energy.

The usefulness of solar energy in Antarctica seems questionable in comparison since only for a short period in the summer is there an abundance of solar radiation, and because on average insolation rates are low (3.92 kWh/m^2.day annual average insolation at SANAE IV). There are currently only two large PV installations in Antarctica (out of 17 installed renewable energy systems) aimed at significant displacement of diesel. These systems are also never found preceding the installation of a wind turbine. Nonetheless, the difficulty and cost involved in transporting fuel to stations should make this energy generation method desirable in some instances.

Yet, from table 4.7 the potential for utilising solar thermal devices before wind turbines or photovoltaic panels seems doubtful. The following section presents an investigation of how solar thermal devices are expected to perform at SANAE IV, and the energy savings that should be generated from such systems.

4.3.1 Selection of a Solar Thermal Collector

A number of criteria were considered in the selection of a solar thermal device. For instance, from the investigation in chapter 2 it was found that the diffuse fraction of radiation incident at SANAE IV is extremely high. In fact there is only 2.04 kWh/m^2.day of beam radiation available on average throughout the year to a non-tracking optimally tilted surface in comparison to the 3.92 kWh/m^2.day of global insolation available to flat-plate collectors. Thus more than half of the average global radiation is diffuse. Ambient temperatures were also considered, and it should be noted that operating temperatures of flat-plate solar thermal collectors will be far lower than concentrating devices; an important consideration for conditions where energy losses to the cold surroundings are already high even at relatively low process temperatures. The marked difficulties in installing the *"…complicated drive system* …[with] *high energy requirement"* (Tamm, 2005) required for concentrating systems are also a concern, especially since extremely strong winds (often gusting at more than 120 km/hr) common at SANAE IV could most likely damage such a system and probably also cause misalignments and vibrations that resulted in the noticeable efficiency reductions at Eskom's Stirling Dish test facility in South Africa (van Heerden, 2003).

Therefore a simple and convenient solar thermal device is the flat-plate solar collector. This collector will not only operate at lower process temperatures, but will also be: less susceptible to wind related efficiency losses, more resistant to wind related damage, utilise both the beam and diffuse components of radiation, allow for easier maintenance, and is readily available locally.

Figure 4.8: The solar thermal system installed at Australia's Davis station (AAD, 2005)

FLAT PLATE SOLAR COLLECTORS

Three products sourced from companies in South Africa and the United States of America were investigated to estimate probable efficiencies of solar thermal collectors at SANAE IV. Solahart, an Australian based company, manufactures two of these three products (the Bt and Mt collectors) and is not only a supplier to South Africa but also currently the only company to have installed a solar thermal product in Antarctica (see figures 4.8 and 4.14). The second company, Thermomax, is a manufacturer of solar thermal vacuum tube collectors and will be used for comparative purposes. The products manufactured by Thermomax are not readily available in South Africa and require packaging and shipment from overseas.

The performance characteristics of the Solahart and Thermomax products are presented in figure 4.9 (also refer to appendix D.3 to D.5), while figure 4.10 illustrates how the suggested solar thermal system will be incorporated into the current diesel only electricity generation system.

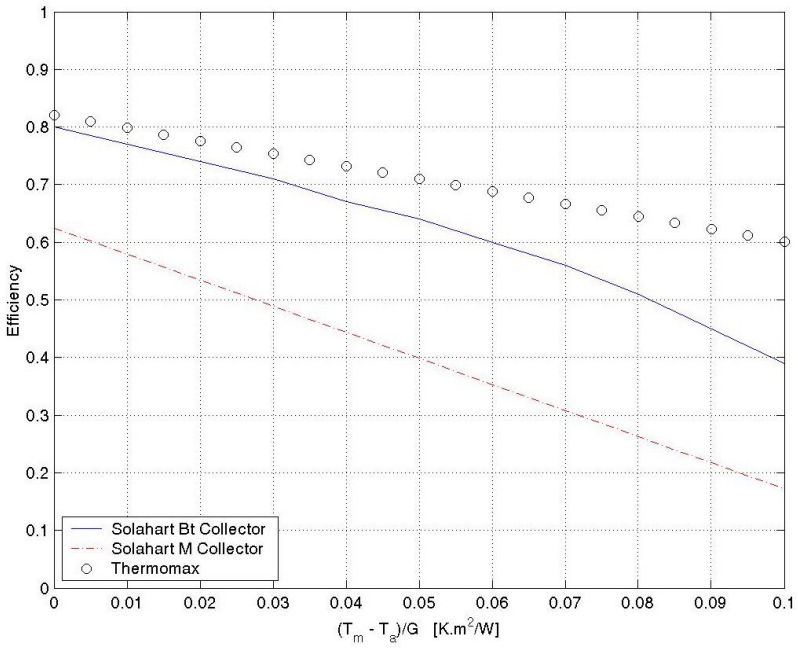

Figure 4.9: Efficiencies of three available flat-plate solar thermal collectors

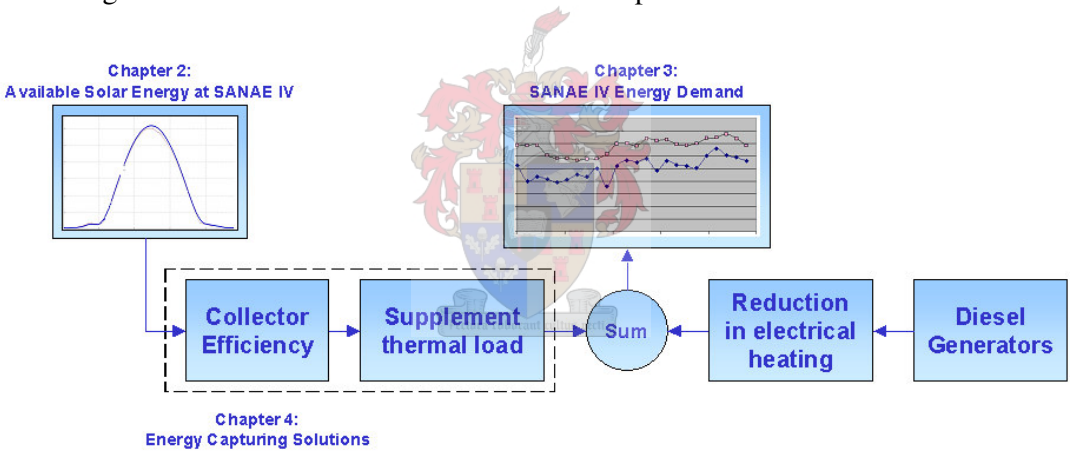

Figure 4.10: SANAE IV solar energy system implementing solar thermal collectors

Of all the thermal loads at SANAE IV the snow smelter was identified in chapter 3 as the most appropriate for supplementing with solar energy. Mainly this was due to the fact that summer H&V loads at the station are negative (implying that the base requires cooling and no contributions from a solar thermal device) and because the Primary Hot Water System already plays an important role in cooling the generators during the summer (and therefore has no use for excess heat, refer to chapter 3). The most significant remaining thermal load, the snow smelter, is not only the cause of excessive generator power consumption, but also a good load to supplement in order to generate greater amounts of fresh-water during the summer takeover period (as explained in section 3.2.2).

To assist in this investigation a simulation programme of the snow smelter operation was created with Matlab V6.1 code using the already existent PLC logic (see appendix D.2 to D.6) and the efficiency curves of the products presented in figure 4.9. In this manner various parameters within the system could be altered (such as collector tilt angle, insolation rate, overall heat transfer coefficient of the heat exchanger, size of the thermal store etc.) and the contribution of the solar thermal collector was analysed.

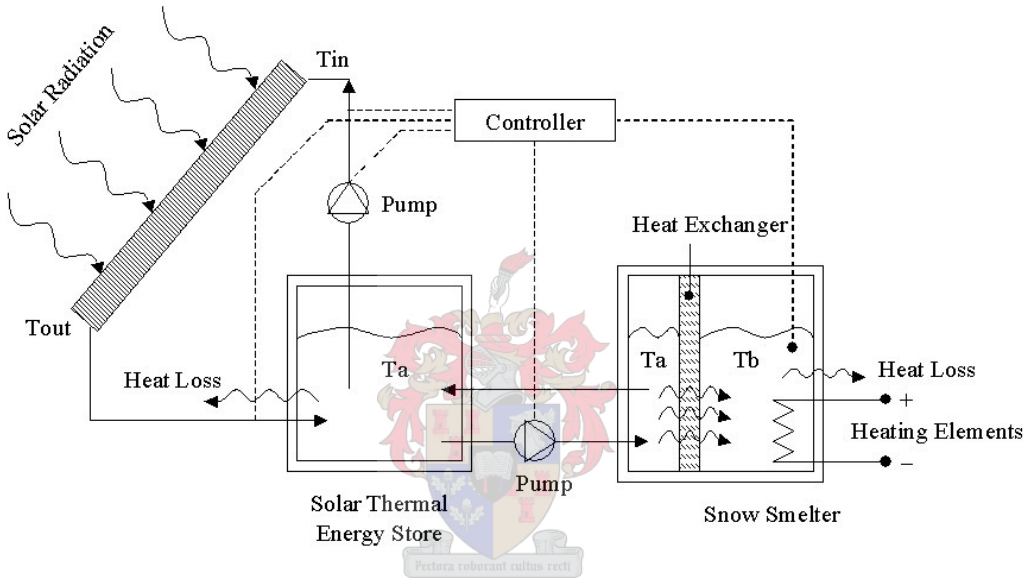

Figure 4.11: Physical connection of solar thermal collector to snow smelter system

Figure 4.11 shows the recommended split solar system, with a solar thermal energy storage tank added to the current snow smelter set-up. The fluid circulating through the thermal energy store and the collector contains anti-freeze (isolated from the main snow smelter), and the collected energy is transferred to the snow smelter's cold-side through a heat exchanger. Pumps are controlled by a PLC and activated such as to prevent either the transfer of heat to the environment through the collector or the transfer of heat from the snow smelter to the energy store. The programme's logic and sample results are presented in figures 4.12 and 4.13, and estimated savings for the Bt collector have been tabulated in tables 4.8 and 4.9. Refer to appendix D.7 for values relating to the Mt and Thermomax collectors.

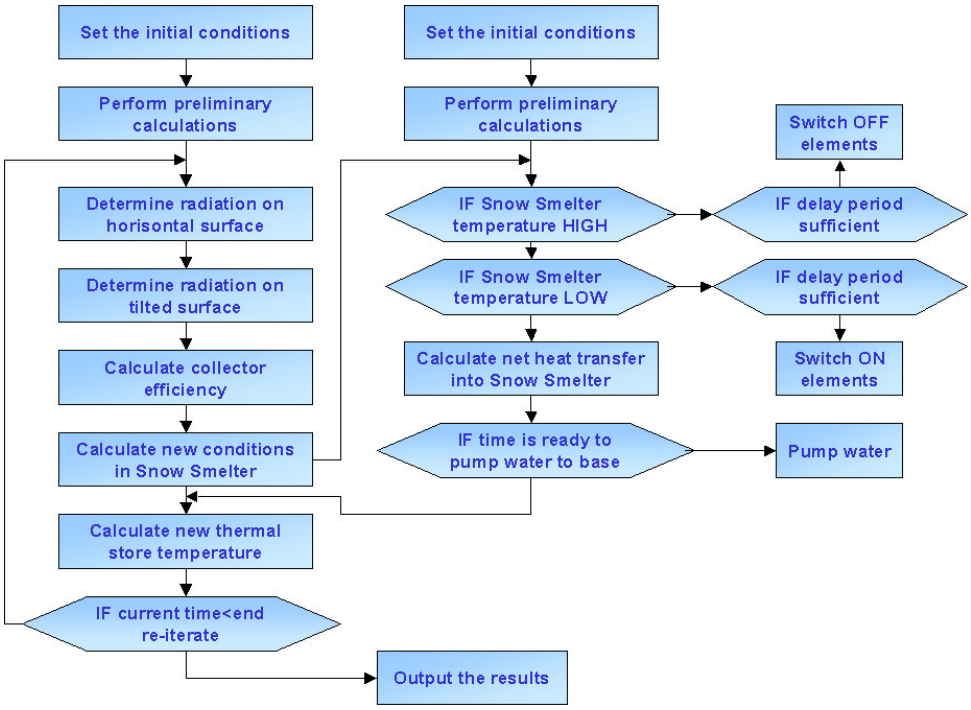

Figure 4.12: Basic logic behind snow smelter simulation programme

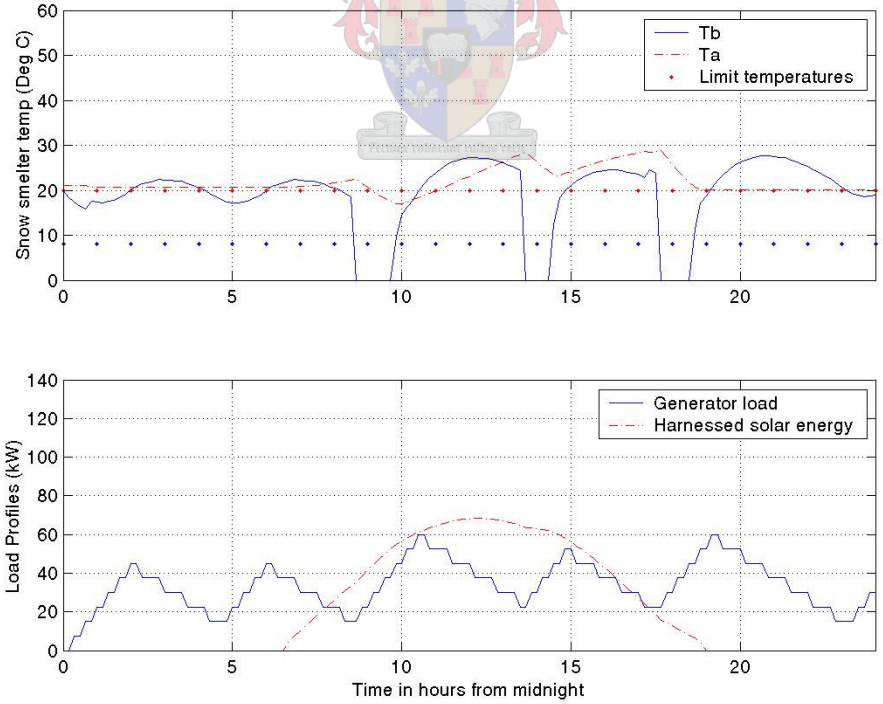

Figure 4.13: Sample results from snow smelter simulation programme

Table 4.8: Estimated daily load for snow smelter with and without Bt collector system

ESTIMATED DAILY GENERATOR LOAD FROM SNOW SMELTER (kWh/day)																		
Collector Size	NONE (0 PANELS)						MEDIUM (24 PANELS)						LARGE (72 PANELS)					
Tresponse (min)	*30*	*10*	*30*	*10*	*30*	*10*	*30*	*10*	*30*	*10*	*30*	*10*	*30*	*10*	*30*	*10*	*30*	*10*
Tmax (°C)	*30*	*30*	*20*	*20*	*10*	*10*	*30*	*30*	*20*	*20*	*10*	*10*	*30*	*30*	*20*	*20*	*10*	*10*
January	1715	1578	1485	1313	1318	1069	1628	1428	1388	1153	1209	891	1464	1294	1129	906	916	554
February	1715	1578	1485	1313	1318	1069	1655	1479	1415	1204	1249	951	1533	1361	1267	1205	1003	686
March	1315	1157	1115	865	663	569	1280	1106	856	759	530	429	1135	1041	682	657	250	296
April	1315	1157	1115	865	663	569	1303	1140	939	770	530	447	1195	1097	853	714	374	337
May	1315	1157	1115	865	663	569	1315	1157	1115	865	663	569	1315	1157	1115	865	663	569
June	1315	1157	1115	865	663	569	1315	1157	1115	865	663	569	1315	1157	1115	865	663	569
July	1315	1157	1115	865	663	569	1315	1157	1115	865	663	569	1315	1157	1115	865	663	569
August	1315	1157	1115	865	663	569	1315	1157	1115	865	663	569	1315	1157	1115	865	663	569
September	1315	1157	1115	865	663	569	1303	1140	939	770	530	447	1195	1097	853	714	374	337
October	1315	1157	1115	865	663	569	1280	1106	856	759	530	429	1135	1041	682	657	250	296
November	1315	1157	1115	865	663	569	1024	1003	677	623	354	281	788	769	380	359	77	32
December	1315	1157	1115	865	663	569	987	956	595	574	296	260	683	610	283	250	28	15

Table 4.9: Energy savings generated at snow smelter from Bt collector system

DAILY SAVINGS (kWh)												
Collector Size	MEDIUM (24 PANELS)						LARGE (72 PANELS)					
Tresponse (min)	*30*	*10*	*30*	*10*	*30*	*10*	*30*	*10*	*30*	*10*	*30*	*10*
Tmax (°C)	*30*	*30*	*20*	*20*	*10*	*10*	*30*	*30*	*20*	*20*	*10*	*10*
January	87	150	97	160	109	178	251	284	356	407	402	515
February	60	99	70	109	69	118	182	217	218	108	315	383
March	35	51	259	106	133	140	180	116	433	208	413	273
April	12	17	176	95	133	122	120	60	262	151	289	232
May	0	0	0	0	0	0	0	0	0	0	0	0
June	0	0	0	0	0	0	0	0	0	0	0	0
July	0	0	0	0	0	0	0	0	0	0	0	0
August	0	0	0	0	0	0	0	0	0	0	0	0
September	12	17	176	95	133	122	180	116	433	208	413	273
October	35	51	259	106	133	140	120	60	262	151	289	232
November	291	154	438	242	309	288	527	388	735	506	586	537
December	328	201	520	291	367	309	632	547	832	615	635	554
Average	*72*	*62*	*166*	*100*	*116*	*118*	*183*	*149*	*294*	*196*	*279*	*250*

The following points should be noted concerning tables 4.8 and 4.9. In these tables *Tmax* is the temperature at which the heating elements in the storage tank of the snow smelter are switched off (i.e. the design temperature of water in the snow smelter). The value *Tresponse* is the enforced delay time programmed into the PLC between switching heating elements off (one at a time and only after *Tmax* is reached) in minutes. The standard design values for these parameters are; *Tmax* = 30ºC and *Tresponse* = 30 minutes. Furthermore, the savings listed in table 4.9 have all been calculated with respect to each corresponding "No-Collector" column in table 4.8. In

other words, savings indicate the effect of the collector system only, and not the savings achieved due to any adjustments of the snow smelter PLC logic.

The data shown in the tables above are for the Solahart Bt-Collector. The Thermomax vacuum-tube collectors slightly outperformed the Bt collectors on a cost basis (refer to appendix D.7 and table D.6), however the Bt-Collector was preferred due to its availability in South Africa. The Bt's reliability (Solahart has proven this technology in cold weather on a number of occasions), and ruggedness also played a role in selecting this device.

Because snow has a latency period while melting during which the addition of energy does not raise the temperature it is unlikely that a solar thermal collector system will be able to remove the peaks from the load profile. All heating elements in the snow smelter will switch on during filling, even if only for a short period, due to the sudden drop in water temperature. Of course the addition of solar energy would reduce the total load on the generators. Hence, only total daily energy consumption is reduced, and not the peak or maximum demands. In addition it should be noted that the simulation programme used to estimate the savings in table 4.9 could not account for local heating phenomenon around the elements that play an important role in calculating the actual, as opposed to theoretical energy consumption of the snow smelter. For instance, the fluid around the heating elements might measure 30 ºC (as well as around the PLC temperature sensor), while much of the rest of the snow smelter is still filled with snow.

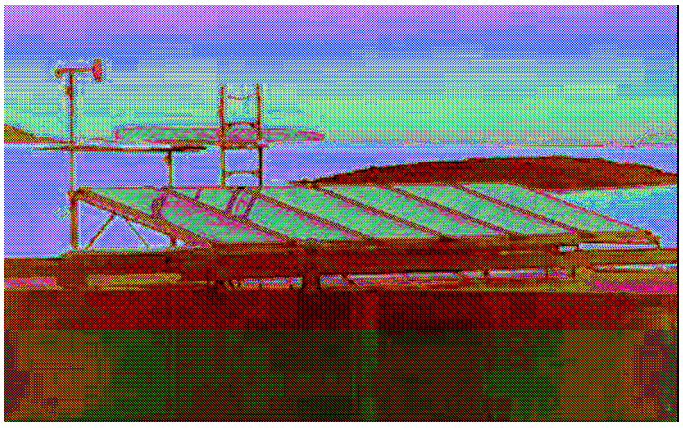

Figure 4.14: The Solahart PowerPack system installed at the Davis Station (Solahart, 2005)

4.4 Summary

In this chapter approximations of potential energy savings have been made using the expected amounts of insolation (studied in chapter 2), the nature of energy loads at SANAE IV (investigated in chapter 3) and estimates of solar energy system characteristics (calculated in chapter 4) as shown in figure 4.1. These approximations of energy savings pertain particularly to application at the station's electrical mini-grid and snow smelter as described above. It was found that photovoltaic and solar thermal collectors both present good opportunities for utilising solar energy at SANAE IV.

Notably, commissioning a PV system for use with the SANAE IV electrical mini-grid could be accomplished without utilising expensive storage equipment. The relatively large base demand of the station (60 kW) would allow a substantial system to be designed around feeding energy directly into the electrical mini-grid, which, in view of the economic results obtained in chapter 5, is very expedient.

It was found from the methodology suggested by RETScreen that mono-crystalline modules could capture solar radiation at an average efficiency of approximately 14 % (from collector to energy consumer), while it was noted from the AAD that installing tracking mechanisms is not advisable. Annual power generation savings from tilted collectors could therefore potentially reach 200 kWh/m^2.year (calculated using the information in tables 4.6 and 2.3).

Although used less readily in Antarctica than devices such as wind turbines and PV panels, solar thermal collectors presented a unique opportunity for application at SANAE IV's snow smelter. Known characteristics of three flat-plate products were used in a snow smelter simulation programme, and results from each were tabulated and compared in table 4.9 and appendix D.7. It is likely that more than 420 kWh/m^2.year could be available in thermal energy from such a system, and that further energy savings from the snow smelter could be realised by adjusting the PLC logic of this device (i.e. the set-point temperatures and pre-set delays).

Chapter 5 – Economic Analysis

5.1 Introduction

To a large extent the economic evaluation of the suggested solar thermal and PV systems is the main criteria upon which the feasibility of utilising solar energy at SANAE IV will be determined. Therefore the effect of less tangible system changes, such as those in pollution and emissions, must also be included in the study to properly account for all costs and savings in monetary terms. These *externalities* have previously been investigated and quantified for conditions similar to those at SANAE IV in research projects such as the one by Isherwood et al. (1999), and form part of this analysis.

The basic methodology of the ensuing economic evaluation is presented in the report created by the South African Department of Environmental Affairs and Tourism entitled "*Cost Benefit Analysis*" (DEAT, 2005). The report stipulates the manner in which projects that fall under the administration of DEAT should be evaluated, and as a result the ensuing economic analysis has been constructed largely from the information provided in this document. However, a number of quantitative values used in the investigation have also been obtained from other resources. Two particularly relevant publications in this regard were the articles entitled "*Towards New Energy Systems for Antarctic Stations*" authored by Guichard (1994) and the "*Technical and Economic Evaluation of the Utilisation of Wind Energy at the SANAE IV Base in Antarctica*" authored by Teetz (2002).

Significant difficulties were encountered in forecasting fuel prices for the future, and as a result a sensitivity analysis was conducted using low, medium and high price projections at the end of this chapter. In this regard information provided by Helm (2005) in "*The Assessment: The New Energy Paradigm*" and by the International Energy Agency (IEA) proved to be particularly helpful resources.

In the ensuing economic feasibility study of chapter 5 a short summary of all the project costs involved are first provided in sections 5.2 to 5.7. Following this results for the solar PV system and solar thermal systems are calculated in sections 5.8.1 and 5.8.2 respectively and lastly table 5.8 provides estimates of the financial feasibility criteria employing assumptions other than those used up to that point. Sample calculations have been presented in Appendix E.

5.2 Basic Investment Costs

The basic investment costs of the proposed energy system include all the expenditures that are required to commission the project, excluding the ancillary costs listed in section 5.3. These costs are varied and numerous, and can be categorised as follows (Teetz, 2002):

1. Feasibility study
    a. Site investigation
    b. Solar energy resource assessment
2. Development
    a. Permits and approval
    b. Project management
3. Engineering
    a. Design of solar energy system
    b. Mechanical design
    c. Electrical design
4. Renewable energy equipment
    a. Solar thermal collector and/or PV modules
    b. Spare parts and special tools
    c. Control system
    d. Transportation
5. Balance of plant
    a. Transport by ship
    b. Transport from ship to base
    c. Solar energy system foundations
    d. Solar energy system erection
    e. Electrical connection
    f. Commissioning of system
6. Miscellaneous
    a. Training
    b. Contingencies

5.3 Investment Costs of Supplementary Infrastructure and Electrical Connections to SANAE IV's Electrical Grid

The investment costs of supplementary infrastructure and electrical connections are sometimes less obvious than the basic investment costs listed in section 5.1, however, no less important. They include (Teetz, 2002):

1. Cost of access roads
2. Cost of cables, poles, transformers, etc.
3. Testing costs
    a. System testing under normal conditions
    b. System testing in Antarctic conditions
    c. Electrical grid connection testing at SANAE IV
    d. Complete system testing

In the ensuing investigation the costs mentioned above in sections 5.2 and 5.3 (viz. basic investment costs, and the investment costs of supplementary infrastructure and electrical connections to SANAE IV's electrical mini-grid) will be grouped together under the term *capital investment*. This capital investment represents the entire cost required to commission the proposed energy system at SANAE IV, and does not include recurring costs that will be incurred cyclically due to maintenance and other expenditures. These recurring costs are listed below in section 5.4.

5.4 Annual Recurring Costs and Savings

The implementation of any renewable energy system at SANAE IV will result in a number of costs and savings occurring cyclically throughout the lifetime of the project. By considering the magnitude of these cyclic costs and savings along with the capital investment, the feasibility of the project can be determined. These recurring costs (or savings) may or may not exceed the initial capital investment depending on their amounts and temporal nature (i.e. at what time during the lifetime of the system they occur), and which for the purposes of this investigation include (Teetz, 2002):

1. Energy system operation and maintenance costs

2. Labour costs
3. Interest on capital investment
4. Fuel savings due to reduction in diesel consumption
5. Operation and maintenance savings due reduction in generator use
6. Labour savings due to reduced generator usage

The installation of a solar energy system will therefore result in an increase of capital, maintenance and labour costs, yet also in a reduction in fuel consumption and external penalties. This relationship can be expressed as:

$$LCC = C_{pw} + M_{pw} + L_{pw} + F_{pw} + X_{pw} \qquad 5.1$$

Where the lifecycle cost (LCC) is the present worth (PW) sum of capital (C), maintenance (M), labour (L), fuel (F) and external (X) expenses. The present worth of each annual cost is calculated by multiplying a future sum of money by a Present Worth Factor (PWF):

$$PWF(i,n) = \frac{1}{(1+i)^n} \qquad 5.2$$

Where the present worth factor ($PWF(i,n)$) is a function of the relevant interest rate (i) and number of years between the present and expected future date of cash flow (n). Sample calculations of the economic evaluation have been provided in appendix E.

5.5 Economic Viability Criteria Necessary to Evaluate Investments for Solar Energy Systems

The methods used in this thesis to investigate the economic feasibility are presented in a document entitled "*Cost Benefit Analysis*" (DEAT, 2005) that, *"…aim*[s] *…to provide general information on techniques, tools and processes for environmental assessment and management"*. They include calculating:

1. Net present value (NPV),
2. Internal Rate of Return (IRR),

3. Benefit-Cost Ratio (BC Ratio) and
4. Cost of Energy Production (R/kWh)

5.6 Externalities

Externalities refer to those factors that lie beyond the immediate system costs under consideration (i.e. the costs mentioned in sections 5.2, 5.3 and 5.4) yet which still have a significant impact on the decision making process. In this instance the relevant externalities concern the environment, or in other words, the cost to the environment of the current energy generation methods. Reducing the operating intensity of energy generation methods becomes immediately beneficial to the environment if it is possible to assuage emissions, waste or the risk of oil spills. These are assigned a monetary value and accounted for in the economic analysis.

In table 5.1 the estimated air pollutants that are emitted into the atmosphere by the diesel-electric generators at SANAE IV each year are presented.

Table 5.1: Total annual emissions from generators (Taylor et al., 2002)

	VOC	CO	NO_x	SO_2	CO_2	PM
Lower Estimate (tons)	0.341	0.533	13.451	0.076	744	0.198
Upper Estimate (tons)	0.546	0.853	13.451	0.076	744	0.317

The Rand values of these emissions have been estimated (adapted with 1 % per annum compound increase from Teetz, 2002) and are presented in table 5.2.

Table 5.2: Cost of pollutants (Teetz, 2002)

POLLUTANT	COST (R/kg)	AMOUNT PRODUCED (LOWER LIMIT, TONS)	AMOUNT PRODUCED (UPPER LIMIT, TONS)	COST
VOC	41.59	0.34	0.55	R 22 709.92
CO	41.59	0.53	0.85	R 35 479.04
NO_X	25.40	13.45	13.45	R 341 613.97
SO_2	62.76	0.08	0.08	R 4 769.43
CO_2	0.20	744.00	744.00	R 145 643.35
PM	36.62	0.20	0.32	R 11 607.56
			TOTAL COST:	*R 561 823.26*

According to table 5.2 a maximum saving of approximately R 560 000 in externalities currently exists at SANAE IV (which translates into a value of 1.88 R/L or 0.30 US$/L) if the total savings is divided by the annual fuel consumption of the generators (297 872 L). Note, however, that the expected fuel savings of the suggested solar system would not entirely eliminate the use of fuel at the station, and therefore the actual savings would in reality be significantly less than the total of R 560 000.

Teetz (2002) also provided a second estimate of the cost of externalities by assigning a Rand value to each litre of fuel consumed as suggested by El-Kordy et al. (2001). This value of 0.87 US$/L (adapted with 3 % per annum compound increase from Teetz, 2002) also accounts for the impact of fuel spills, yet is 290 % higher than the estimate derived from table 5.2.

The following relevant points should be noted in this regard. The cost to the environment of cleaning spills and waste are significantly higher than the cost of air pollutants alone. In the case of SANAE IV shipping and storage add considerably to non-emission type environmental costs since snow has to be collected from the station and transported back to South Africa. These costs should therefore be included in the economic assessment and support the use of the value suggested by El-Kordy above. Furthermore, a case in point concerns the snow smelter at SANAE IV that may in the future experience water contamination problems due to the melting of contaminated snow. Fuel spills are immediately frozen in the snow, however, warmer weather tends to melt the top layer of this snow allowing the fuel to seep down towards the snow smelter that lies at a lower elevation. To correct this problem would require re-locating the snow smelter entirely. The second value suggested by El-Kordy et al. and used by Teetz (2002) in his investigation at the South African station will therefore also be used here.

5.7 Diesel Fuel Price

Three estimates of diesel point-of-use costs are presented in table 5.3 for comparison. As a rule of thumb the purchase price of fuel in the country of origin can be tripled to obtain a rough estimate of final costs (Guichard, 1996), however, the extensive study undertaken by the AAD in 1991 (Steel, 1993) suggests a factor of 3.70 and is most probably the more accurate estimate. For the purposes of this study a factor of 3 will be applied since it coincides with the results obtained by Teetz (2002) which considered factors specific to the conditions at SANAE IV. It is also slightly more conservative than the value suggested by the AAD. Since the current purchase

price of SAB Diesel in South Africa for DEAT is 5.36 R/L the point-of-use cost will therefore be 16.08 R/L in the ensuing investigation.

Table 5.3: Diesel costs for use in Antarctica

	TEETZ[Δ] (RAND/L)	GUICHARD[Ŧ] (AUD/L)	STEEL[Ψ] (AUD/kWh)	GUICHARD[Å] (US$/kWh)
Purchase cost	1.932	± 0.33	± 0.10	0.0275
Final cost	5.847	± 1.00	± 0.37	0.0785
Factor	*3.026*	*± 3.00*	*± 3.70*	*2.8545*

[Δ]Teetz (2002); [Ŧ]Guichard (1996); [Ψ]Steel (1993); [Å]Guichard (1994)

5.8 Economic Assessment

The economic assessment of the solar energy systems at South Africa's SANAE IV station has been undertaken in two parts. In the first part the economic feasibility of installing a PV system is investigated in detail, followed in the second part by an identical consideration of the suggested flat-plate solar thermal system. Unless otherwise stated the methods employed consider the time value of money by using a hurdle rate of 8 % as suggested by DEAT (2005) (also referred to as the Minimum Attractive Rate of Return [MARR]), and are presented in real terms (i.e. not actual or nominal values). The fuel-price escalation rate used in the investigation was assumed to be 5 %, and all other assumptions have been listed in tables 5.4 and 5.6.

5.8.1 Photovoltaic Energy System Assessment

The financial assessment of the proposed PV system at SANAE IV is presented below. All assumptions have been listed in table 5.4, and as mentioned above the investigation utilises the following tools to determine feasibility:

1. Net Present Value,
2. Internal Rate of Return,
3. Benefit Cost Ratio and
4. Cost of energy produced.

Table 5.4: Essential data and system characteristics of PV System

Solar Energy Characteristics and Data:		
Total Number of Panels (Dependent on inverter size)	572.00	No.
Solar System Efficiency	13.00	%
Panel Watts Peak (SANYO HIT 63S1)	63.00	Wp
Total Available Titled Insolation	1 430.80	kWh/m^2.year
Area per panel	0.47	m^2
Annual solar system operating hours	8 640.00	hr
Expected design life of solar system	25	years
Solar panels unit purchase price	-R 35.00	R/Wp
Solar panels total purchase price	-R 1 261 260.00	Rand
Auxiliary equipment (Trace Engineering 2x20 kW PV-series inverter)	-R 214 782.08	Rand
Installation cost (cables, module support frames, infrastructure)	-R 147 604.21	Rand
Transportation cost	-R 29 520.84	Rand
Estimated annual maintenance & operation cost	-R 73 802.10	Rand
Estimated annual labour cost	-R 1 000.00	Rand
Solar system energy penetration factor	100.00	%
Complete solar system cost	-R 1 653 167.13	Rand
Annual power production	48 795.63	kWh
Installed area	265.98	m^2
Installed Watts (peak)	36	kWp
Fuel saved annually due to solar system energy capture	9 958.29	L
Diesel Generator Characteristics and Data:		
Diesel purchase price	-5.36	Rand/L
Diesel point-of-use price for SANAE IV	-16.08	Rand/L
Estimated annual maintenance & operation cost	-30000.00	Rand
Estimated annual labour cost	-20000.00	Rand
Annual power production	1 061 971	kWh
Annual power generation hours	11304.00	hr
Estimated diesel generator efficiency (considering summer HVAC conditions)$^{\phi}$	50.00	%
Fuel energy density	9.80	kWh/L
Annual generator diesel consumption	297 872	L
Estimated saving in L and M due to reduced operating time	0.00	%
Economic Data:		
Value of Externalities (on every litre of fuel saved)	5.32	R/L
Interest rate on lent capital	10.00	%
Estimated maintenance and labour cost escalation per year	1.00	%
Estimated fuel cost escalation	5.00	%
General inflation rate (August 2005)	3.50	%
Crude Oil Price (US$/barrel)	61.00	US$/barrel
Exchange rate (R to US$)	6.46	Rand/US$
Estimated escalation rate of external costs	1.00	%
MARR (hurdle rate)	8.00	%

$^{\phi}$ During summer there is a net *heat gain* in SANAE IV. Waste-heat is therefore not completely utilised.

NET PRESENT VALUE (NPV)

In figure 5.1 the NPV of all the costs incurred by the diesel-only and hybrid-PV systems are illustrated throughout the expected 25-year project lifetime. The results have been calculated using equation 5.1 excluding externalities for the moment. It is evident for the hybrid system that until the 21st year total costs remain greater than those of a diesel only system (i.e. no breakeven point is reached through the mitigation of fuel consumption), and that only after such a time net profits are made. Note that, as stated above, the time value of money in this figure has been accounted for by using a hurdle rate of 8 % meaning that these investments must be able to outperform the equivalent profits that could be obtained from an alternative investment (at a bank for instance) with an interest rate of that amount.

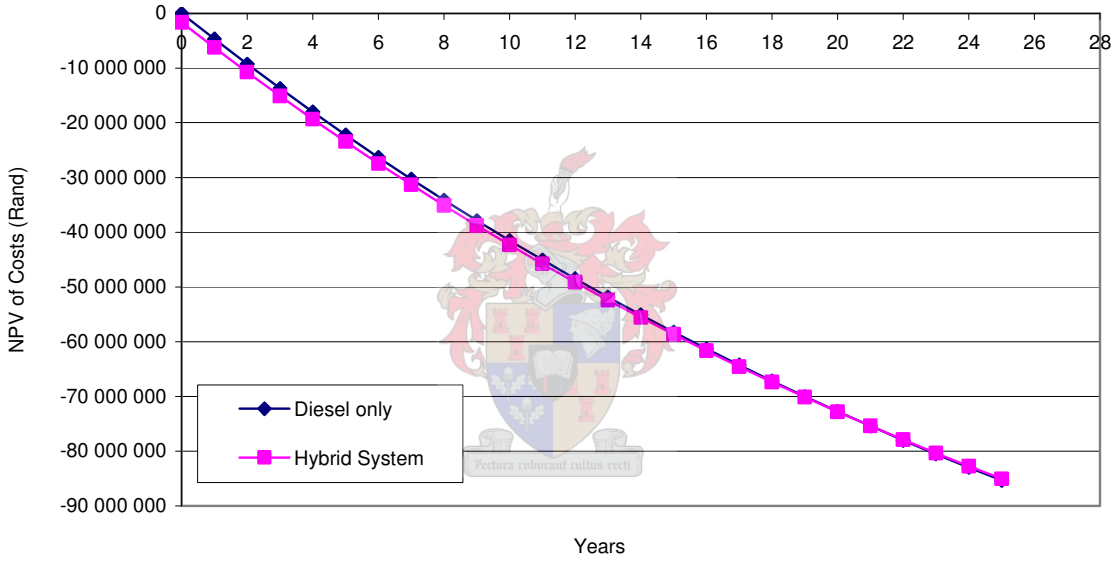

Figure 5.1: NPV of costs incurred during expected project lifetime

In figure 5.2 expected payback periods for the system at different interest rates (viz. 8 % and 0 %) with and without externalities (see section 5.6) are shown. From the figure it is evident that regardless of the hurdle rate or environmental costs the PV system will struggle to rapidly recover investment costs sunk into the project assuming that an eighteen to twenty-four month payback is optimal. Nonetheless, even under the most stringent assumptions (viz. 8 % hurdle rate and excluding externalities) costs can be recovered within the lifetime of the system, and with increasing promise as emphasis is placed on more desirable funding methods and external costs.

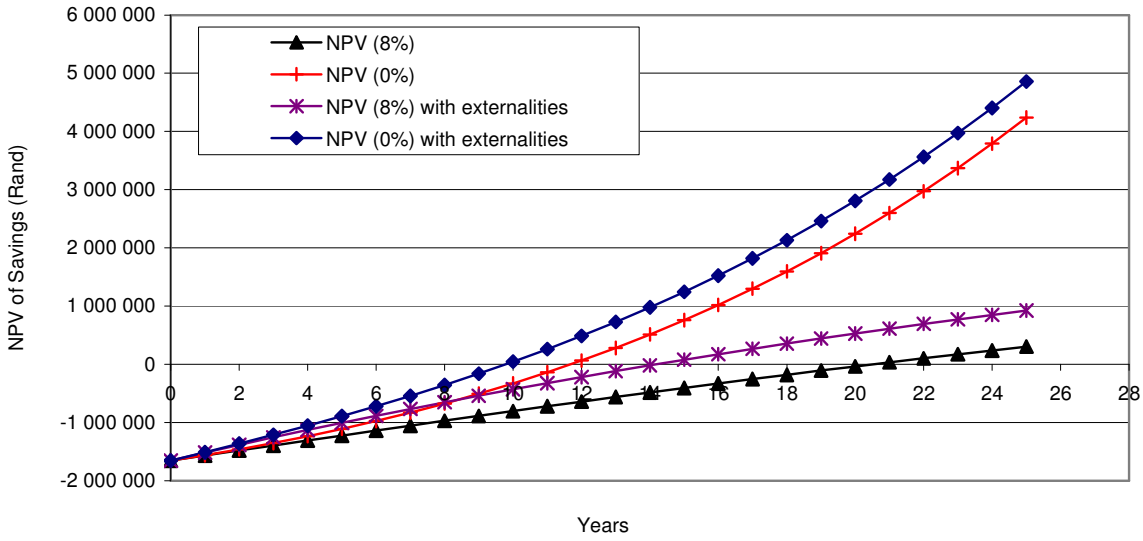

Figure 5.2: NPV of the difference between the costs of the two alternatives

A comparison of initial capital investment and the consequent net savings is given in figure 5.3. From the figure it is evident that an initial capital investment of R 1 900 000 will result in a breakeven point after approximately 25 years. Capital outlay should therefore be less than approximately this amount to make a profit within the system lifetime utilising an 8 % interest rate criteria (without externalities) and the assumptions listed in table 5.4.

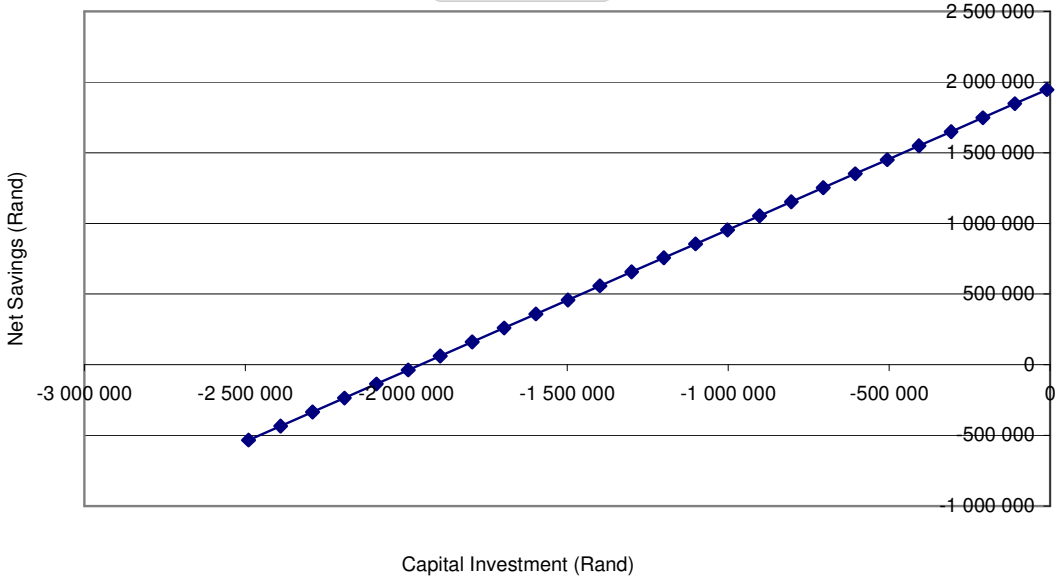

Figure 5.3: NPV after 25 years at various initial capital investments (8 % MARR)

INTERNAL RATE OF RETURN (IRR)

The IRR method (otherwise known as the profitability index or discounted cash flow method) is defined as that method which, *"…solves for the interest rate that equates the equivalent worth of an investment's cash inflows (receipts or savings) to the equivalent worth of cash outflows"* (Sullivan et al., 2003). Consequently the breakeven interest rate, or that interest rate which will result in a zero net profit over the lifetime of the investment, is determined. If this rate of return calculated is higher than a company's minimum attractive rate from alternative investments, it stands to reason that the investment is desirable.

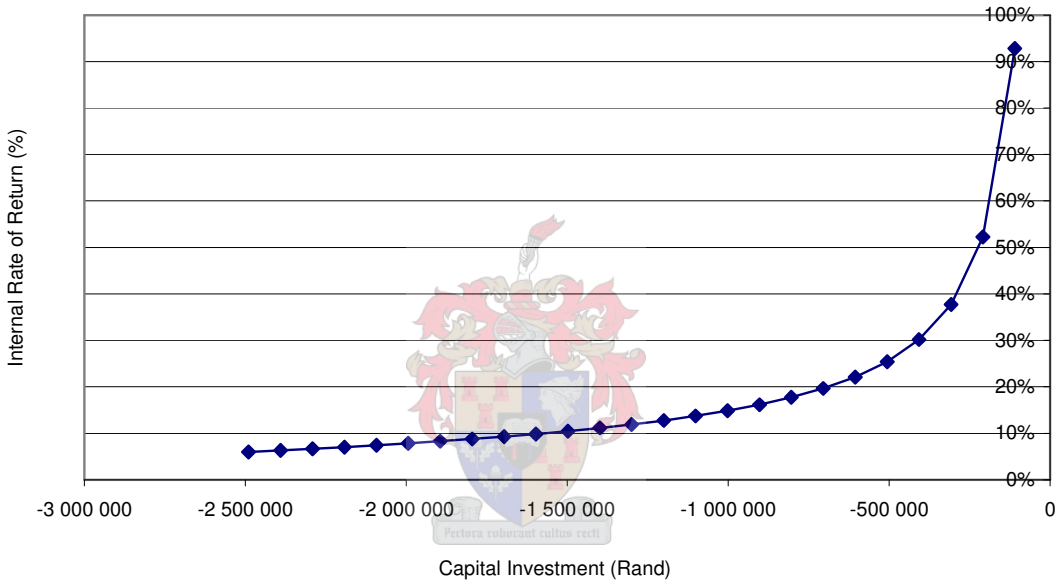

Figure 5.4: IRR at various initial capital investments

From figure 5.4 an IRR of 9.52 % was calculated, compared to the Minimum Attractive Rate of Return that was set at 8 %. The Net Annual Worth and Present Values are listed in table 5.5 (again at an 8 % hurdle rate) and should be compared to figure 5.2 for a comparison of possible NPVs using alternative assumptions.

Table 5.5: PV System results after 25 years

CRITERIA	AMOUNT
NPV (R)	302 915
IRR (%)	9.52
NAW (R)	26 907

BENEFIT COST RATIO (BC RATIO)

A BC Analysis is useful for estimating the relative worth of savings against costs. In this investigation (where a value of unity suggests that savings are equal in magnitude to costs) a value greater than unity indicates that potential revenues generated by an investment exceed the associated costs, and indicates a desirable alternative to the current method of investment.

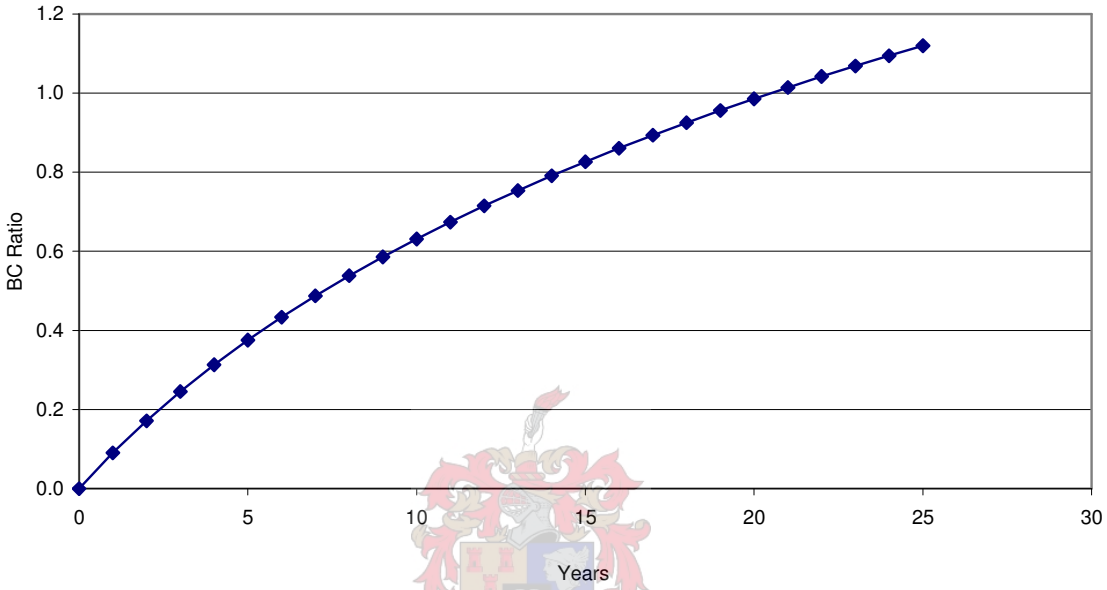

Figure 5.5: BC Ratio over lifespan of project

The suggested PV system is able to recover the costs after a period of 21 years (at an 8 % hurdle rate and without the inclusion of externalities in the system savings) as was also found in figures 5.1 and 5.2. The trend also illustrates that a longer system lifetime equates to greater potential benefits derived from the investment, albeit with a smaller differential gain after each year.

Referring to figure 5.6 it is again evident that the breakeven point should occur for an initial capital outlay of R 1 900 000 or less, a value that corresponds with information given by figures 5.3 and 5.4. Note that revenues are markedly increased with a reduction in initial capital investment and an extension of the project lifetime. For the suggested PV system an estimated capital investment of R 1 653 167 will be required (as stated in table 5.4).

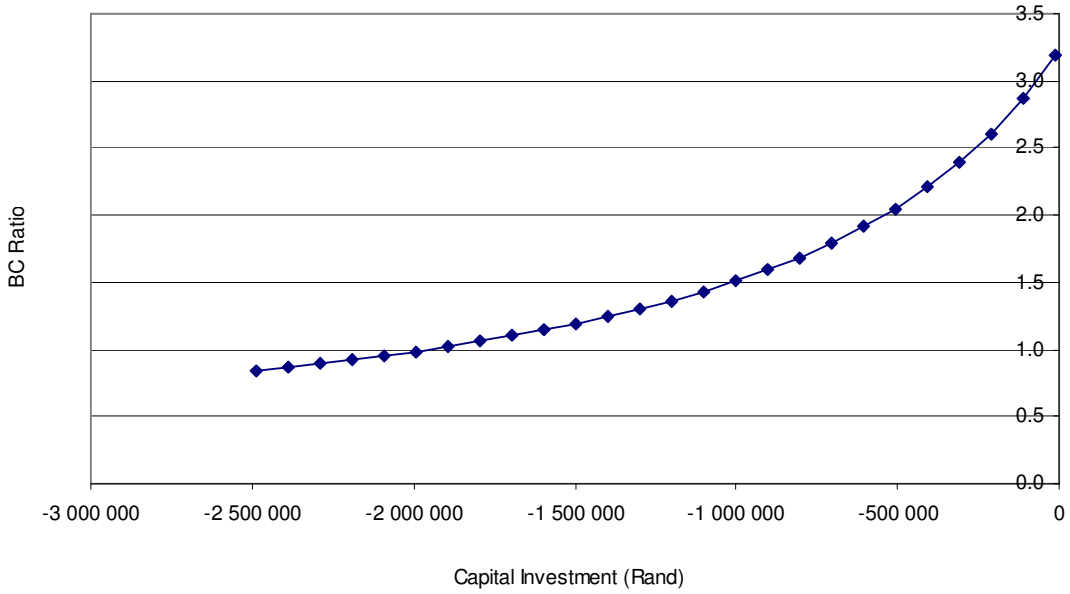

Figure 5.6: BC Ratio at various capital investments

COST OF ENERGY GENERATION (R/kWh)

The cost of energy generation at SANAE IV for hybrid and diesel-only systems has been calculated by summing the project expenses (given in equation 5.1 but excluding externalities) over the expected 25 year lifetime and dividing by energy consumption over the same period (approximately 1 062 MWh annually). Therefore, and referring to figure 5.7, it is evident that diesel-only system energy costs amount to roughly 3.21 R/kWh (since the associated capital investment costs are zero) and that diesel-PV systems could generate energy at a cost of 3.20 R/kWh.

Standard off-peak domestic rates of electrical energy in South Africa are currently approximately 0.30 R/kWh, and therefore almost 11 times cheaper than the estimated current diesel-only cost of energy generated at SANAE IV. This is a value that correlates reasonably well with the reference by Steel (1993) to the detailed cost analysis completed by the Energy Section of the AAD in 1991. Results from this investigation showed that the final cost of energy consumption in Antarctica amounted to approximately 7 times the domestic price of electricity in Tasmania, and 14 times the off-peak charge. In this investigation carried out by the AAD the cost of the fuel itself represented approximately 55 % of this final value, while equipment depreciation and maintenance represented the other 45 %.

From figure 5.7 the minimum attractive PV-system capital investment associated with this diesel-only-system energy cost is again estimated at approximately R 1 900 000, while the actual investment of the PV system, as mentioned above, is in the order of R 1 653 167. This capital investment corresponds with an energy production price of approximately 3.20 R/kWh, and represents a reduction in fuel generation costs of less than 1 %. Teetz (2002) estimated that wind generation would be able to reduce fuel generation costs in the order of 20 %.

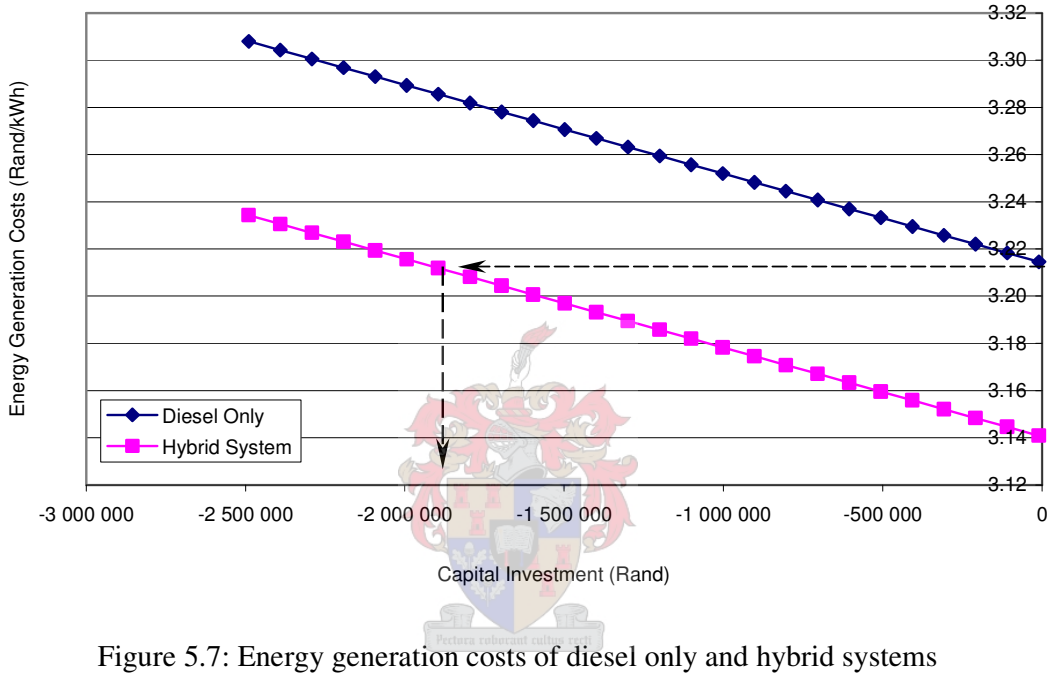

Figure 5.7: Energy generation costs of diesel only and hybrid systems

5.8.2 Solar Thermal Energy System Assessment

The suggested solar thermal system described here shows more potential for financial and energy savings than the photovoltaic collectors assessed above. Assumptions have been tabulated in table 5.6 and illustrations of the costs are provided as before. Estimated fuel savings have again been calculated based on a generator efficiency of 50 % (refer to table 5.4) since waste-heat recovery is relatively insignificant during the summer period owing to the high inside station temperatures. Even though the Domestic Hot Water System utilises a small portion of the waste heat during the summer months the suggested percentage is still conservative.

Table 5.6: Essential data and system characteristics of solar thermal system

Solar Energy Characteristics and Data:		
Number of panels (either 24 or 72)	72	No.
Tmax (stable smelter temperature)	20	℃
Tresponse (for switching elements off)	10	min
Total available titled insolation on non-tracking surface	1 430.80	kWh/m^2.year
Area per panel	1.98	m^2
Expected design life of solar system	25	years
Solar panels unit purchase price	-R 7 000.00	R/Panel
Solar panels total purchase price	-R 504 000.00	Rand
Cost of Accessories (Thermal Energy Store, pumps, controller & pump room)	-R 170 000.00	Rand
Installation cost	-R 134 800.00	Rand
Transportation cost	-R 33 700.00	Rand
Estimated annual maintenance & operation cost	-R 33 700.00	Rand
Estimated annual labour cost	-R 5 000.00	Rand
Solar system energy penetration factor	100.00	%
Complete solar system cost	-R 881 200.00	Rand
Annual power production	60 000	kWh
Installed area	142.56	m^2
Fuel saved annually due to solar system energy capture	12 244.90	L
Estimated Annual System Efficiency	29.42	%
Diesel Generator Characteristics and Data:		
Diesel purchase price	-5.36	Rand/L
Diesel point-of-use price for SANAE IV	-16.08	Rand/L
Estimated annual maintenance & operation cost	-30 000.00	Rand
Estimated annual labour cost	-20 000.00	Rand
Annual power production	1 061 971	kWh
Annual power generation hours	11 304.00	hr
Estimated diesel generator efficiency (considering summer HVAC conditions)$^{\phi}$	50.00	%
Fuel energy density	9.80	kWh/L
Annual generator diesel consumption	297 872	L
Estimated saving in L and M due to reduced operating time	0.00	%
Economic Data:		
Value of Externalities (on every litre of fuel saved)	5.32	R/L
Interest rate on lent capital	10.00	%
Estimated maintenance and labour cost escalation per year	1.00	%
Estimated fuel cost escalation	5.00	%
General inflation rate (August 2005)	3.50	%
Crude Oil Price (US$/barrel)	61.00	US$/barrel
Exchange rate (R to US$)	6.46	Rand/US$
Estimated escalation rate of external costs	1.00	%
MARR (hurdle rate)	8.00	%

$^{\phi}$ During summer there is a net *heat gain* in SANAE IV. Waste-heat is therefore not completely utilised.

NET PRESENT VALUE (NPV)

In figure 5.8, as in figure 5.2, the expected payback periods for the solar system at different interest rates and with externalities (see section 5.6) are shown. Costs are recovered within 6 years from the initial investment, and the system worth at the end of the project duration under the assumptions listed in table 5.6 is estimated at R 2 148 811 (with an initial investment of R 881 200).

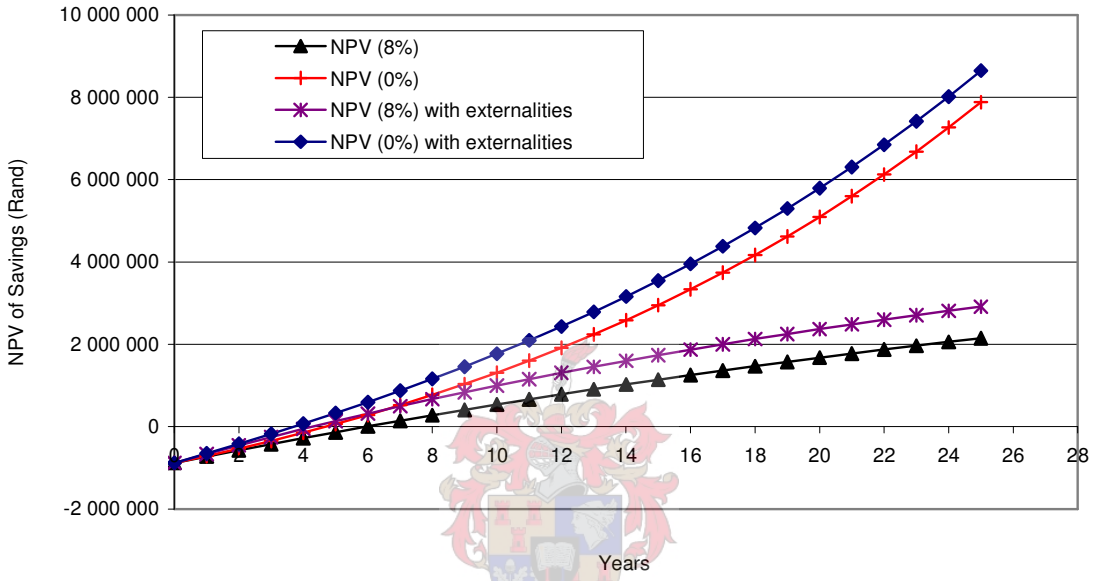

Figure 5.8: NPV of the difference between the costs of the two alternatives

Thus the economic characteristics of the solar thermal system described here show potential for breakeven on the short to medium term of the project. This is unlike the photovoltaic system that was not able to recover the costs as rapidly, and contrary to the expectations of the discussion in section 4.3. Mainly this is because the snow smelter presents the unique opportunity to utilise solar thermal energy at reasonably low process temperatures, during the summer, with relative ease of installation.

Note that the solar thermal system currently under investigation is large (72 collector panels), however it should be remembered that these collectors are modular and that any smaller combination is possible. Savings generated in these instances will not be of the same magnitude as those presented above yet breakeven periods will still take place in the same amount of time.

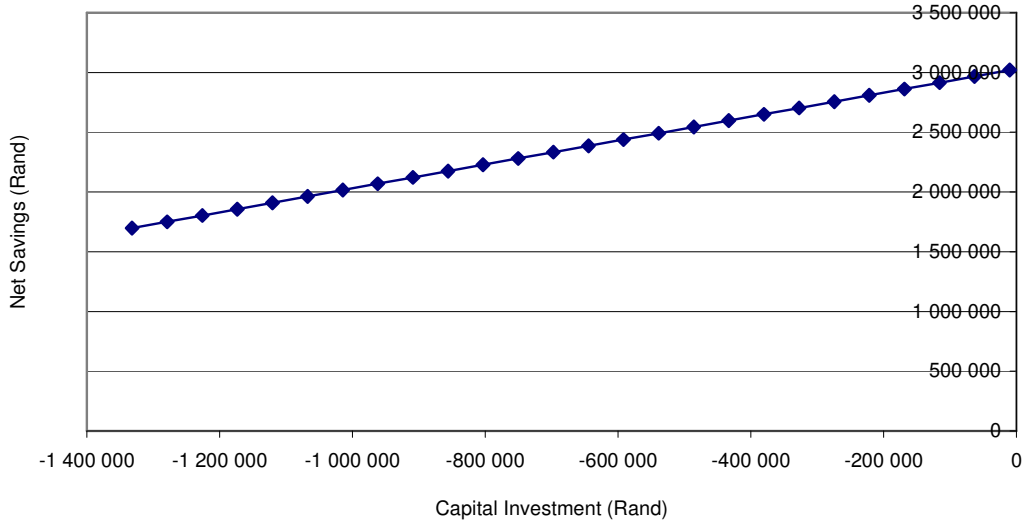

Figure 5.9: NPV after 25 years at various initial capital investments (8 % MARR)

INTERNAL RATE OF RETURN (IRR)

The IRR of the suggested solar thermal system shown in figure 5.10 has been calculated as 24 % (from an initial investment of R 881 200), while smaller systems show slightly lower yet still consistently large rates of around 15 % (as compared to the MARR of 8 %). Refer to table 5.7 for estimates of the expected NAW and NPV of the system after 25 years and to figure 5.8 for estimates of the NPV using different assumptions.

Table 5.7: Solar thermal system results after 25 years

CRITERIA	AMOUNT
NPV (R)	2 148 811
IRR (%)	24.47
NAW (R)	190 873

BENEFIT COST RATIO (BC RATIO) AND COST OF ENERGY GENERATION (R/kWh)

Following figure 5.10 (which illustrates the IRR) graphs of BC Ratio and cost of energy generation are illustrated in figures 5.11 and 5.12 below. The results correlate well with those discussed so far, and show that a thermal collector system used to supplement the energy demand of the snow smelter has the ability to recover the cost of the initial investment well within the lifetime of the project. A breakeven point is expected on the short to medium term, as

well as under various adverse conditions (such as low fuel price escalation rates, high initial investment costs, high labour expenses, etc.). The cost of energy generation in this instance has been calculated at 3.13 R/kWh, as opposed to the 3.20 R/kWh of the PV system in section 5.8.1, and is approximately 3 % cheaper than the cost of 3.21 R/kWh for diesel-only power generation.

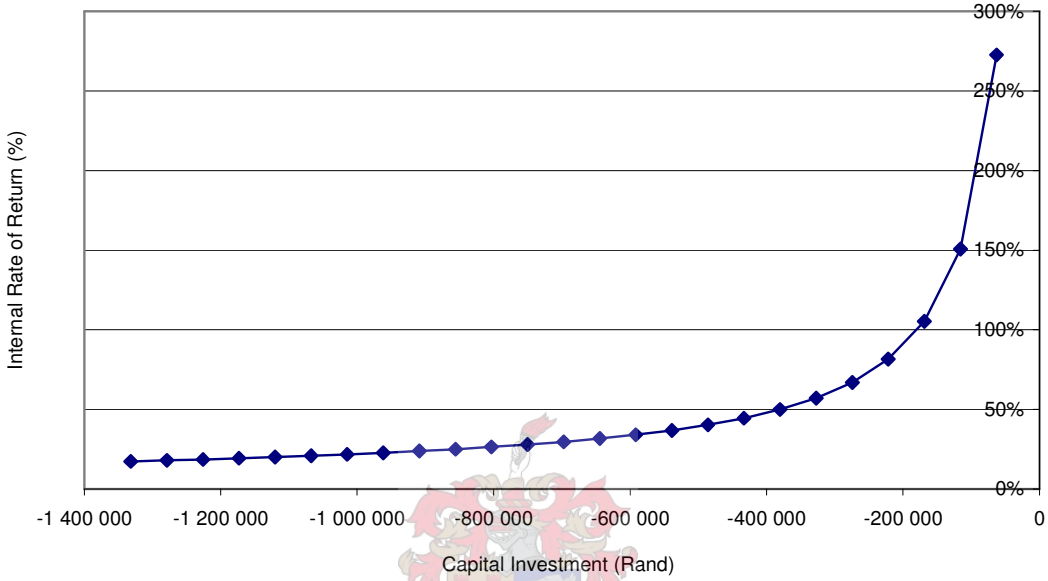

Figure 5.10: IRR at various initial capital investments

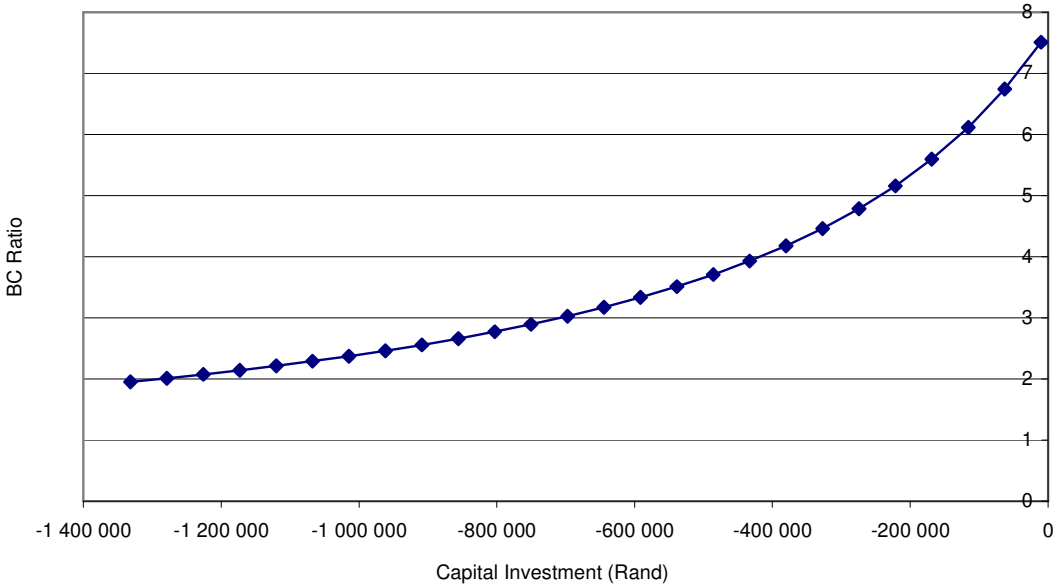

Figure 5.11: BC Ratio at various capital investments

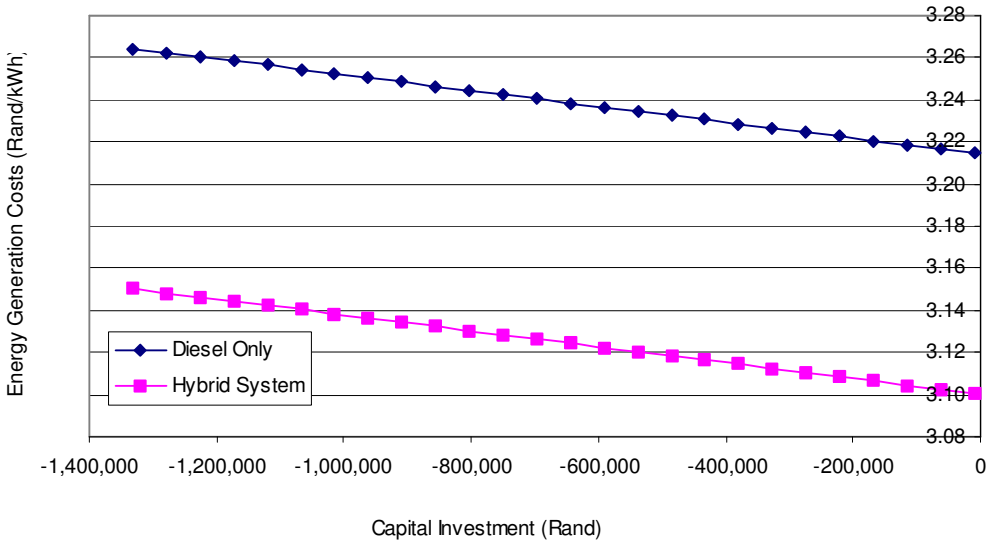

Figure 5.12: Energy generation costs of diesel only and hybrid systems

5.8.3 Economic Performance Criteria at Various Financial Conditions

Due to the difficulties involved with predicting criteria such as future fuel price escalation rates and a fair MARR, the performance of the PV and solar thermal systems under various economic conditions have been presented in table 5.8. These values serve as an indication of how sensitive the systems' financial criteria are to change, showing that although the solar thermal system is a relatively low risk investment the success of the PV systems depends on the realisation of expected future scenarios. Any significantly unfavourable economic conditions would result in a net financial loss related to the installation of a PV system.

Table 5.8: Financial outcomes under various economic conditions

	SOLAR PHOTOVOLTAIC			SOLAR THERMAL		
MARR	*8%*					
Fuel Price Escalation	*7 %*	*5 %*	*3 %*	*7 %*	*5 %*	*3 %*
Breakeven period (years)	16	21	N/A	6	6	7
IRR (%)	12	10	7	27	24	22
NAW (Rand after 25 years)	91 037	26 907	-21 335	269 729	190 873	131 554
NPV (Rand after 25 years)	1 024 882	302 915	-240 183	3 036 554	2 148 811	1 481 007
BC (after 25 years)	1.40	1.10	0.90	3.25	2.50	2.00
MARR	*4 %*					
Fuel Price Escalation	*7 %*	*5 %*	*3 %*	*7 %*	*5 %*	*3 %*
Breakeven period (years)	13	15	18	5	5	6
IRR (%)	12	10	7	27	25	22
NAW (Rand after 25 years)	170 969	91 622	33 498	330 651	233 083	161 614
NPV (Rand after 25 years)	2 956 406	1 584 322	579 252	5 717 633	4 030 493	2 794 640
BC (after 25 years)	2.00	1.50	1.20	4.75	3.50	2.75

5.9 Summary

It is evident from chapter 5 that with proper implementation the suggested solar energy systems should be capable of recovering their initial capital investment within the project lifetime. Therefore these systems represent not only economically feasible investments, but also good opportunities for improving living conditions at SANAE IV during the summer as discussed in chapter 3.

The average cost of generating electricity after commissioning a solar thermal system with a 143 m^2 collector field (assuming a real hurdle rate of 8 % and fuel price escalation rate of 5 %) would be approximately 3.13 Rand/kWh, as opposed to the 3.21 Rand/kWh of the current diesel-only system. Annual fuel savings associated with such a system were calculated as 12 245 litres. The project would arrive at a breakeven point after approximately 6 years, and represent a NPV of 2 148 811 Rand after 25 years. By further considering environmental factors such as the cost of removing soiled snow from Antarctica and diesel fuel emissions the magnitude of the net present savings would increase by approximately 500 000 Rand.

The 40 kW photovoltaic system that was investigated was only able to fully recover the initial costs after 21 years. It is expected that installing such a system would equate to a NPV of 302 915 Rand at the end of the 25 year system lifetime, saving 9 958 litres of diesel annually in the process and generating energy at a cost of 3.20 Rand/kWh. It should be noted, however, that under more ideal conditions (i.e. less attractive alternative investment opportunities, higher fuel price escalation rates and a stronger emphasis on environmental concerns) investment into a photovoltaic system could potentially breakeven after approximately 10-15 years, while simultaneously significantly improving base operation.

The opportunity to install a solar energy system at SANAE IV therefore warrants action. There is potential not only to generate savings over the operational lifetime but also to preserve the environment in accordance with the desires of the Antarctic Treaty. It is firmly believed that with careful planning and implementation such a project can and should be successfully undertaken.

Chapter 6 – Conclusion

At the start of this project four questions were posed that, together, would determine the technical and economic feasibility of utilising solar energy at South Africa's SANAE IV station in Antarctica (refer to chapter 1). These questions have been addressed in chapters 2 through to 5, and the necessary information obtained from each. Results were compared with information contained in relevant sources and where applicable with data measured during the 2004/2005 takeover at SANAE IV, as detailed in sections 2.3.1 and 3.2. Various financial outcomes resulting from different economic scenarios were also considered. At the close of this study it is therefore possible to summarise the information obtained, draw important conclusions and suggest a future course of action.

As described in chapter 2, the annual-average global horizontal insolation at SANAE IV was found to be relatively low (2.87 kWh/m^2.day, or 10.33 MJ/m^2) compared with other locations on Earth. The insolation is characterised by significant seasonal fluctuations and comprised large components of diffuse radiation. Except for clear-sky days when tilted surfaces may be exposed to radiation of up to 1 300 W/m^2, the diffuse component contributes to an estimated 1.74 kWh/m^2.day, or approximately 60 % of the annual average global insolation. In comparison to other resources these estimates of radiation at SANAE IV are very similar to the conditions at its closest neighbour, the German Neumeyer station, as shown in figure 2.12. The required collector tilt angles were also found to be relatively high, starting at 50° in the peak of summer and increasing to 90° in the winter. This makes it difficult to design small and compact collector fields since, due to the high tilt angles, it is not possible to place collectors directly behind each other.

After investigating the energy consumption of SANAE IV (chapter 3) the station's electrical mini-grid and snow smelter were highlighted as favourable electrical and thermal loads respectively for the application of solar energy systems. It was evident that, due to the difficulties synonymous with generating electricity during the summer takeover period, supplementing these systems with solar energy would prove to be particularly beneficial for the station. During this time the generators are prone to overheating, even disrupting normal grid operation, and there is a restricted supply of fresh water from the snow smelter to the base. These loads therefore present opportunities for a twofold gain by implementing a solar energy system; firstly, by

generating financial savings and, secondly, by reducing some of the pressure placed on the station's energy systems during the summer months.

It was calculated that under ideal assumptions the snow smelter would consume approximately 820 kWh daily while creating fresh water during the takeover period (when base population totals approximately 80 people). However, as shown later (in section 4.3.1), if heat losses and the snow smelter PLC logic are accounted for then the actual value is most likely more than double this amount. The consequent load on the generators required for the snow smelter is therefore on average 34 to 68 kW, with peaks that could reach up to 94 kW during the day.

The investigation described in section 3.3.1 revealed that the electrical mini-grid was characterised by large daily demand fluctuations, making it unreasonable to use an average daily load profile as a method of approximating demand during the summer period. It is important to account for the high load-profile variability when matching renewable energy systems with energy storage devices to the demand of the station. From this study the base load of SANAE IV was calculated to be 60 kW, and thus a PV system with a rated power smaller than this size was investigated (viz. a 40 kW system).

Here again emphasis was placed on the suggestion that was made in section 3.2.3 to improve the working computer simulation model of all the energy systems at the station. This would result in a number of benefits, but particularly it would help to better understand the effect that any changes will have on the station by accounting for the complex interaction of all existing systems in a way that simple calculations cannot. Furthermore, it would also make the identification of savings opportunities at the station much easier.

In section 3.2.4 it was recommended that additional methods of supplying fresh air to the plant-room should be investigated. Any added contribution of fresh air to the room would noticeably improve the working conditions during the summer. Attention was also given to some of the difficulties involved with PLC control (c.f. section 3.2.5) and heat losses to the environment (c.f. section 3.3). All of these areas justify efforts to improve the current status of the energy system.

In chapter 4 factors related to determining suitable PV and solar thermal collectors for the conditions in Antarctica were investigated. Although the purchase of photovoltaic panels in South Africa poses no problems for the implementation of a solar energy system at SANAE IV it

was more difficult to find suitable locally manufactured solar thermal devices. By far the least complicated of these thermal systems is the flat-plate collector, a choice supported by considering the low ambient temperatures, high fractions of diffuse radiation and the collector tracker device reliability for instance (refer to section 4.3.1).

For the PV system some difficulty was encountered in establishing what type of inverter is most suitable for use at the base. Even though no acceptable products are currently available for purchase in South Africa, overseas markets manufacture three-phase grid-tie inverters that automatically lock onto and feed into an existing grid. Since the generators at SANAE IV output electrical energy at three-phase, 380 VAC and 50 Hz, there is no problem in obtaining an inverter that will supply electrical energy at these standard values.

The performance characteristics of the PV and solar thermal collectors under typical Antarctica conditions were also investigated, as described in chapter 4. Three methods of estimating PV efficiencies were presented in section 4.2.3 and subsequently summarised in table 4.6. The results indicate that total systems' efficiencies of PV systems should average approximately 14 % during the year, collecting approximately 200 kWh/m^2.year. In comparison, the average efficiency of the recommended solar thermal collector was calculated as 29 %, or 420 kWh/m^2.year. Results for the solar thermal systems are presented in table 4.9 and appendix D.7.

It was established in chapter 5 that a 40 kW PV system could save as much as 9 958 litres of fuel annually, and that during the same amount of time a solar thermal system (with 72 collector panels) supplementing the snow smelter could save 12 245 litres of fuel. The solar thermal collector system required a lower capital expense, thus it is not surprising that of these two options the latter is also financially more secure. Maintenance and installation of the solar thermal system requires slightly more substantial efforts, yet such efforts are still considered very reasonable within the scope of work that is required to be completed by the summer takeover maintenance crew.

The payback period for the thermal collector system was estimated at six years under the standard investment assumptions, although under more favourable conditions (high fuel price escalation rates and a lower MARR) this amount of time could be reduced to a five-year horizon. The system, which would realise an IRR of 25%, and a NPV of R 2 148 811 after 25 years, is therefore an attractive investment. The PV system, on the other hand, would only be able to

break even towards the end of the project lifetime, although under the more ideal conditions of high fuel price escalation rates, lower MARRs, low attractiveness of other investment opportunities and a stronger emphasis on environmental considerations a breakeven point could potentially be realised within 13-16 years.

It should be noted, however, that a PV system is capable of reducing the size of peak electrical loads on the generators while a solar thermal device is only able to shorten the length of these peaks. Each system must be evaluated on its own merits, and each presents its own unique opportunities.

It is clear that there is ample scope for the utilisation of solar energy at South Africa's SANAE IV station in Antarctica. The suggested solar energy systems present good opportunities for reducing station load and improving living conditions during the summer, and with the proper implementation the initial capital investment can be recovered within the project lifetime (PV only towards the end of the project lifetime, and solar thermal more certainly within six years). Although these solar energy systems may seem large, it should be remembered that they could be scaled to smaller versions of those suggested, and that under these conditions they would most likely recover their capital investment in a similar period of time to that identified here.

It is recommended that an assessment of available funds be made within DEAT in order to establish what financial resources are available for the future implementation of a renewable energy system at SANAE IV. Once it has been established under what conditions these resources could be used (i.e. lending rates and available amount) a refinement of the above assessment may be performed in order to re-assess the economic implications of such a decision if necessary. Over and above the direct savings and improvements which could be realised by installing solar energy systems at SANAE IV, the increased global awareness of environmental change and greenhouse gasses should motivate a careful consideration of the benefits that renewable energy systems have to offer SANAP.

References

Antarctic Renewable Energy, *Earthbeat*, an interview by Alexandra de Blas with Antoine Guichard the Executive Secretary of the Council of Managers of the National Antarctic Programmes, http://www.abc.net.au/rn/science/earth/stories/s99156.htm

AAD (2005), *Australian Antarctic Division*, homepage of the Australian Antarctic Division, www.aad.gov.au

Bronicki, LY (2001), *Sustainable Energy for Rural Areas of the Developing Countries*, A paper presented at the 18th Congress of the World Energy Council in Buenos Aires, October 2001, No. 01-03-03, DS3

Cencelli, N (2002), *Energy Audit and Study of the Heating and Ventilation System of the SANAE IV Base*, BEng Thesis, Department of Mechanical Engineering, University of Stellenbosch

COMNAP (2005), *Council of Managers of National Antarctic Programmes*, homepage http://www.comnap.aq/comnap/comnap.nsf/P/Pages/Operations.ENMANET/

Corkish, R (1997), *Can Solar Cells Ever Recapture the Energy Invested in their Manufacture*, Australia and New Zealand Solar Energy Society, Solar Progress, vol. 18, no. 2, pp. 16-17

de Wet, B (2005), figure A.2 was printed with the permission of its owner Mr de Wet who was team leader of the overwintering party at SANAE IV during 2004

DEAT (2005), *Cost Benefit Analysis*, Section 8 of the Integrated Environmental Management Information Series produced for the South African Department of Environmental Affairs and Tourism (DEAT), http://www.environment.gov.za/Documents/Publications/2005Jan7/Book3.pdf

Duffie, JA and Beckman, WA (1991), *Solar Engineering of Thermal Processes*, John Wiley and Sons Inc., New York, ISBN 0-471-51056-4

El-Kordy, M, Badr, M, Abed, K and Ibrahim, S (2001), *Economical Evaluation of Electricity Generation Considering Externalities*, Renewable Energy, February 2002, vol. 25 (2), pp. 317-328

EPIA (2005), *European Photovoltaic Industry Association*, homepage of the European Photovoltaic Industry Association, homepage http://www.epia.org/

Erbs, DG, Klein, SA and Duffie, JA (1982), *Estimation of the Diffuse Radiation Fraction for Hourly, Daily, and Monthly-Average Global Radiation*, Solar Energy, vol. 28, pp. 293-302

Gleick, P (2005), *Hyperforum on Long Term Sustainability*, produced from the World Resource Institute, http://www.hf.caltech.edu/hf/b3/library/kio-wat/w_table4.html

Guichard, A, Brown, C and Lyons, D (1996), *Analysis of the Potential for Wind and Solar energy Systems in Antarctica*, Institute of Antarctic and Southern Ocean Studies, University of Tasmania, Hobart, Australia.

Guichard A (1994), *Towards New Energy Systems for Antarctica*, proceedings of the Sixth Symposium on Antarctic Logistics and Operations, Rome, Italy, August 1994, pp. 81-95

Helm, D (2005), *The Assessment: The New Energy Paradigm*, Oxford Review of Economic Policy, vol. 21 (1), pp. 1-18

Henryson, M and Svensson, M (2004), *Renewable Power for the Swedish Antarctic Station Wasa*, Master of Science Thesis, Department of Energy and Technology, Stockholm, Sweden

Hottel, HC (1976), *A Simplified Model for Estimating the Transmittance of Direct Solar Radiation through Clear Atmospheres*, Solar Energy, vol. 18, pg. 129-134

Huang, BJ, Petrenko, VA, Samofatov, IY and Shchetninina, NA (2001), *Collector Selection for Solar Ejector Cooling System*, Solar Energy, vol. 71 (4), pp. 269-274

Isherwood, W, Smith, J, Aceves, S, Berry, G, Clark, W, Johnson, R, Das, D, Goering, D and Seifert, R (1999), *Remote Power Systems with Advanced Storage Technologies for Alaskan Villages,* Lawrence Livemore National Laboratory (LLNL), USA

Liu, BYH and Jordan, RC (1960), *The Interrelationship and Characteristic Distribution of Direct, Diffuse and Total Solar Radiation*, Solar Energy, vol. 4 (3), pp. 1-19

Liu, BYH and Jordan, RC (1963), *Long Term Average Performance of Flat-Plate Solar Energy Collectors*, Solar Energy, vol. 7 (2), pp. 53-74

Madrid Protocol (1991), *Protocol on Environmental Protection to the Antarctic Treaty (the Madrid Protocol)*, http://www-old.aad.gov.au/information/treaty/protocoltxt.asp

Maycock, PD (1999), *The World Photovoltaic Market 1975-1998*, Warrenton, Virginia, PV Energy Systems Inc., pg. A-3

Mills, AF (1999), *Heat Transfer*, second edition, Prentice Hall, Upper Saddle River, New Jersey, ISBN 0-13-947624-5

Neumeyer (2005), German Neumeyer Antarctic Station, homepage of the German Neumeyer Antarctic Station http://www.awi-bremerhaven.de/

Norris, DJ (1968), *Correlation of Solar Radiation with Clouds*, Pergamon Press, Great Britain, Solar Energy, vol.12, pp.107-112

Olivier, JR (2005), photographs were taken by the author during a field trip to the SANAE IV station in the 2004/2005 takeover period

Perez, R, Stewart, R, Seals, R and Guertin, T (Oct. 1988), *The Development and Verification of the Perez Diffuse Radiation Model*, Sandia National Laboratories Contractor Report SAND88-7030

Perry-Castañeda Library Map Collection (2005), *Polar Regions and Ocean Maps*, United States Central Intelligence Agency, homepage http://www.lib.utexas.edu/maps/polar.html

RETScreen (2005), *Renewable Energy Technology (RET) Screen International Clean Energy Decision Support Centre*, homepage http://www.retscreen.net

SANAE IV database (2005), SANAE IV computer network at the station, a number of electronic documents are available from the network, no images from this database have been printed without permission

SANAP (2005), *South African National Antarctic Programme*, South Africa's homepage to SANAE IV, http://home.intekom.com/sanae/index.html

SCAR (2005), *Scientific Committee on Antarctic Research*, a recognised research body active in Antarctic co-ordinating scientific research between the twelve original Antarctic Treaty signatories and a growing number of other member states, homepage http://www.scar.org/

Schmidt, T, Langlo, GK (1994), *Radiation Measurements at the German Antarctic Station Neumeyer 1982-1992*, Reports on Polar Research, vol. 146, ISSN 0176-5027

Solahart (2005), Solahart South Africa, Bryanston, P O Box 69560, e-mail jim@solahart.co.za, homepage http://www.solahart.com

Steel, JD (1993), *Alternative Energy Options for Antarctic Stations*, Graduate Diploma Thesis, Institute of Antarctic and Southern Ocean Studies (IASOS), University of Tasmania

Sullivan, WG, Wicks, EM, Luxhoj, JT (2003), *Engineering Economy*, Twelfth Edition, International Edition, Prentice Hall, Pearson Education Inc., Upper Saddle River, New Jersey, ISBN 0-13-039555-2

Surface Radiation Budget (SRB) dataset (2005), Langley Research Centre of NASA, http://eosweb.larc.nasa.gov/PRODOCS/srb/table_srb.html

Surface Meteorology and Solar Energy (SSE) dataset (2005), Langley Research Centre of NASA, http://eosweb.larc.nasa.gov/sse/

Tamm, G, Tomson, T (2005), *Performance of Flat Plate Collectors with Two-Positional Active Tracking*, Department of Civil and Mechanical Engineering, United States Military Academy, West Point, NY 10996, USA

Taylor, AB, Gunaselvam, J, Bester, W and Stone, A (2002), *Investigation into Reducing the Impact of Diesel Engines on the Antarctic Environment with Associated Maintenance Benefits*, Department of Mechanical Engineering, University of Stellenbosch

Teetz, H (2000), *Heating and Ventilation System Analysis and Redesign of the SANAE IV Base in Antarctica*, BEng Thesis, Department of Mechanical Engineering, University of Stellenbosch

Teetz, H (2002), *Technical and Economic Evaluation of the Utilisation of Wind Energy at the SANAE IV Base in Antarctica*, MSc Thesis, Department of Mechanical Engineering, University of Stellenbosch

Theodora Maps (2005), database of maps from around the world found on the website of Theodora Maps, homepage http://www.theodora.com/maps/

Thermomax (2005), 5560 Sterret Place, Suite 115, Columbia, MD 21044, e-mail info@thermotechs.com, homepage http://www.thermotechs.com

Van Heerden, L (2005), Research operations manager at Eskom Research, Development and Demonstration (Eskom R,D&D), homepage http://www.sabregen.co.za/

Yates, TA (2003), *Solar Cells in Concentrating Systems and Their High Temperature Limitations*, BSc Thesis, Department of Physics, University of California, Santa Cruz

Appendix A: Additional Information to Introduction

A.1 Additional Information

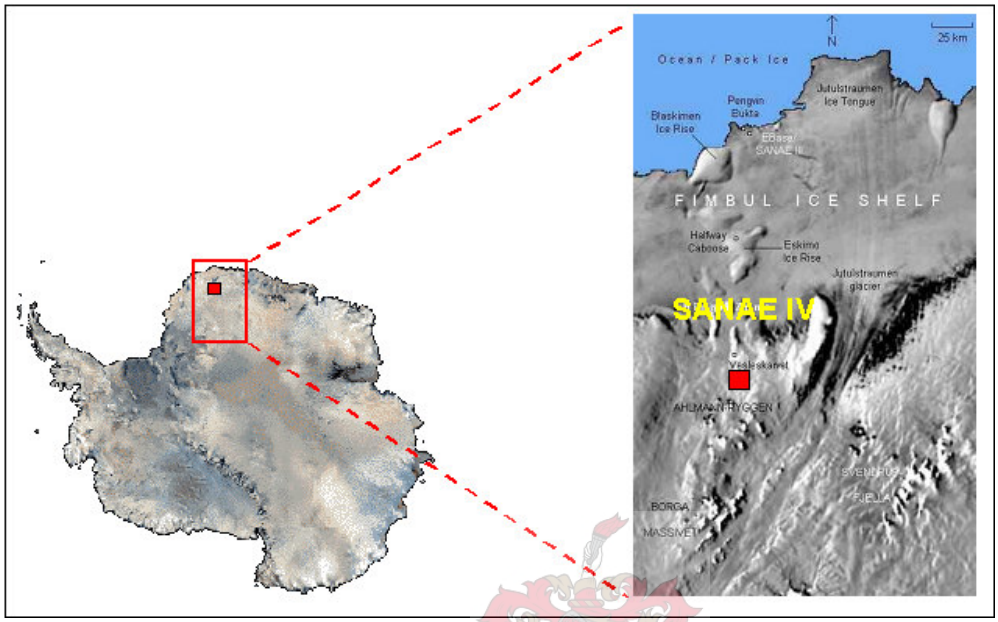

Figure A.1: SANAE IV in Queen Maud Land, Antarctica (Theodora Maps, 2005)

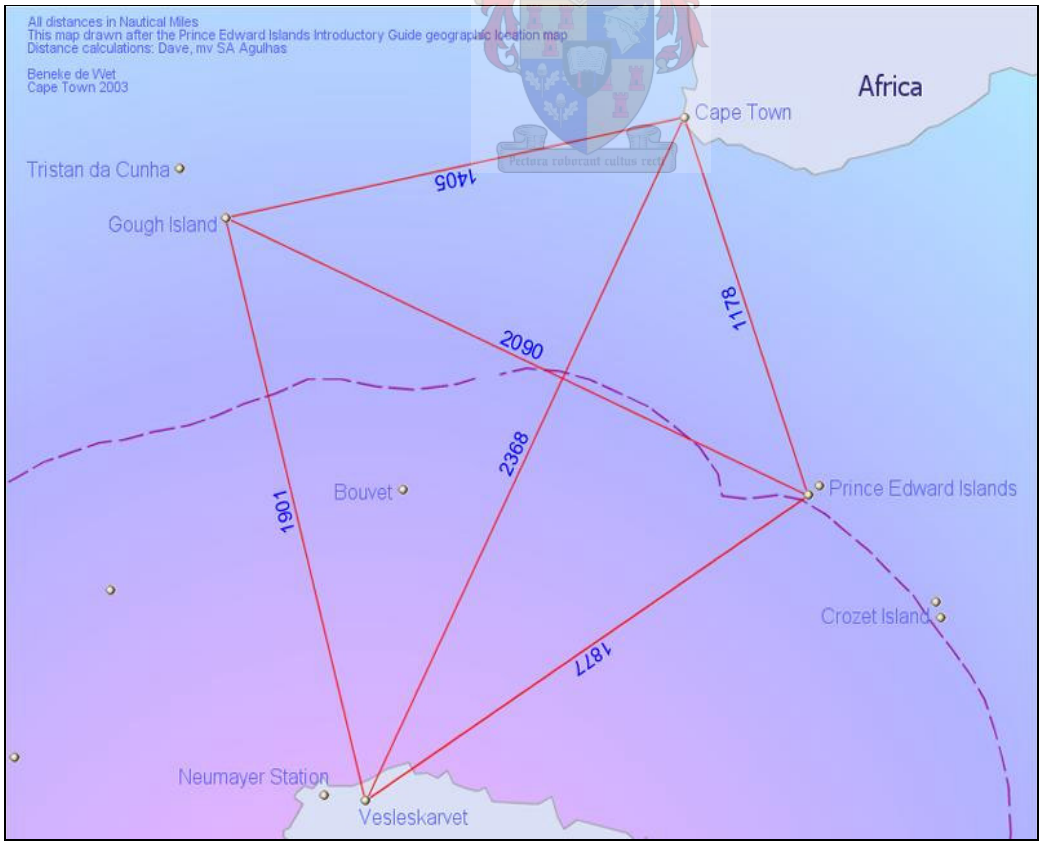

Figure A.2: SANAE IV, distances in Nautical Miles (de Wet, 2005)

Figure A.3: Territorial claims and overwintering stations (Perry-Castañeda, 2005)

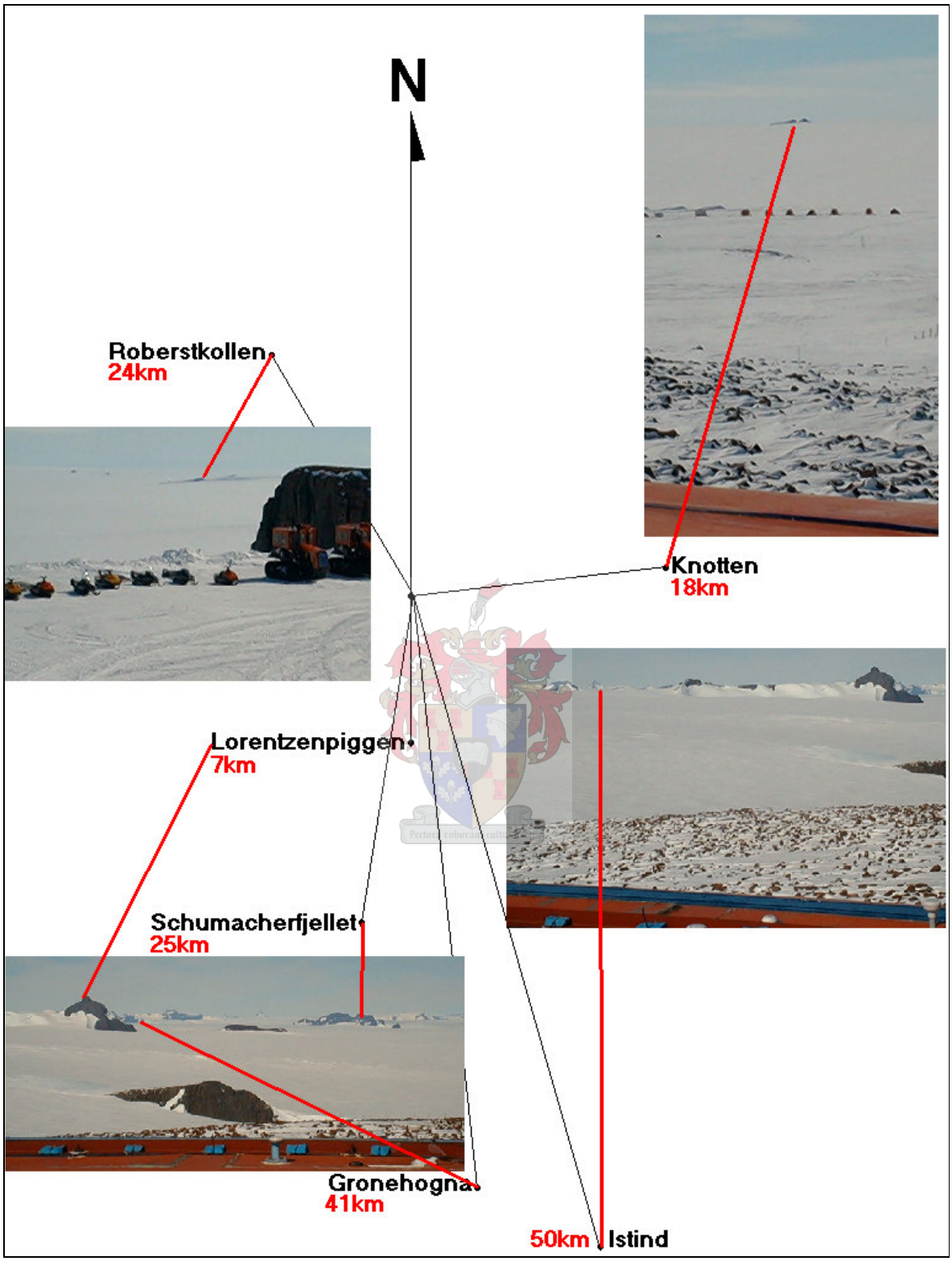

Fig A.4: View from SANAE IV (SANAE IV database, 2005)

Table A.1: Dimensions of SANAE IV

DIMENSION	UNIT	VALUE
BLOCK A		
Length of block	[m]	44.7
Width of block	[m]	12.3
Height of block	[m]	6.5
Area of roof	[m^2]	550.3
Area of sidewalls	[m^2]	707.2
Area of floor	[m^2]	550.3
BLOCK B		
Length of block	[m]	44.7
Width of block	[m]	14.2
Height of block	[m]	6.5
Area of roof	[m^2]	662.0
Area of sidewalls	[m^2]	707.8
Area of floor	[m^2]	662.0
BLOCK C		
Length of block	[m]	44.7
Width of block	[m]	15.3
Height of block	[m]	7.1
Area of roof	[m^2]	682.1
Area of sidewalls	[m^2]	816.5
Area of floor	[m^2]	682.1
CONNECTING BLOCKS		
Length of block	[m]	44.7
Width of block	[m]	12.3
Height of block	[m]	6.5
Area of roof	[m^2]	550.3
Area of sidewalls	[m^2]	707.2
Area of floor	[m^2]	550.3

A.2 Excerpt From the Antarctic Treaty of 1959 (SCAR, 2005)

"The Governments of Argentina, Australia, Belgium, Chile, the French Republic, Japan, New Zealand, Norway, the Union of South Africa, the Union of Soviet Socialist Republics, the United Kingdom of Great Britain and Northern Ireland, and the United States of America,

Recognizing that it is in the interest of all mankind that Antarctica shall continue for ever to be used exclusively for peaceful purposes and shall not become the scene or object of international discord;

Acknowledging the substantial contributions to scientific knowledge resulting from international cooperation in scientific investigation in Antarctica;

Convinced that the establishment of a firm foundation for the continuation and development of such cooperation on the basis of freedom of scientific investigation in Antarctica as applied during the International Geophysical Year accords with the interests of science and the progress of all mankind;

Convinced also that a treaty ensuring the use of Antarctica for peaceful purposes only and the continuance of international harmony in Antarctica will further the purposes and principles embodied in the Charter of the United Nations;

Have agreed as follows:

Article I

1. *Antarctica shall be used for peaceful purposes only. There shall be prohibited, inter alia , any measure of a military nature, such as the establishment of military bases and fortifications, the carrying out of military manoeuvres, as well as the testing of any type of weapon.*

2. *The present Treaty shall not prevent the use of military personnel or equipment for scientific research or for any other peaceful purpose.*

Article II

Freedom of scientific investigation in Antarctica and cooperation toward that end, as applied during the International Geophysical Year, shall continue, subject to the provisions of the present Treaty.

Article III

1. *In order to promote international cooperation in scientific investigation in Antarctica, as provided for in Article II of the present Treaty, the Contracting Parties agree that, to the greatest extent feasible and practicable:*

a. *information regarding plans for scientific programs in Antarctica shall be exchanged to permit maximum economy of and efficiency of operations;*

b. *scientific personnel shall be exchanged in Antarctica between expeditions and stations;*

c. *scientific observations and results from Antarctica shall be exchanged and made freely available."*

A.3 Excerpt From the Protocol on Environmental Protection to the Antarctic Treaty of 1991 (Madrid Protocol, 1991)

"The States Parties to this Protocol to the Antarctic Treaty, hereinafter referred to as the Parties,

Convinced of the need to enhance the protection of the Antarctic environment and dependent and associated ecosystems;

Convinced of the need to strengthen the Antarctic Treaty system so as to ensure that Antarctica shall continue forever to be used exclusively for peaceful purposes and shall not become the scene or object of international discord;

Bearing in mind the special legal and political status of Antarctica and the special responsibility of the Antarctic Treaty Consultative Parties to ensure that all activities in Antarctica are consistent with the purposes and principals of the Antarctic Treaty;

Recalling the designation of Antarctica as a Special Conservation Area and other measures adopted under the Antarctic Treaty system to protect the Antarctic environment and dependent and associated ecosystems;

Acknowledging further the unique opportunities Antarctica offers for scientific monitoring of and research on processes of global as well as regional importance;

Reaffirming the conservation principles of the Convention on the Conservation of Antarctic Marine Living Resources;

Convinced that the development of a Comprehensive regime for the protection of the Antarctic environment and dependent and associated ecosystems is in the interest of mankind as a whole;

Desiring to supplement the Antarctic Treaty to this end;

Have agreed as follows:

Article 2

Objective and Designation

The Parties commit themselves to the comprehensive protection of the Antarctic environment and dependent and associated ecosystems and hereby designate Antarctica as a natural reserve, devoted to peace and science."

Appendix B: Radiation Calculations

B.1 Predicted Available Average Radiation at SANAE IV

The following equations have been derived by increasing radiation levels suggested by SSE (2005) with 20 %, as explained in sections 2.3.3 and 2.4.

For January (where x is any number from 0 to 24):

$$G = -0.0003187 \cdot x^6 + 0.024072 \cdot x^5 - 0.64063 \cdot x^4 + 6.8013 \cdot x^3 - 22.662 \cdot x^2 + 33.863 \cdot x + 6.5175 \quad B.1$$

$$Gd = -0.0001608 \cdot x^6 + 0.012169 \cdot x^5 - 0.32434 \cdot x^4 + 3.4278 \cdot x^3 - 11.02 \cdot x^2 + 16.759 \cdot x + 11.998 \quad B.2$$

For February (where x is any number from 3.493 to 21.360):

$$G = -0.0012182 \cdot x^6 + 0.090864 \cdot x^5 - 2.5999 \cdot x^4 + 35.673 \cdot x^3 - 245.63 \cdot x^2 + 866.61 \cdot x - 1219.3 \quad B.3$$

$$Gd = -0.0007333 \cdot x^6 + 0.054576 \cdot x^5 - 1.5697 \cdot x^4 + 21.958 \cdot x^3 - 158.09 \cdot x^2 + 597.99 \cdot x - 899.57 \quad B.4$$

For March (where x is any number from 5.860 to 18.760):

$$G = -0.0025561 \cdot x^5 + 0.25082 \cdot x^4 - 8.521 \cdot x^3 + 114.08 \cdot x^2 - 640.82 \cdot x + 1230.9 \quad B.5$$

$$Gd = -0.0012648 \cdot x^5 + 0.10078 \cdot x^4 - 2.9637 \cdot x^3 + 36.676 \cdot x^2 - 163.52 \cdot x + 193.12 \quad B.6$$

For April (where x is any number from 8.193 to 16.193):

$$G = -0.0026532 \cdot x^5 + 0.2618 \cdot x^4 - 8.9646 \cdot x^3 + 132.14 \cdot x^2 - 826.19 \cdot x + 1748.4 \quad B.7$$

$$Gd = -0.0022056 \cdot x^5 + 0.10044 \cdot x^4 - 1.6247 \cdot x^3 + 5.1313 \cdot x^2 + 115.6 \cdot x - 768.2 \quad B.8$$

For May (where x is any number from 10.590 to 13.657):

$$G = -8.2884 \cdot 10^{-14} x^4 + 4.0637 \cdot 10^{-12} \cdot x^3 - 2.483 \cdot x^2 + 60.204 \cdot x - 359.08 \quad B.9$$

$$Gd = -0.0020699 \cdot x^4 + 0.1488 \cdot x^3 - 5.3644 \cdot x^2 + 79.098 \cdot x - 386.72 \quad B.10$$

For June and July (where x is any number from 11.999 to 12.001):

$$G = 0 \qquad B.11$$

$$Gd = 0 \qquad B.12$$

For August (where x is any number from 8.867 to 15.667):

$$G = 2.3785 \cdot 10^{-15} \cdot x^4 - 1.5383 \cdot 10^{-13} \cdot x^3 - 3.4373 \cdot x^2 + 84.331 \cdot x - 477.51 \qquad B.13$$

$$Gd = -0.063729 \cdot x^4 + 3.1409 \cdot x^3 - 59.386 \cdot x^2 + 509.44 \cdot x - 1643.5 \qquad B.14$$

For September (where x is any number from 6.5582 to 17.665):

$$G = -0.0014105 \cdot x^5 + 0.26263 \cdot x^4 - 10.501 \cdot x^3 + 162.37 \cdot x^2 - 1030.1 \cdot x + 2269.8 \qquad B.15$$

$$Gd = 0.06291 \cdot x^4 - 2.9828 \cdot x^3 + 46.624 \cdot x^2 - 265.9 \cdot x + 465.31 \qquad B.16$$

For October (where x is any number from 4.005 to 20.100):

$$G = -0.0015866 \cdot x^6 + 0.11482 \cdot x^5 - 3.2308 \cdot x^4 + 44.536 \cdot x^3 - 317.69 \cdot x^2 + 1181.3 \cdot x - 1785.9 \qquad B.17$$

$$Gd = -0.0008765 \cdot x^6 + 0.06435 \cdot x^5 - 1.8296 \cdot x^4 + 25.799 \cdot x^3 - 191.5 \cdot x^2 + 751.82 \cdot x - 1194.3 \qquad B.18$$

For November (where x is any number from 0 to 24):

$$G = -0.00049941 \cdot x^6 + 0.035343 \cdot x^5 - 0.88544 \cdot x^4 + 8.9745 \cdot x^3 - 29.957 \cdot x^2 + 39.632 \cdot x + 4.4457 \qquad B.19$$

$$Gd = -0.00025896 \cdot x^6 + 0.018308 \cdot x^5 - 0.45638 \cdot x^4 + 4.5441 \cdot x^3 - 14.133 \cdot x^2 + 17.913 \cdot x + 7.9901 \qquad B.20$$

For December (where x is any number from 0 to 24):

$$G = -1.6487 \cdot 10^{-8} \cdot x^{10} + 1.9982 \cdot 10^{-6} \cdot x^9 - 9.8769 \cdot 10^{-5} \cdot x^8 + 0.0025415 \cdot x^7 - \ldots.$$

$$\ldots.0.035956 \cdot x^6 + 0.27337 \cdot x^5 - 1.094 \cdot x^4 + 3.0168 \cdot x^3 - 4.9394 \cdot x^2 + 25.783 \cdot x + 29.969 \qquad B.21$$

$$Gd = -3.8755 \cdot 10^{-9} \cdot x^{10} + 5.001 \cdot 10^{-7} \cdot x^9 - 2.5358 \cdot 10^{-5} \cdot x^8 + 0.00063774 \cdot x^7 - \ldots.$$

$$\ldots.0.0080792 \cdot x^6 + 0.043821 \cdot x^5 - 0.049655 \cdot x^4 + 0.21121 \cdot x^3 - 1.6514 \cdot x^2 + 16.667 \cdot x + 25.387 \qquad B.22$$

B.2 MATLAB V6.1 Programmes Used to Calculate Insolation and Radiation at SANAE IV on a Tilted Surface

B.2.1 Programme used to calculate Insolation at SANAE IV on a tilted surface

```
%%-------------------------------------------------------------------------------------------------------------%%
%%  PROGRAMME TO ESTIMATE INSOLATION ON A TILTED PLANE AT SANAE IV              %%
%%-------------------------------------------------------------------------------------------------------------%%
%This programme provides the basic code for calculating what happens when a solar collecting surface
%at SANAE IV is tilted away from the horizontal using isotropic and anisotropic sky conditions.
%The algorithm can be found in Duffie and Beckman (1991, pg.109 and onwards)

%%-----------------------------------------------------------------------%%
%%  Define all the variables                                             %%
%%-----------------------------------------------------------------------%%
%Haverage: is the global radiation value on the horizontal surface that will be transformed to a value on a tilted surface
%Hdaverage: is the diffuse radiation value on the horizontal surface that will be transformed to a value on a tilted surface
%day: is any day of that month under consideration, where the correct day is calculated from F_DayOfTheYear.m (Duffie and Beckman, 1991,
pg 14)
%roug: is the ground reflectivity (high due to snow cover)
%gam: is the surface azimuth angle (where 0=pointing South and 180=pointing North)
%phi: is the latitude of SANAE IV
%month: is that month of the year under consideration (1=January)
%Angle: is the collector tilt angle
%n: is the correct day is calculated from F_DayOfTheYear.m (Duffie and Beckman, 1991, pg 14)
%decl: is the earth's declination from the solar plane on the given day
%thetazd: is the zenith angle of the sun in degrees (Duffie and Beckman, 1991, pg. 13)
%gammaS: is the solar azimuth angle in degrees (Duffie and Beckman, 1991, pg. 13)
%omegaS: is the sunset hour angle in degrees
%w: is the hour angle in degrees

%%-----------------------------------------------------------------------------%%
%%  Preliminary calculations (used in all sub-portions of code)          %%
%%-----------------------------------------------------------------------------%%
close all
clear all
clc

%Estimated monthly-average daily values for Januray that will be used to calculate what the value on the
%tilted plane is. See appendix B1.
Haverage=[7.3 3.98 1.78 0.60 0.01 0.00 0.00 0.15 1.28 3.25 5.17 6.48]*1000*3600;    %In J/m^2
Hdaverage=[4.36 1.64 0.84 0.21 0 0 0 0 0.54 1.27 2.13 2.66]*1000*3600;              %In J/m^2
day=17;
month=1;

        %%-------------------------------------------------------------------------------------------------------------%%
        %%                                                                                                           %%
        %%    HOURLY-TOTAL ALGORITHMS OF ISOTROPIC AND ANISOTROPIC CONDITIONS                                        %%
        %%                                                                                                           %%
        %%-------------------------------------------------------------------------------------------------------------%%

%%-----------------------------------------------------------------------------%%
%%  Calculate the 3Hrly diffuse radiation using the Neumeyer 5-yr averages %%
%%-----------------------------------------------------------------------------%%
%Define all the neacessary initial and input conditions below
datenumber=datenum([2005,month,day,0,0,0]);
Beta=0:10:140;
dt=1/3600;          %This is a VERY IMPORTANT parameter in the logic that follows. The timestep is exactly a second long, therefore...
                %...when integrating W/m^2 no factor has to be applied and the SUM function can simply be used

%Determine the diffuse radiation for every hour of the day...
x1=0:1/3600:0.5;
[G,Gd,x]=F_MonthlyProfiles(month,x1);
for j=1:23;
   x1=j-0.5:1/3600:j+0.5;
   [G,Gd,x]=F_MonthlyProfiles(month,x1);
   I(j+1)=sum(G);
   Id(j+1)=sum(Gd);
end
```

```
%%-------------------------------------------------------------------------%%
%%  For the anisotropic sky conditions (Duffie pg.99)                      %%
%%-------------------------------------------------------------------------%%
%Following is code that illustrates the use of the Perez et al. model
s=1;
roug=[0.1:0.7:1];
for R=roug          %roug;         %Various reflectances are investigated
   t=1;
   for Bet=Beta    %Beta    %And various tilt angles are investigated
      for j=0:1:23
         q=datenum([2005,month,day,j,0,0]);
         if (Id(j+1)>0)
            [It(j+1),Idt(j+1),Ibt(j+1)]=F_TiltANISOSKY(q,Bet,I(j+1),Id(j+1),R,180);   %Assumes isotropic-sky conditions
         else
            It(j+1)=0; Idt(j+1)=0; Ibt(j+1)=0;
         end
      end
      Htilt(t,s)=sum(It);
      Htiltd(t,s)=sum(Idt);
      Hbeam(t,s)=sum(Ibt);
      t=t+1;
   end
   s=s+1;
end
%Also plot the results
Htilt=Htilt/1e6;
Htiltd=Htiltd/1e6;
Hbeam=Hbeam/1e6;

figure(100)
hold on
for i=1:length(roug)
   %Plot the total insolation
   plot(Beta,Htilt(:,i))
   %Plot the beam radiation
   % plot(Beta,Hbeam(:,i),'r-')
   %Plot the diffuse insolation
   % plot(Beta,Htiltd(:,i),'k-')
end
plot(Beta,Htilt(:,1))
grid on
xlabel('Slope of Collector Surface {\beta}'), ylabel('Insolation [MJ/m^2]')
%axis([0 Beta(end) 0 35])

%Find the maximums of the global horisontla radiation series'
for i=1:length(Htilt(1,:))
   [maxesR,maxesC]=max(Htilt(:,i));
   [maxesRb,maxesCb]=max(Hbeam(:,i));
   [maxesRd,maxesCd]=max(Htiltd(:,i));
   % plot(Beta(maxesC),maxesR,'rv',Beta(maxesCb),maxesRb,'rv',Beta(maxesCd),maxesRd,'rv')
end
hold off

%For the highest ground reflectivity under investigation...
disp(['the avialable global insolation on the horizontal surface is: '])
disp([num2str(Htilt(1,1)*1000/3600), ' kWh'])

disp(['the avialable beam insolation on the horizontal surface is: '])
disp([num2str(Hbeam(1,1)*1000/3600), ' kWh'])

disp(['the optimum global insolation tilt angle is: '])
disp([num2str(Beta(maxesC)), ' degrees'])

disp(['the optimum beam tilt angle is: '])
disp([num2str(Beta(maxesCb)), ' degrees'])

disp(['the avialable global insolation on the tilted surface is: '])
disp([num2str(maxesR*1000/3600), ' kWh'])

disp(['the avialable beam insolation on the tilted surface is: '])
disp([num2str(maxesRb*1000/3600), ' kWh'])
```

```
%%-------------------------------------------------------------------------%%
%%  For the isotropic sky conditions (Duffie pg.94)                        %%
%%-------------------------------------------------------------------------%%
%Now calculate the total insolation on a tilted panel with the relevant hourly I and Id values
s=1;
roug=0.5:0.5:1;
for R=roug;        %Various reflectances are investigated
   t=1;
   for Bet=Beta    %And various tilt angles are investigated
      for j=0:1:23
         q=datenum([2005,month,day,j,0,0]);
         [It(j+1),Idt(j+1)]=F_TiltISOSKY(q,Bet,I(j+1),Id(j+1),R,180);   %Assumes isotropic-sky conditions
      end
      Htilt(t,s)=sum(It);
      Htiltd(t,s)=sum(Idt);
      t=t+1;
   end
   s=s+1;
end
%Also plot the results
Htilt=Htilt/1e6;
Htiltd=Htiltd/1e6;
figure(200)
grid on
for i=1:length(roug)
   hold on
   plot(Beta,Htilt(:,i),'b-')
   hold off
end
xlabel('Slope of Collector Surface {\beta}'), ylabel('Insolation [MJ/m^2]')
axis([0 Beta(end) 0 35])
%axis([Beta(1) Beta(end) 0 35]);
```

B.2.2 Programme used to calculate Radiation at SANAE IV on a tilted surface

```
%%-------------------------------------------------------------------------%%
%%  PROGRAMME TO COMPUTE  INSTANTANEOUS RADIATION AT SANAE IV ON A TILTED PLANE   %%
%%-------------------------------------------------------------------------%%
%This programme provides the basic code for calculating what happens when a solar collecting surface
%at SANAE IV that is tilted away from the horizontal using isotropic and anisotropic sky conditions.
%The algorithm can be found in Duffie and Beckman (1991, pg.109 and onwards)
close all
clear all
clc

%%-------------------------------------------------------------------------%%
%%  Preliminary calculations (used in all sub-portions of code)            %%
%%-------------------------------------------------------------------------%%
%Define all the necessary initial and input conditions below
dt=1;
A=0.840;
month=1;
day=15;
%Beta=70;
Beta=[52 63 74 84 86 86 86 88 78 69 52 48]; %Which are the optimum tilt angles of every month
gamma=180;
flag1=1; %Determines whether the Hottel clear-sky prediction is used (flag=1, only valid for January), or the measured global horizontal data
flag2=0; %Determines whether the Anisotropic (flag2=0) or isotropic conditions must be used for tilting the collector
flag3=0; %Determines whether measured data must be plotted (flag3=1)
flag4=0; %Determines whether the average radiation profiles must be used (flag4=1) instead of Hottel

        %%-------------------------------------------------------------------------%%
        %%                                                                         %%
        %%    INSTANTANEOUS ALGORITHMS OF ISOTROPIC AND ANISOTROPIC CONDITIONS     %%
        %%                                                                         %%
        %%-------------------------------------------------------------------------%%


if (flag1==1) & (flag4==0)     %If it is desired that the Hottel clear-sky correlation is used
```

```
%%-------------------------------------------------------------------------%%
%%  Determine the clear-sky radiation on the given day                     %%
%%-------------------------------------------------------------------------%%
%Hottel and Liu and Jordan clear sky models
A0Star=0.4237-0.00821*(6-A)^2;
A1Star=0.5055+0.00595*(6.5-A)^2;
KStar=0.2711+0.01858*(2.5-A)^2;
r0=0.99;
r1=0.99;
rk=1.02;
a0=r0*A0Star;
a1=r1*A1Star;
k=rk*KStar;
kk=0.45*KStar; %NOTE: This is a personal fit of the extinction co-efficient

%The beam transmittance and horizontal beam radiation is calculated as...
s=1;
q=datenum(2005,month,day,0,0,0);    %The day of the year under investigation
stepsize=1/24/60;
for i=q:stepsize:q+1
   [zenithd,gammaS,b]=F_SolarAngles(i);
   n=F_DayOfTheYear(q);

   taub=a0+a1*exp(-k/cos(zenithd*pi/180));
   taubb=a0+a1*exp(-kk/cos(zenithd*pi/180)); %This is a personal fit of the extinction co-efficient
   Gon=1367*(1+0.033*cos(360*n/365*pi/180));
   Gcb(s)=Gon*taub*cos(zenithd*pi/180);
   Gcbb(s)=Gon*taubb*cos(zenithd*pi/180); %This is a personal fit of the extinction co-efficient

   taud=0.271-0.294*taub;
   Gd(s)=taud*1367*(1+0.033*cos(360*n/365*pi/180))*cos(zenithd*pi/180);

   s=s+1;
end

%The total horizontal radiation is defined as the sum of the clear-sky beam
%and the clear sky diffuse
Gtot=Gcbb+Gd; %This is a personal fit of the extinction co-efficient
%Now make a x-axis vector for plotting that runs from 0 to 1 (a day in length)
r=length(Gtot);
ex=(0:1/(r-1):1)*24;
elseif (flag1==0) & (flag4==0)
%Retrieve the measured data on the relevant day
[M]=D_DataCompareMain(day);
M(:,1:2:end)=M(:,1:2:end)*24;
for i=1:length(M(:,1))
   if M(i,1)>=24
      M(i,1:2:end)=M(i,1:2:end)-24;
   end
end
Gtot=M(:,2);
Gd=M(:,6);
r=length(Gtot);
ex=M(:,1)';
elseif flag4==1;
ex=0:1/60*10:24;
[Gtot,Gd,ex]=F_MonthlyProfiles(month,ex);
end

%%-------------------------------------------------------------------------%%
%%  For the isotropic sky conditions (Duffie pg.99)                        %%
%%-------------------------------------------------------------------------%%
%Following is code that illustrates the use of the Perez et al. model
s=1;
for R=0.7;        %Various reflectances are investigated
   t=1;
   for Bet=Beta(month)    %And various tilt angles are investigated
      p=1;
      for x=ex
         hourr=floor(x);
         minn=floor((x-floor(x))*60);
         secc=(x-hourr-minn/60)*3600;
         q=datenum([2005,1,day,hourr,minn,secc]);
         if flag2==0
            [Gt(p),Gdt(p),Gbt(p)]=F_TiltANISOSKY(q,Bet,Gtot(p),Gd(p),R,gamma);   %Assumes anisotropic-sky conditions
         elseif flag2==1
```

```
            [Gt(p),Gdt(p),Gbt(p)]=F_TiltISOSKY(q,Bet,Gtot(p),Gd(p),R,gamma);   %Assumes isotropic-sky conditions
          end
          p=p+1;
       end
       t=t+1;
    end
    s=s+1;
end

if flag3==1
    figure(300)
    %Plot the daily profile of the tilted surface
    hold on
    plot(M(:,1),M(:,2),'bv','markersize',3)
    plot(ex,Gt,'r.','markersize',3)
    plot(M(:,13),M(:,14),'bo','markersize',3), grid on
    %plot(M(:,1),M(:,2))
    hold off
    xlabel('Time of day (in hours from midnight)'), ylabel('Radiation [W/m^2]')
    legend('Measured global horizontal radiation','Predicted radiation at tilt angle', 'Measured radiation at tilt angle')
    axis([0 24 0 1600])

    %Caclulate the percentage difference between predicted and measured curves
    xx=0:1/3600:24;
    yy1=spline(M(:,13),M(:,14),xx);
    tot1=sum(Gt);
    yy2=spline(ex,Gt,xx);
    tot2=sum(M(:,14));
    percentage=tot2/tot1*100
else
    figure(300)
    %Plot the daily profile of the tilted surface
    hold on
    plot(ex,Gt,'r-','markersize',3)
    %plot(M(:,1),M(:,2))
    hold off
    xlabel('Time of day (in hours from midnight)'), ylabel('Radiation [W/m^2]')
    legend('Predicted radiation at tilt angle')
    axis([0 24 0 1600])
end
```

B.3 MATLAB V6.1 Functions Used in Conjunction with the Programmes in B2 to Calculate Radiation on a Tilted Surface

B.3.1 Function F_TiltANISOSKY.m

```
function [It,Idt,Ibt]=F_TiltANISOSKY(q,B,I,Id,roug,g)
%%-- Duffie and Beckman (John Wiley and Sons, Inc., 1991, pg 97)
%This programme calculates the amount of insolation incident on a tilted surface if the
%Perez et al. anisotropic sky (1988) method is used. NB - Input values are in J/m^2.

%%-------------------------------------------------------------------------%%
%%  Convert the daynumber to its component values                          %%
%%-------------------------------------------------------------------------%%
[datenumber]=F_SolarTime(q);
[y,month,day,h,mn,s]=datevec(datenumber);

%%-------------------------------------------------------------------------%%
%%  Main Programme                                                         %%
%%-------------------------------------------------------------------------%%
Ib=I-Id;
if I<=Id
    I=Id;
    Ib=0;
end

%Calculate the values required for determining Rb
phi=-71.67305556;
```

```
n=F_DayOfTheYear(datenumber);
decl=23.45*sin(pi/180*360*(284+n)/365);

%Calculate the hour angle (equals 15 degrees per hour).
[thetazd,gammaS,omegaS,w]=F_SolarAngles(datenumber);

%Convert to radians
declR=decl*pi/180;
phiR=phi*pi/180;
wR=w*pi/180;
BR=B*pi/180;
thetazR=thetazd*pi/180;
gR=g*pi/180+pi; %The "+180" is to correct for a convention that says 0=pointing South
gsR=gammaS*pi/180;

% %Calculate Rb - RETScreen method (...doesn't seem to work)
% denominator=cos(thetazR);
% gsR=asin(sin(wR)*cos(declR)/sin(thetazR));
% numerator=cos(thetazR)*cos(BR)+(1-cos(thetazR))*(1-cos(BR))*(cos(gsR-gR));
% Rb=numerator/denominator;

% %Calculate Rb - Duffie method (...works when predicting instantaneous radiation values)
% numerator=cos(phiR+BR)*cos(declR)*cos(wR)+sin(phiR+BR)*sin(declR);
% denominator=cos(thetazR);
% Rb=numerator/denominator;

%Calculate Rb - Duffie method (...works when predicting instantaneous radiation values)
numerator=cos(thetazR)*cos(BR)+sin(thetazR)*sin(BR)*cos(gsR-gR);
denominator=cos(thetazR);
Rb=numerator/denominator;

% %Calculate Rb - Duffie extended method (...works when predicting instantaneous radiation values)
% gammasd=180/pi*(atan(sin(wR)/(sin(phiR)*cos(wR)-cos(phiR)*tan(declR))));
% omegaew=180/pi*(acos(tan(declR)/tan(phiR)));
% if abs(w)<omegaew
%     C1=1;
% else
%     C1=-1;
% end
% if (phi*(phi-decl))>=0
%     C2=1;
% else
%     C2=-1;
% end
% if w>=0
%     C3=1;
% else
%     C3=-1;
% end
% if abs(tan(declR)/tan(phiR))>1
%     C1=1;
% end
% gsR=(C1*C2*gammasd+C3*((1-C1*C2)/2)*180)*pi/180;
% numerator=cos(thetazR)*cos(BR)+sin(thetazR)*sin(BR)*cos(gsR-gR);
% denominator=cos(thetazR);
% Rb=numerator/denominator;

if Rb<0
   Rb=0;
end
%Calculate the total insolation on the tilted surface
a=max([0,cos(thetazR)]);
b=max([cos(85*pi/180),cos(thetazR)]);

In=Rb*I;
epsilon=(((Id+In)/Id)+(5.535e-6)*thetazd^3)/(1+(5.535e-6)*thetazd^3);
m=1/cos(thetazR);
Ion=4.921e6*(1+0.0333*cos(pi/180*360*n/365));
delta=m*Id/Ion;

if 0<=epsilon & epsilon<1.065
   f11=-0.196; f12=1.084; f13=-0.006; f21=-0.114; f22=0.180; f23=-0.019;
elseif 1.065<=epsilon & epsilon<1.230
   f11=0.236; f12=0.519; f13=-0.180; f21=-0.011; f22=0.020; f23=-0.038;
elseif 1.230<=epsilon & epsilon<1.500
   f11=0.454; f12=0.321; f13=-0.255; f21=0.072; f22=-0.098; f23=-0.046;
```

```
elseif 1.500<=epsilon & epsilon<1.950
   f11=0.866; f12=-0.381; f13=-0.375; f21=0.203; f22=-0.403; f23=-0.049;
elseif 1.950<=epsilon & epsilon<2.800
   f11=1.026; f12=-0.711; f13=-0.426; f21=0.273; f22=-0.602; f23=-0.061;
elseif 2.800<=epsilon & epsilon<4.500
   f11=0.978; f12=-0.986; f13=-0.350; f21=0.280; f22=-0.915; f23=-0.024;
elseif 4.500<=epsilon & epsilon<6.200
   f11=0.784; f12=-0.913; f13=-0.236; f21=0.173; f22=-1.045; f23=0.065;
elseif 6.200<=epsilon
   f11=0.318; f12=-0.757; f13=0.103; f21=0.062; f22=-1.698; f23=0.236;
end

F1=max([0,(f11+f12*delta+thetazR*f13)]);
F2=f21+f22*delta+thetazR*f23;

Ibt=Ib*Rb;
It=Ib*Rb+Id*(1-F1)*((1+cos(BR))/2)+Id*F1*a/b+Id*F2*sin(BR)+I*roug*((1-cos(BR))/2);
%Idt=Id*((1-F1)*((1+cos(BR))/2)+F1*a/b+F2*sin(BR));
Idt=It-Ibt;
```

B.3.2 Function F_TiltISOSKY.m

```
function [Itot,Idt,Ibt]=F_TiltISOSKY(datenumber,B,I,Id,roug,g)
%%-- Duffie and Beckman (John Wiley and Sons, Inc., 1991, pg 94)
%This programme calculates the amount of insolation incident on a tilted surface if the
%Liu and Jordan isotropic sky (1960) method is used. NB - Input values are in J/m^2.

%%-------------------------------------------------------------------------%%
%%  Convert the daynumber to its component values                          %%
%%-------------------------------------------------------------------------%%
[datenumber]=F_SolarTime(datenumber);
[y,month,day,h,mn,s]=datevec(datenumber);

%%-------------------------------------------------------------------------%%
%%  Main Programme                                                         %%
%%-------------------------------------------------------------------------%%
Ib=I-Id;
if I<=Id
   I=Id;
   Ib=0;
end

%Calculate the values required for determining Rb
phi=-71.67305556;
n=F_DayOfTheYear(datenumber);
decl=23.45*sin(pi/180*360*(284+n)/365);

%Calculate the hour angle (equals 15 degrees per hour).
[thetazd,gammaS,omegaS,w]=F_SolarAngles(datenumber);

%Convert to radians
declR=decl*pi/180;
phiR=phi*pi/180;
wR=w*pi/180;
BR=B*pi/180;
thetazR=thetazd*pi/180;
gR=g*pi/180+pi; %The "+180" is to correct for a convention that says 0=pointing South;
gsR=gammaS*pi/180;

% %Calculate Rb - RETScreen method (...doesn't seem to work for Southern Hemisphere)
% denominator=cos(thetazR);
% gsR=asin(sin(wR)*cos(declR)/sin(thetazR));
% numerator=cos(thetazR)*cos(BR)+(1-cos(thetazR))*(1-cos(BR))*(cos(gsR-gR));
% Rb=numerator/denominator;

%Calculate Rb - Duffie method (...works when predicting instantaneous radiation values)
numerator=cos(phiR+BR)*cos(declR)*cos(wR)+sin(phiR+BR)*sin(declR);
denominator=cos(thetazR);
Rb=numerator/denominator;

% %Calculate Rb - Duffie method (...works when determining instantaneous radiation values)
% numerator=cos(thetazR)*cos(BR)+sin(thetazR)*sin(BR)*cos(gsR-gR);
% denominator=cos(thetazR);
```

```
% Rb=numerator/denominator;

% %Calculate Rb - Duffie extended method (...works when determining instantaneous radiation values)
% gammasd=180/pi*(atan(sin(wR)/(sin(phiR)*cos(wR)-cos(phiR)*tan(declR))));
% omegaew=180/pi*(acos(tan(declR)/tan(phiR)));
% if abs(w)<omegaew
%     C1=1;
% else
%     C1=-1;
% end
% if (phi*(phi-decl))>=0
%     C2=1;
% else
%     C2=-1;
% end
% if w>=0
%     C3=1;
% else
%     C3=-1;
% end
% if abs(tan(declR)/tan(phiR))>1
%     C1=1;
% end
% gsR=(C1*C2*gammasd+C3*((1-C1*C2)/2)*180)*pi/180;
% numerator=cos(thetazR)*cos(BR)+sin(thetazR)*sin(BR)*cos(gsR-gR);
% denominator=cos(thetazR);
% Rb=numerator/denominator;

if Rb<0
   Rb=0;
end
%Calculate the total insolation on the tilted surface
Ibt=Ib*Rb;
Irt=I*roug*((1-cos(BR))/2); %The reflected component
Idt=Id*((1+cos(BR))/2) + Irt;

Itot=Ibt+Idt;
```

Appendix C: Additional Information to SANAE IV Energy Demand

C.1 Heating and Ventilation System Energy Audit

SANAE IV's Heating and Ventilation System (H&V System) is responsible for maintaining comfortable temperatures, humidity levels and good circulation of fresh air in the base. The system does not re-cycle any component of the heated inside air but instead uses only 100 % fresh outside-air. This is an expensive practice, since more heating energy is required, yet one often used in applications where health concerns are significant (such as in operating theatres at hospitals for instance). At SANAE IV the outside air is heated by air-handling units (AHUs), which transfer energy received from the FCU Water System to the fresh air blown in from the outside. Varying the speed of the AHU-fans that blow the outside air past the AHUs can therefore control the station's inside temperature. This is because the amount of energy passing from the FCU Water System into the air is regulated in this manner and the air can be heated to the exact temperature required to offset heat losses from the base.

Cencelli (2002) estimates that the amount of heat lost to the surroundings during summer and winter varies between 39 kW and 72 kW respectively, reaching up to 120 kW during very cold spells (also refer to paragraphs 4 and 5 of section 3.2.2). The processes of conduction through walls, radiative heat transfer and air leakage through poor seals or other openings ultimately cause this heat loss. Fortunately many appliances used in the base (such as computers, lights, kitchen appliances etc.) provide much of the required heat themselves, while the remainder is made up by heating outside air to the required temperature in the AHUs as explained above. With 100 % fresh-air ventilation requirements and the very low ambient temperatures in Antarctica this task of keeping the station warm is nonetheless extremely expensive.

A quick calculation will be performed to determine the energy required by the FCUs. Here Q is the heat load demanded by the H&V System [J] and ΔT is the necessary temperature difference [K] between the supply duct (at temperature T) and room conditions (at temperature T_{inside}).

$$\dot{Q} = \dot{m} \cdot C_p \cdot \Delta T \qquad C.1$$

And,

$$T = \Delta T + T_{inside} \qquad C.2$$

Where T is the temperature of the H&V supply air. Therefore,

$$T = \frac{\dot{Q}}{\dot{m} \times C_p} + T_{inside} \qquad C.3$$

The air leaving the FCU and moving into the supply ducts must be heated from ambient to T, thus the amount of energy required to do this is:

$$\dot{Q}_{FCU} = \dot{m} \times C_p \times (T - T_{ambient}) \qquad C.4$$

However, using equation C.2 for T,

$$\dot{Q}_{FCU} = \dot{m} \times C_p ((\frac{\dot{Q}}{\dot{m} \times C_p} + T_{inside}) - T_{ambient}) \qquad C.5$$

From equation C.5 and values for the variables provided by Cencelli (also given in table C.1) graphs have been created and plotted in figure C.1. It is clear that the most energy-intensive part of the current system is that portion of heating required to bring the cold outside air to room temperature (the y-intercept). Consider the plot of the required FCU thermal summer contribution with 15 % re-circulation (by mass) for instance. A 15 % re-circulation results in a 55 % FCU energy demand reduction.

The present investigation also revealed that a direct link with mass flow-rate and energy requirements exists (i.e. a 10 % reduction or increase in mass flow-rate results in a corresponding 10 % reduction or increase in FCU energy requirements).

Table C.1: A-Block summer and winter conditions suggested by Cencelli (2002)

PARAMETER	SUMMER	WINTER
Estimated heat loss from base due to conduction etc. (kW)	12.6	24.1
Mass flow-rate of air through FCUs (kg/s)	3.23	1.87
Specific heat capacity of air (J/kg.K)	1008	1008
Inside temperature (°C)	22	18
Ambient Temperature (°C)	-10	-55

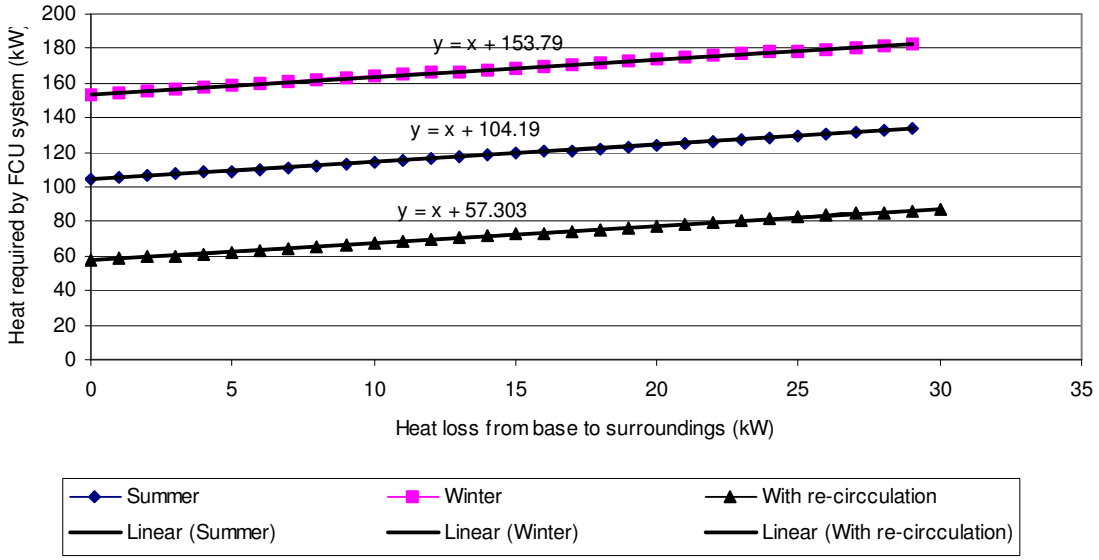

Figure C.1: Contribution required by A-Block FCU to compensate for heat losses from the base

Implementing re-circulation to reduce the FCU energy demand is not practical during the summer, however, even though it is well suited to winter conditions. During the summertime it is necessary to use the H&V System as a means of removing heat from the station (as described in section 3.2.2). A better energy-savings solution would be to control the mass flow-rate instead by running the current FCU-fans at a wider range of speeds in place of, as is currently the case (Cencelli, 2002), just two discreet settings. Furthermore, also note that the FCU-Water System does not presently operate at its set-point temperatures and requires adjustment.

From the discussion above and the information provided in section 3.2.2 it is evident that the H&V System is 180 degrees "out of phase" with the availability of solar energy. During the summer there is ample heat available from the generators to keep the base warm (in fact it is necessary to cool the base) while conversely the winter periods are characterised by cold inside temperatures. With the obvious lack of sunshine during the winter periods it is evident that the Heating and Ventilation System is not an ideal application for the utilisation of solar energy.

The above investigation was not meant as a comprehensive study, but rather as an introduction to the processes of the H&V System. This system is very complex and changes to it should only be considered while simultaneously accounting for the resultant effects on other systems in the station (like for instance the Primary Hot Water System). It is believed that updating the existing computer based simulation programme of SANAE IV (which is entirely separate from the

station's actual control systems and simply models a number of cause and effect relationships at the base) could be very useful in investigating and improving the current performance of SANAE IV.

An energy management and data capture system was once operational at the station, however, difficulties in maintaining the system's hardware have led to its decommissioning. The programme referred to in this instance however is unlike the energy management system and completely based in software. Utilisation of such a programme would mean, firstly, that the entire base operating system will become currently and technically documented. Secondly, this exercise would result in the identification of all the best opportunities for improvements at the base, with a resultant quantification of return on investment. Thirdly, the performance of the base could be monitored constantly and potential problems would therefore be identified soon. It is the opinion of the author that together with the opportunity of ensuring that the base does not lose any heat unnecessarily to the surroundings (through unsealed openings and cracks particularly at the hangar doors, seals around windows and any unplugged cable outlets) such a simulation programme poses a significant opportunity to generate savings.

As an aside, also note that the relative humidity of the base has for a long time been unsatisfactory (Cencelli, 2002). Due to the extremely cold temperatures water vapour in Antarctica tends to freeze and settle out as snow leaving the air dry and uncomfortable. Although humidifiers are installed in all three blocks of the station they exacerbate the problem of water shortages and for this reason are sometimes not used in the summer. However, they only consume a very low 500 W of electrical energy. If one could ensure a greater supply of water to the station then this system could be used more freely and would improve the living conditions at SANAE IV.

C.2 List of Electricity Consuming Devices in SANAE IV (Dec 2004)[¥]

Table C.2: A-Block electricity consumers

A-BLOCK			
SITUATED	**ITEM**	**QUANTITY**	**kW**
Science Lab Top			
	Computers	10	1.56
	Laptops	2	0.13
	Lights (9W)	2	0.02
	Lights (24W)	14	0.34
	Dome Heaters	3	2.50
	Skirting Heaters (0.75 kW)	4	3.00
	UPS	9 amps at 220V	1.56
Science Lab Bottom			
	Computers	10	1.56
	Laptops	4	0.22
	Lights (24W)	32	0.77
	Skirting Heaters (1.5 kW)	1	1.50
	Skirting Heaters (0.75 kW)	6	4.50
	UPS	14 amps at 220V	2.18
Top Passage			
	Lights (9W)	11	0.10
Stairwells			
	Lights (9W)	6	0.05
	Skirting Heaters (0.75 kW)	2	1.50
Top Bedrooms (17 in total)	Lights (9W)	36	0.32
	Lights (24W)	72	1.73
	Computers	0	0.00
	Laptops	6	0.39
	Skirting Heaters (0.75 kW)	18	13.50
Laundry			
	Lights (9W)	0	0.00
	Lights (24W)	8	0.19
	Tumble Dryer (5kW)	2	10.00
	Skirting Heaters (0.75 kW)	1	0.75
	Washing Machine (240V, 5Amps)	2	1.56
Top Men's Bathroom			
	Lights (9W)	14	0.13
Top Ladie's Bathroom			
	Lights (9W)	9	0.08
Bottom Passage			
	Lights (9W)	10	0.09
Bottom Rooms			
	Computers	13	2.02
	Laptops	6	0.39
	Fridge (230V, 0.87Amps)	1	0.14
	Lights (24W)	125	3.00
	Lights (9W)	15	0.14
	Skirting Heaters (0.75 kW)	25	18.75
AB-Link			
	Lights (9W)	27	0.24
	Lights (24W)	12	0.29
	Computers	1	0.16
	Skirting Heaters (1.5 kW)	3	4.50
Heating and Ventilation			
	Fan motor	1	2.20
	Humidifier	1	0.50
	Exhaust fans	1	2.50
	Extraction fan	1	2.50
	Operating theatre	1	0.18
Totals			
	Computers	**34**	**5.29**
	Laptops	**18**	**1.17**
	Lights (9W)	**130**	**1.17**
	Lights (24W)	**263**	**6.31**
	Skirting Heaters (1.5kW)	**4**	**6.00**
	Skirting Heaters (0.75kW)	**56**	**42.00**
	UPS	**14 Amps at 220V**	**2.18**
Graph			
	Heaters		**50.50**
	Lights		**7.48**
	Ventilation and humidification		**7.88**
	Washing machines and driers		**11.56**
	Computers and Laptops		**6.46**

[¥] All data presented in appendix C.2 was collected by the author during the 2004/2005 SANAE IV takeover.

Table C.3: B-Block electricity consumers

B-BLOCK			
SITUATED	**ITEM**	**QUANTITY**	**kW**
Top Passage			
	Lights (9W)	12	0.11
	Fridge (220V, 0.7 Amps)	1	0.11
	Freezer (220V, 0.7 Amps)	1	0.11
Stairwells			
	Lights (9W)	4	0.04
	Skirting Heaters (0.75 kW)	2	1.50
Top TV Lounge			
	Lights (24W)	12	0.29
	Skirting Heaters (0.75 kW)	2	1.50
Top Library			
	Lights (24W)	24	0.58
Top Stores			
	Lights (24W)	8	0.19
	Lights (9W)	4	0.04
	Skirting Heaters (0.75 kW)	2	1.50
Top Bedrooms (11 in total)	Lights (9W)	22	0.20
	Lights (24W)	44	1.06
	Laptops	2	0.13
	Skirting Heaters (0.75 kW)	11	8.25
Laundry			
	Lights (24W)	8	0.19
	Tumble Dryer	3	15.00
	Washing Machine (240V, 5Amps)	3	2.33
Top Men's Bathroom			
	Lights (9W)	20	0.18
Top Ladie's Bathroom			
	Lights (9W)	9	0.08
Bottom Passage			
	Lights (9W)	7	0.06
Bottom Stairwell Stores			
	Lights (9W)	6	0.05
Waste Room			
	Lights (24W)	18	0.43
	Lights (9W)	2	0.02
	Skirting Heaters (0.75 kW)	2	1.50
Bottom TV Lounge			
	Small Spotlights (50W, 2 Amps per 3 lights)	12	3.73
	Lights (24W)	12	0.29
	Skirting Heaters (0.75 kW)	2	1.50
Bottom Bar			
	Small Spotlights (50W, 2 Amps per 3 lights)	19	
	Lights (9W)	1	0.01
	Skirting Heaters (0.75 kW)	1	0.75
	Ice Maker		
	Refrigerator		
Bottom Games Room			
	Small Spotlights (50W, 2 Amps per 3 lights)	2	
	Lights (24W)	31	0.74
	Skirting Heaters (0.75 kW)	2	1.50
Dry Room Store			
	Lights (24W)	15	0.36
	Skirting Heaters (0.75 kW)	2	1.50
Freezer Room			
	Lights (9W)	18	0.16
	Refrigeration Equipment		
	10 HorseP Compressor	*7.46kW*	
	Condensation Fan	*0.37kW*	
	Evaporation Fans	*0.467kW x 3*	
	3/4 HP Compressor	*5.56kW*	
	Evaporation Fans	*0.778kW x 2*	
	Condensation Fan	*0.2kW*	
	Total		11.546
Kitchen			
	Lights (24W)	10	0.24
	Convection Oven (6.5 kW per phase)	1	19.50
	Deep Frier (12kW)	1	12.00
	Snackwich Machine	1	3.00
	Heating Plates (3kW)	1	3.00
	Solid Top Oven (6kW /phase)	1	18.00
	Electric Mixer	2	0.66
	Defy Oven (16 Amps)	1	2.49
Dining Room			
	Lights (9W)	48	0.43
	Skirting Heaters (0.75kW)	6	4.50
	Ice Maker	1	1.00
	Microwave (1.3kW)	1	1.30
	Fridge (0.7 Amp)	1	0.70
	Toaster (3.15 kW)	1	3.15
	Baine Marie	1	2.50
	Drinking Fountain	1	0.20
	Snackwich Machine (2.5kW)	1	2.50
BC-Link			
	Lights (9W)	27	0.24
	Lights (24W)	14	0.34
	Skirting Heaters (1.5 kW)	4	6.00
Heating and Ventilation			
	Fan motor	1	2.20
	Humidifier	1	0.50
	Exhaust fans	2	5.00
	Fresh air supply (kitchen)	1	5.00
	Extraction fan	1	2.50
Totals			
	Lights (9W)	**180**	**1.62**
	Lights (24W)	**196**	**4.70**
	Small Spotlights (50W)	**33**	**10.27**
	Skirting Heaters (0.75kW)	**36**	**27.00**
	Panel Heaters (1.5kW)	**4**	**6.00**
	Freezer Room	**1**	**11.546**
	Kitchen Equipment	**1**	**58.65**
Graph			
	Heaters		**33.00**
	Lights		**16.59**
	Ventilation and Humidification		**15.20**
	Washing machines and driers		**17.33**
	Freezer Room		**11.546**
	Dining Room		**11.35**
	Kitchen		**58.65**

Table C.4: C-Block electricity consumers

C-BLOCK			
SITUATED	**ITEM**	**QUANTITY**	**kW**
Gym			
	Lights (24W)	14	
	Lights (9W)	4	
	Skirting Heaters (0.75W)	4	
Upstairs Passage			
	Lights (9W)	22	
Upstairs Lab			
	Lights (24W)	4	
Upstairs Offices			
	Lights (24W)	22	
	Lights (9W)	0	
	Laptops	2	
	Computers	3	
	Skirting Heaters (0.75W)	3	
Upstairs Stores			
	Lights (24W)	28	
	Lights (65W)	4	
Sauna			
	Lights (24W)	2	
	Lights (9W)	2	
	Sauna (12kW)	1	12.00
Hanger			
	Lights (24W)	32	
Plant Room			
	Lights (24W)	32	
	Lights (58W)	8	
Welding Room			
	Lights (24W)	14	
	Lights (58W)	4	
Daytank Room			
	Lights (20W)	2	
Cat Store			
	Lights (24W)	12	
Sewage Plant			
	Lights (20W)	6	
Downstairs Passage			
	Lights (9W)	3	
Heating and Ventilation			
	Fan motor	1	1.10
	Humidifier	1	0.50
	Exhaust motor (W. purification)	1	2.30
	Hangar Extraction	1	1.10
	Exhaust fan (plantroom)	1	2.20
	Hangar Rejection Unit	1	4.00
Miscellaneous			
	Water purification plant	1	6.75
	Fire System	1	0.08
	Radio Room	1	3.30
Plant Room			
	Primary Hot Water pumps	2	4.00
	Domestic Hot Water pumps	2	1.10
	FCU Water pumps	2	7.50
	Cold Water pumps	2	4.00
Inline heaters			
	Cold water system	1	15.00
	Hot water system	1	15.00
	FCU system	1	90.00
Totals			
	Lights (9W)	**31**	**0.28**
	Lights (20W)	**8**	**0.16**
	Lights (24W)	**160**	**3.84**
	Lights (58W)	**12**	**0.70**
	Lights (65W)	**4**	**0.26**
	Skirting Heaters (0.75kW)	**7**	**5.25**
Graph			
	Heaters		**5.25**
	Lights		**5.24**
	Ventilation and humidification		**11.20**
	Sauna		**12.00**
	Plant room		**16.60**
	Inline heaters		**120.00**
	Snow Smelter		**94.00**

C.3 Graphical Representation of C2 (Electricity Consumption)[¥]

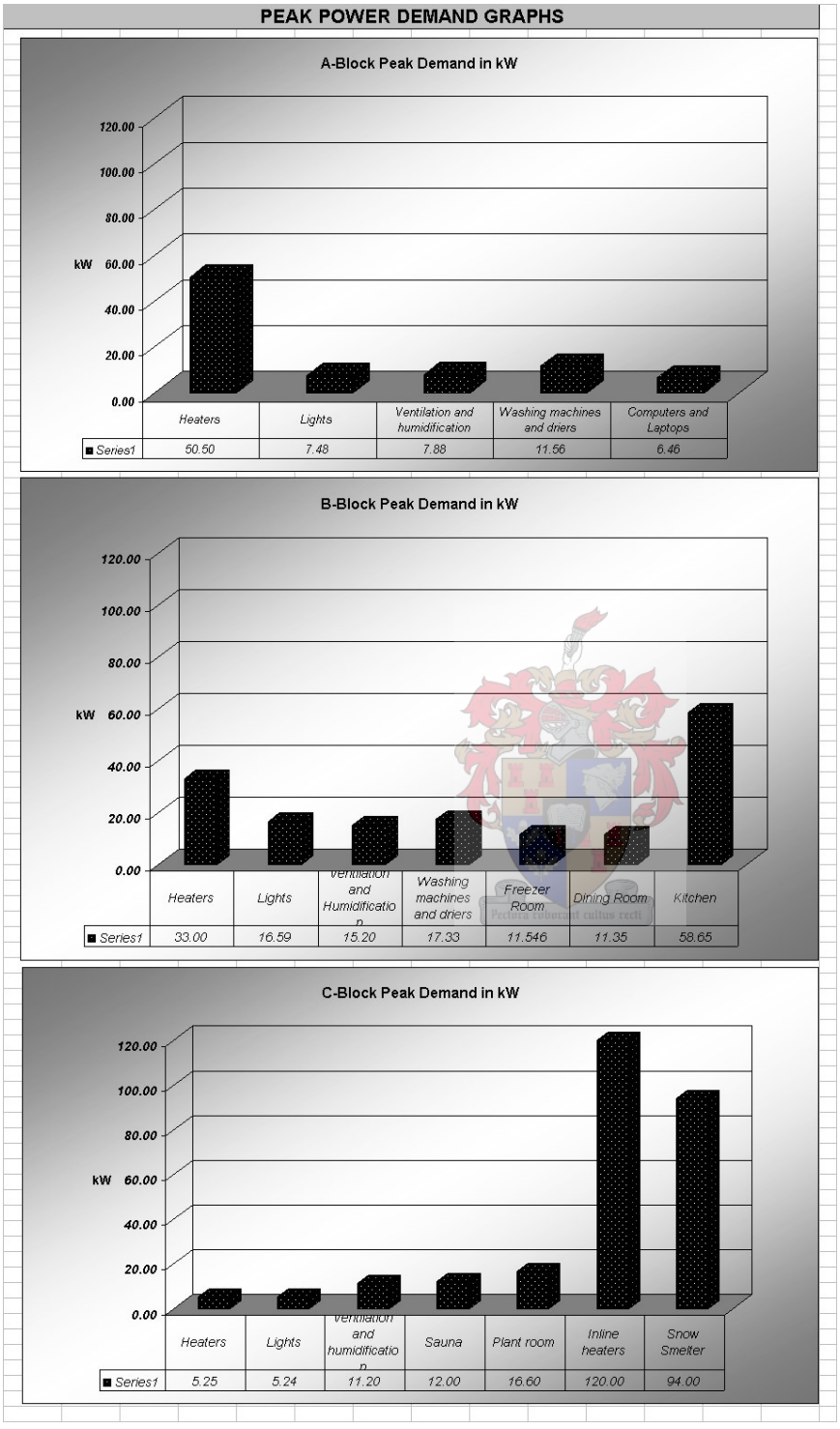

Figure C.2: Graphs of electricity consumers in each block

[¥] All data presented in appendix C.3 was collected by the author during the 2004/2005 SANAE IV takeover.

C.4 Assimilated Data on Generator Output (used for determining load profiles)

Table C.5: Data collected on generator load profiles

HISTORICAL AND RECORDED SUMMER TAKEOVER GENERATOR DATA														
Previous load profile measurements (Cencelli 2002, Taylor 2002, Teetz 2002, Olivier 2004)												Everyone's Average		
Time	Cencelli				Taylor		Teetz	Olivier				MIN	TIME	AVG
0.00	165.00	131.00	131.00				165.00	123.30	105.00			105.00	0.00	136.72
0.02								112.00	90.00			90.00		
0.04	175.00	125.00	118.00	170.00			150.00	138.00	80.00			80.00	0.04	136.57
0.06								140.00	84.30			84.30		
0.08	176.00	120.00	118.00	180.00			135.00	142.50	87.00			87.00	0.08	136.93
0.10								138.00	84.30			84.30		
0.13	162.00	118.00	118.00	113.00			125.00	128.00	83.00			83.00	0.13	121.00
0.15									85.00			85.00		
0.17	137.00	118.00	118.00	124.00			122.00		77.80			77.80	0.17	116.13
0.19									78.80			78.80		
0.21	113.00	125.00	125.00	131.00			122.00		82.00			82.00	0.21	116.33
0.23									98.50			98.50		
0.25	110.00	113.00	113.00	130.00			122.00		90.00			90.00	0.25	113.00
0.27									92.00			92.00		
0.29	110.00	106.00	106.00	131.00	130.00	130.00	122.00		87.00			87.00	0.29	115.25
0.31									89.00			89.00		
0.33	110.00	106.00	106.00	131.00	112.00	112.00	130.00		100.00	132.00		100.00	0.33	115.44
0.35									100.00	125.00		100.00		
0.38	110.00	113.00	113.00	134.00	160.00	155.00	142.00	103.00	71.50	130.00		71.50	0.38	123.15
0.40								146.50	148.00	101.00		101.00		
0.42	112.50	120.00	120.00	126.00	168.00	175.00	158.00	150.00	160.30	104.00		104.00	0.42	139.38
0.44								142.00	160.00	142.50		142.00		
0.46	113.00	125.00	125.00	119.00	159.00	162.00	162.00	118.00	178.00	142.50		113.00	0.46	140.35
0.48								172.00	175.00	160.00		160.00		
0.50	130.00	125.00	125.00	156.00	150.00	110.00	161.00	118.00	150.00	133.50		110.00	0.50	135.85
0.52								142.50	139.00	166.00		139.00		
0.54	177.00	118.00	118.00	194.00	145.00	162.00	165.00	137.00	115.00	143.33		115.00	0.54	147.43
0.56								133.80	112.00	142.00		112.00		
0.58	174.00	113.00	113.00	194.00	140.00	165.00	150.00	148.00	96.80	151.00		96.80	0.58	144.48
0.60								142.00	96.80	157.67		96.80		
0.63	170.00	112.00	112.00	156.00	158.00	150.00	140.00	154.00	138.00	167.00		112.00	0.63	145.70
0.65								126.50	150.00	156.40		126.50		
0.67	175.00	106.00	106.00	135.00	135.00	148.00	140.00	112.00	170.00	156.50		106.00	0.67	138.35
0.69								106.00	163.30			106.00		
0.71	180.00	104.00	104.00	152.00	150.00	140.00	150.00	132.80	120.00	137.50		104.00	0.71	137.03
0.73								135.50	87.50			87.50		
0.75	187.00	108.00	108.00	156.00	152.00	155.00	155.00	135.30	101.00			101.00	0.75	139.70
0.77								142.00	142.50	145.50		142.00		
0.79	194.00	120.00	120.00	152.00	148.00	155.00	158.00	145.00	150.00	138.00		120.00	0.79	148.00
0.81								149.00	130.00	156.50		130.00		
0.83	187.00	145.00	145.00	152.00	132.00	144.00	158.00	145.00	136.50			132.00	0.83	149.39
0.85								137.00	130.00	150.00		130.00		
0.88	194.00	152.00	152.00				165.00	145.00	121.00			121.00	0.88	154.83
0.90								136.00	116.00			116.00		
0.92	187.00	132.00	132.00				165.00	151.00	117.50			117.50	0.92	147.42
0.94								155.50	120.00	121.00		120.00		
0.96	170.00	112.00	112.00				158.00	138.00	121.00	145.00		112.00	0.96	136.57
0.98								141.00	113.00	147.00		113.00		
AVG	154.94	119.46	119.08	146.80	145.64	147.36	146.67	136.79	115.07	142.04		105.24	0.48	134.79
MAX	194.00	152.00	152.00	194.00	168.00	175.00	165.00	172.00	178.00	167.00		160.00	0.96	154.83
MIN	110.00	104.00	104.00	113.00	112.00	110.00	122.00	103.00	71.50	101.00		71.50	0.00	113.00

C.5 Generator Diesel Consumption at SANAE IV[¥]

DIESEL DEMAND for JANUARY 2005

FUEL CONSUMPTION				
DATE	BEFORE	AFTER	DIFFERENCE	LITERS
01-Jan	450	204	246	689.784
02-Jan	445	210	235	658.94
03-Jan	477	210	267	748.668
04-Jan	460	200	260	729.04
05-Jan	515	205	310	869.24
06-Jan	510	210	300	841.2
07-Jan	505	215	290	813.16
08-Jan	472.5	220	252.5	708.01
09-Jan	472.5	220	252.5	708.01
10-Jan	560	210	350	981.4
11-Jan	515	215	300	841.2
12-Jan	530	215	315	883.26
13-Jan	490	210	280	785.12
14-Jan	510	215	295	827.18
15-Jan	470	210	260	729.04
16-Jan	500	210	290	813.16
17-Jan	522	215	307	860.828
18-Jan	520	215	305	855.22
19-Jan	555	215	340	953.36
20-Jan	520	215	305	855.22
21-Jan	540	210	330	925.32
22-Jan	510	210	300	841.2
23-Jan	550	210	340	953.36
24-Jan	550	210	340	953.36
25-Jan	532	200	332	930.928
26-Jan	490	210	280	785.12
27-Jan	500	210	290	813.16
28-Jan	500	210	290	813.16
29-Jan	450	210	240	672.96
30-Jan	520	210	310	869.24
31-Jan	553	205	348	975.792

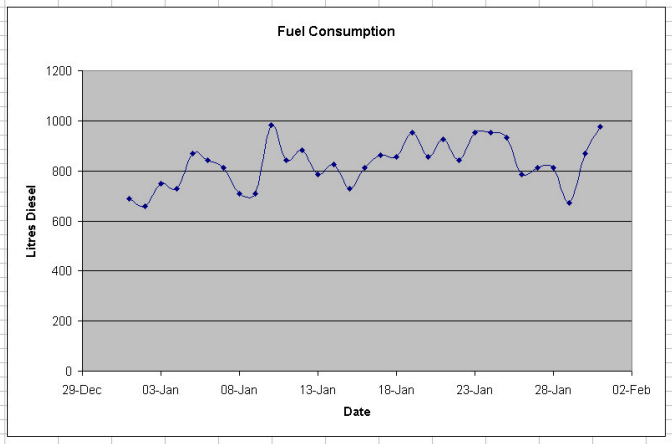

DIESEL DEMAND for 2004

MONTH OF 2004	LITERS DIESEL CONSUMED IN MONTH	MEAN MONTHLY Temp
January	27198	-5.7
February	23731	-9.1
March	33423	-14.3
April	35793	-19.8
May	33397	-22
June	22559	-21.5
July	26887	-25.4
August	24199	-24
September	22891	-22.3
October	22461	-16.6
November	19246	-13.1
December	20060	
Total	**311845**	

Mechanical Engineer's Report		
30-Nov	Bunker diesel remaining on 30 November: 92000 liter	2,3,4 depleted and 5 online
30-Oct		1,2,3,4 depleted and 5 online
30-Sep		1,2,3,4 depleted and 5 online
30-Aug		1,2,3 depleted and 4 online
30-Jul		1,2,3 depleted and 4 online
30-Jun		2 depleted and 3 online
30-May		2 depleted and 3 online
30-Apr		2 depleted and 3 online
30-Mar		1 depleted and 2 online
30-Feb		1 online

380 000 liters received during 2003/2004 takeover
470 000 liters received during 2004/2005 takeover

kWh Readings in 2004	**kWh**	**Difference in kWh**	**Avg**
12-Jun	8076800		
01-Jul	8129060	52260	120.9722
31-Jul	8221740	92680	124.5699

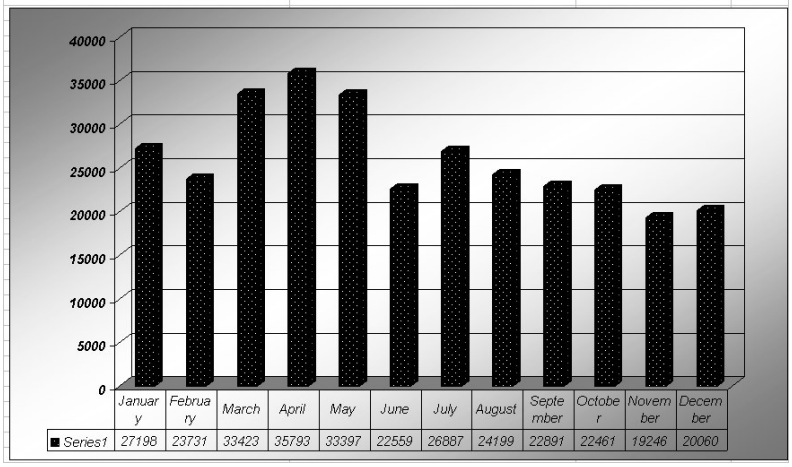

[¥] All data presented in appendix C.5 was collected by the author during the 2004/2005 SANAE IV takeover.

DIESEL DEMAND OF THE BASE

MONTH OF 2000	LITERS DIESEL CONSUMED IN THAT MONTH
Jan	26460
Feb	22960
Mar	28311
Apr	25956
May	26180
Jun	22652
Jul	23352
Aug	21938
Sep	26740
Oct	25550
Nov	23324
Dec	22450
Total	**295873**

MONTH OF 2001	LITERS DIESEL CONSUMED IN THAT MONTH
Jan	25119
Feb	18332
Mar	23680
Apr	23394
May	26250
Jun	25354
Jul	30338
Aug	29019
Sep	28378
Oct	26012
Nov	21350
Dec	21190
Total	**273297**

MONTH OF 2002	LITERS DIESEL CONSUMED IN THAT MONTH
Jan	26538
Feb	19894
Mar	18956
Apr	21784
May	23114
Jun	25102
Jul	25528
Aug	28238
Sep	25984
Oct	24570
Nov	22442
Dec	23204
Total	**285354**

MONTH OF 2003	LITERS DIESEL CONSUMED IN THAT MONTH	Questionable Data (Ommitted)
Jan	29296	
Feb	21168	
Mar	18956	
Apr	26908	
May	24559	
Jun	24080	
Jul	23329	
Aug	28238	
Sep	24959	
Oct	21378	
Nov	18060	
Dec	21266	
Total	**282197**	

MONTH OF 2004	LITERS DIESEL CONSUMED IN THAT MONTH
Jan	27198
Feb	23731
Mar	33423
Apr	35793
May	33397
Jun	22559
Jul	26887
Aug	24199
Sep	22891
Oct	22461
Nov	19246
Dec	20060
Total	**311845**

AVERAGE (WITHOUT OUTLIERS)	LITRES DIESEL CONSUMED IN THAT MONTH	
Jan	26329	26922
Feb	21229	21217
Mar	23649	23649
Apr	23711	24500
May	25181	25000
Jun	23917	25500
Jul	26526	26000
Aug	25849	26326
Sep	25998	25790
Oct	24648	23994
Nov	21591	20884
Dec	21726	21634
Total	290354	288617

AVERAGE (ALL DATA)	LITRES DIESEL CONSUMED IN THAT MONTH
Jan	26328.75
Feb	21229.25
Mar	26092.5
Apr	26731.75
May	27235.25
Jun	23916.75
Jul	26526.25
Aug	25848.5
Sep	25998.25
Oct	24648.25
Nov	21590.5
Dec	21726
Total	**297872**

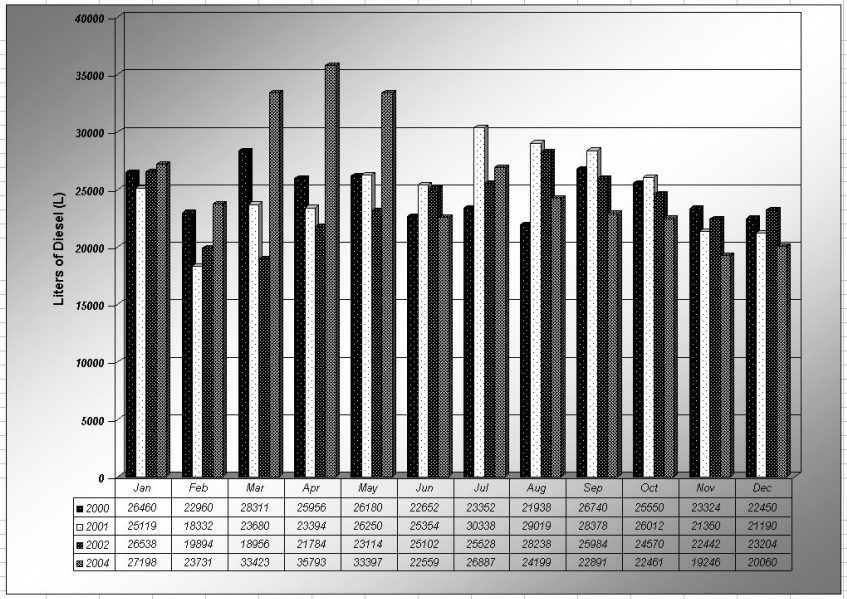

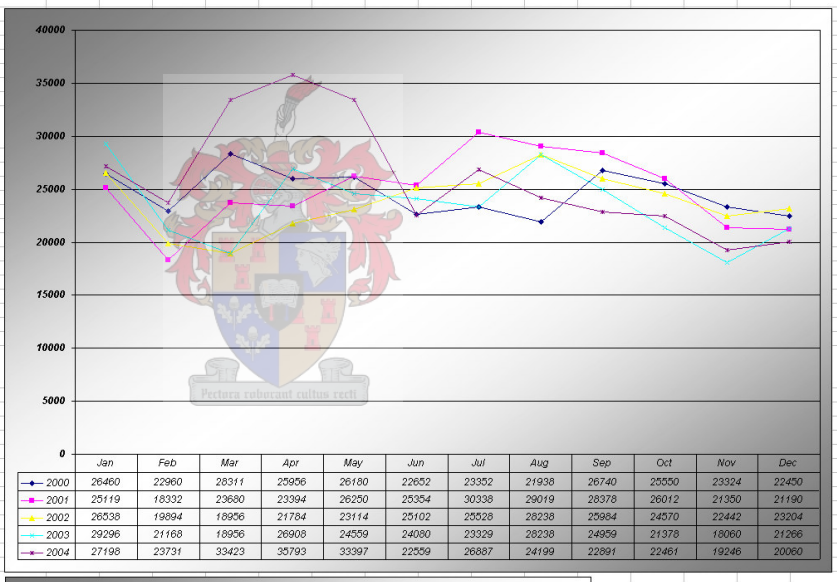

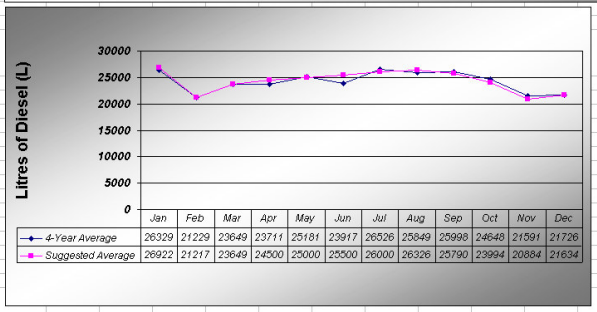

C.6 Associated Amounts of Generator Diesel Consumption and Electrical Output[¥]

Table C.6: Generator diesel consumption and electrical power generation

Jan-05					
DATE	**TIME**	**kWh reading**	**kWh used**	**Average kW**	
06-Jan		43064.90			
16-Jan	**23h48**	43207.16	28452	118.55	
17-Jan	**23h30**	43220.85	2738	115.28	
18-Jan	**21h45**	43235.20	2870	128.99	
19-Jan	**22h00**	43251.37	3234	133.36	
21-Jan	**22h00**	43281.59	6044.00	125.92	
22-Jan	**22h00**	43297.20	3122	130.08	
23-Jan	**17h09**	43309.80	2520	134.04	
24-Jan	**17h15**	43325.75	3190	132.92	
25-Jan	**19h00**	43341.00	3050	118.45	
26-Jan				119.58	
27-Jan				119.58	
28-Jan	**19h00**	43384.05	8610.00	119.58	
29-Jan	**17h15**	43395.25	2240.00	100.67	
30-Jan				128.25	
31-Jan	**18h30**	43425.55	6060.00	128.25	
01-Feb					
02-Feb					
03-Feb					
04-Feb					
05-Feb					
06-Feb					

Coincides with diesel consumption

June to August 2004				
DATE	**kWh reading**	**kWh used**	**Liters diesel used**	**Average kW**
12-Jun	40384.00			
17-Jun	40449.35	13070.00	3650.90	108.92
18-Jun	40462.30	2590.00	687.00	107.92
19-Jun	40475.10	2560.00	707.00	106.67
20-Jun	40486.70	2320.00	656.00	96.67
24-Jun	40542.20	11100.00	3177.00	115.63
25-Jun	40556.80	2920.00	861.00	121.67
26-Jun	40571.50	2940.00	827.00	122.50
27-Jun	40584.50	2600.00	757.00	108.33
28-Jun	40599.20	2940.00	805.00	122.50
29-Jun	40613.40	2840.00	813.00	118.33
30-Jun	40627.80	2880.00	810.00	120.00
01-Jul	40645.30	3500.00	967.00	145.83
02-Jul	40664.50	3840.00	1138.00	160.00
03-Jul	40680.55	3210.00	920.00	133.75
04-Jul	40695.75	3040.00	827.00	126.67
05-Jul	40710.55	2960.00	827.00	123.33
06-Jul	40725.55	3000.00	850.00	125.00
12-Jul	40819.50	18790.00	5201.00	130.49
13-Jul	40834.60	3020.00	869.00	125.83
14-Jul	40848.75	2830.00	757.00	117.92
15-Jul	40863.60	2970.00	791.00	123.75
16-Jul	40876.80	2640.00	782.00	110.00
17-Jul	40892.10	3060.00	875.00	127.50
18-Jul	40907.30	3040.00	841.00	126.67
20-Jul	40937.35	6010.00	1649.00	125.21
21-Jul	40950.40	2610.00	732.00	108.75
23-Jul	40983.60	6640.00	1825.00	138.33
24-Jul	41002.40	3760.00	1175.00	156.67
25-Jul	41018.20	3160.00	875.00	131.67
26-Jul	41032.40	2840.00	794.00	118.33
27-Jul	41046.70	2860.00	765.00	119.17
28-Jul	41061.20	2900.00	819.00	120.83
29-Jul	41077.10	3180.00	878.00	132.50
30-Jul	41093.70	3320.00	892.00	138.33
31-Jul	41108.70	3000.00	838.00	125.00
02-Aug	41136.20	5500.00	1559.00	114.58
03-Aug	41150.85	2930.00	813.00	122.08
04-Aug	41166.10	3050.00	841.00	127.08
05-Aug	41180.10	2800.00	780.00	116.67
06-Aug	41193.60	2700.00	757.00	112.50
07-Aug	41208.10	2900.00	819.00	120.83
08-Aug	41227.50	3880.00	794.00	161.67
09-Aug	41239.00	2300.00	1090.80	95.83
10-Aug	41254.10	3020.00	679.00	125.83
12-Aug	41283.70	5920.00	1601.00	123.33
13-Aug	41297.65	2790.00	847.00	116.25
14-Aug	41312.00	2870.00	802.00	119.58
16-Aug	41339.80	5560.00	1581.00	115.83
17-Aug	41352.20	2480.00	701.00	103.33
18-Aug	41363.75	2310.00	673.00	96.25
19-Aug	41376.80	2610.00	743.00	108.75
20-Aug	41390.00	2640.00	743.00	110.00
21-Aug	41402.90	2580.00	701.00	107.50
25-Aug	41455.30	10480.00	2974.00	109.17
		214260.00	**60136.70**	**120.64**

Generator Efficiency		
Diesel Properties		
	kWh/liter	9.8
Generator Properties		
	kWh/liter	3.56
Generator Efficiency		
	%	**36.36**

[¥] All data presented in appendix C.6 was collected by the author during the 2004/2005 SANAE IV takeover.

C.7 Graphical Representation of C6

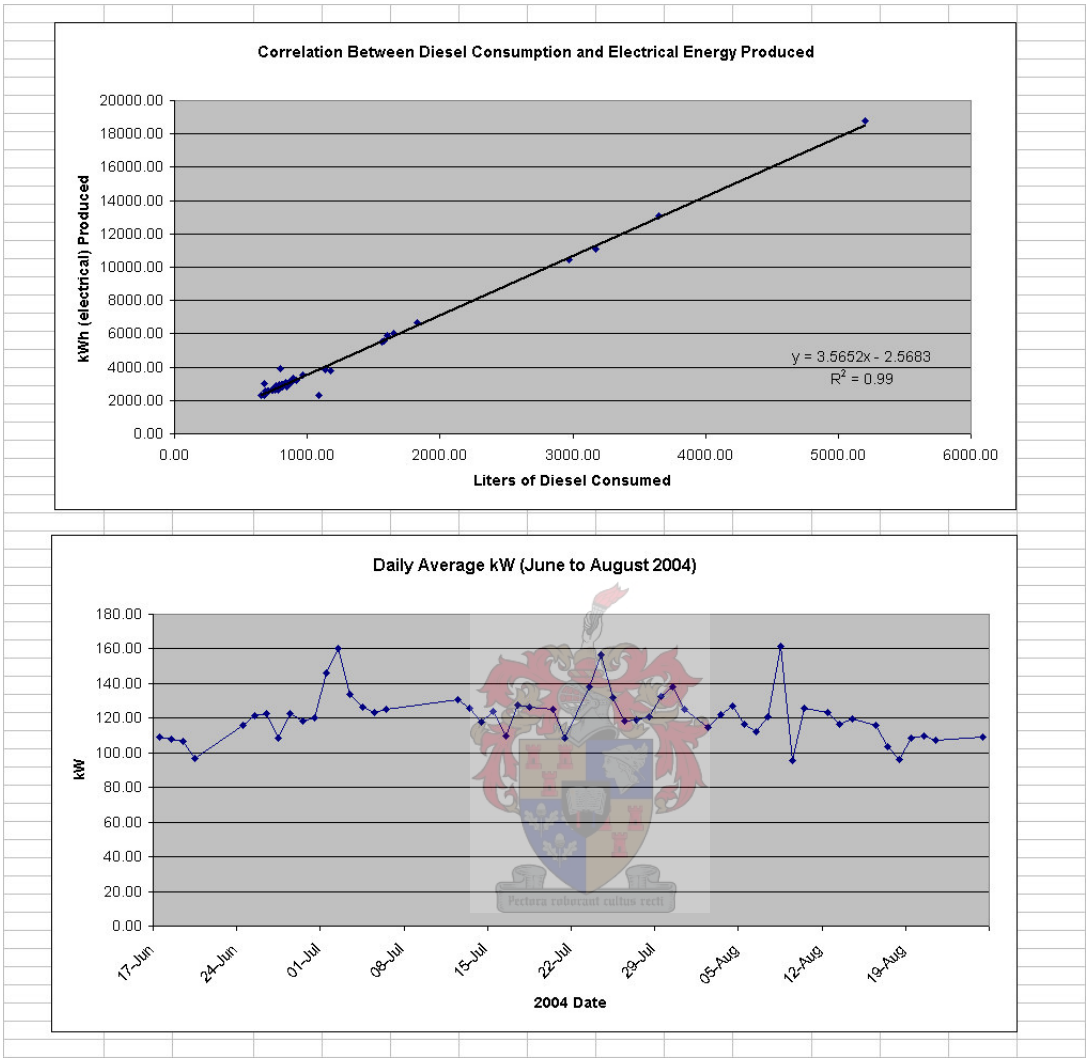

Figure C.3: Graphs of generator diesel consumption and electrical generation

Appendix D: Additional Information to Solar Energy Capturing Solutions

D.1 Energy Capturing Devices

Applications for flat-plate solar thermal collectors were investigated in chapter 3, where it was shown that the energy load of the H&V System at SANAE IV did not match available solar radiation well throughout the year. During the periods of high insolation there was no need to heat the base and in fact the station needed to be cooled, while during winter there was a significant shortage of available solar radiation. It was pointed out, however, that the snow smelter might be a potential point of application. And so, under these assumptions, one would attempt to supplement the current fresh water demand of the station with solar energy captured from a flat-plate solar collector.

Huang et al. (2001) have provided a survey of the three basic commercially available flat-plate solar collectors (viz. Type-A, Type-B and Type-C) as well as their respective average market costs. Type-A is described as a low-cost specially designed single-glazed flat-plate solar collector with selective surface and a 10-centimetre air layer of insulation beneath the glass cover. Type-B is a conventional single-glazed solar collector with selective surface and Type-C is a vacuum-tube collector. A graph of the performance of these collectors is provided below in figure D.1.

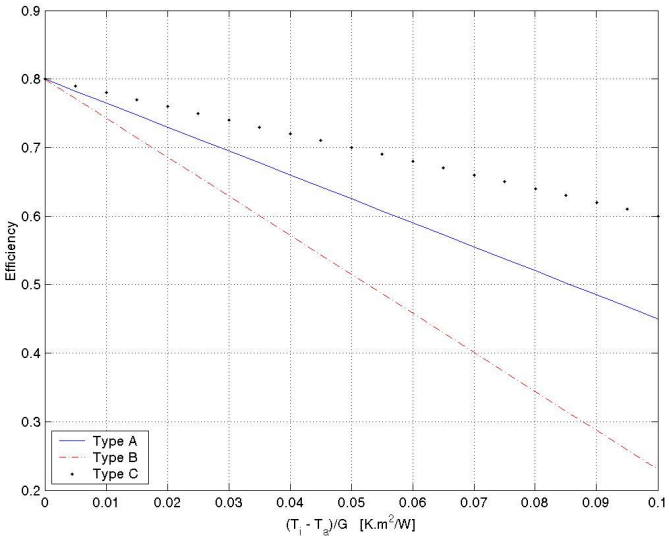

Figure D.1: Characteristics of the standard types of solar collectors (Huang et al., 2001)

The efficiencies of these collectors can therefore be calculated from figure D.1 if the ambient temperature, inlet collector temperature and insolation rate can be estimated. Thus, since the average radiation profile for each month has already been determined, and the average ambient conditions are known, it is only necessary to determine the average collector inlet temperature.

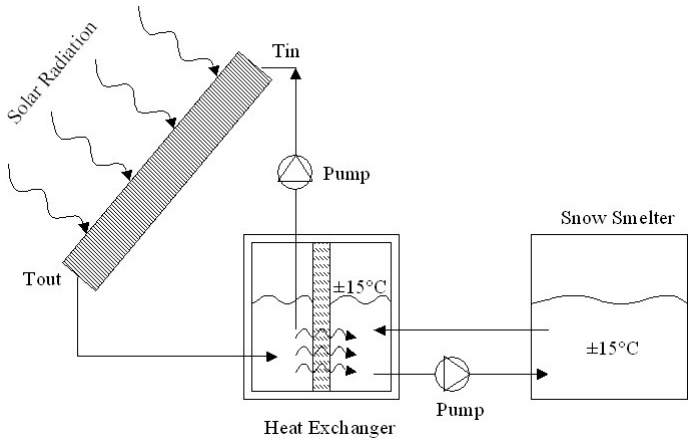

Figure D.2: Potential solar thermal collector set-up

From figure D.2 it is evident that temperature at the collector inlet can be estimated from a simple steady state heat transfer analysis at the heat exchanger, since the snow smelter temperature is fixed and known. Using the equation:

$$Q_{solar} = U_o \cdot A_o \cdot \Delta T \qquad D.1$$

Where Q_{solar} is the heat collected by the flat-plate solar thermal collector [W], U_o is the overall outside heat transfer coefficient of the flat-plate heat exchanger [W/m^{2}K], A_o is the outside area of the flat plate across which heat is exchanged [m^2] and ΔT is the temperature difference across the plate [K]. If we estimate: Q_{solar} as 4752 W (8 panels, each 1.98 m^2, subject to radiation of 500 W/m^2 and a collector efficiency of 50 % which was iterated to convergence), U_o as 1000 W/m^{2}K (Mills, 1999) and the area A_o of the heat exchanger as 1 m^2, the result from equation D.1 is a ΔT of approximately 5 K. Thus (refer to figure D.2) the inlet temperature to the collector would be approximately 20ºC, or 27ºC above the average ambient January temperature. In this manner, using: the performance curves suggested by Huang et al. (2001) shown in figure D.1, the average daily radiation profiles for January described in chapter 1 and the estimated heat exchanger values given above, the average collector efficiencies have been estimated and are presented in table D.1.

Table D.1: Summary of solar thermal collector systems

CRITERIA	TYPE-A	TYPE-B	TYPE-C
Calculated daily January efficiency	0.56	0.45	0.65
Calculated daily December efficiency	0.55	0.44	0.65
Cost (US$/m^2)*	136	121	485
Calculated average January tilted yield (kWh/m^2.day)	4.53	3.63	5.24
Calculated average December tilted yield (kWh/m^2.day)	4.57	3.62	5.36

*These estimates provided by Huang et al. (2001) are low

D.2 Basic Snow Smelter PLC Logic

The following is an extract taken out of the Engineer's training manual (SANAE IV database, 2005) used to explain proper operation and functioning of the snow smelter.

"4.4.2 The basic logic used in the PLC is as follows:

- *The PLC will only switch on elements up to the maximum amount of elements selected by the rotary switches. The reason for this is that you do not want the power consumption to rise to such an extent that a second generator must start unattended.*
- *Once the temperature of the water in each side reaches 30 Degrees Celsius, the PLC will switch off elements to keep the water temperature at 30 Degrees Celsius. This action will happen at 30 minute intervals. (Refer to PLC Manual).*
- *If the temperature drops quickly to below 20 Degrees Celsius as is the case when snow is dumped into the smelly, elements will be switched on at 2 minute intervals. (Refer to PCC Manual).*
- *The level switches are situated in the hot tank. The switches are float level switches which are connected to the indicator lights on the front panel.*
- *When the 100 % level light comes on, the PLC will automatically activate valves 9 and 10 and water will be pumped to the base for a period of 10 minutes. This is just a safety measure to ensure that the tank does not overflow. It would be technically possible to automate the complete pumping action. The reason why it was not done is that at the stage where the level reaches 100 %, the temperature might be 30 Degrees Celsius. The volume of hot water left after 10 minutes of pumping can then be used to melt more snow before it is pumped to the base.*
- *When snow is then added to the cold side of the melter, it must be attempted to stabilise the temperature well above 8 Degrees Celsius after which the pumping action can be started by pressing the pump button for 2 seconds. To stop the pumping action the button must be kept in for 6 seconds."*

D.3 Thermomax Product Prices and Specifications

THERMO TECHNOLOGIES

"Worldwide Leadership in Solar Heating Systems & Services"

Retail Price List 2005

System	Description	Price
MAZ 2-20S	20 Tube Thermomax Collector System (with sloping roof fittings and accessories) 60" x 80", 135 lbs.	$ 1,950.00
MAZ 2-30S	30 Tube Thermomax Collector System (with sloping roof fittings and accessories) 90" x 80", 195 lbs.	$ 2,900.00
MAZ 2-40S	40 Tube Thermomax Collector System (with sloping roof fittings and accessories) 120" x 80", 270 lbs.	$ 3,900.00
MAZ 2-50S	50 Tube Thermomax Collector System (with sloping roof fittings and accessories) 150" x 80", 330 lbs.	$ 4,900.00
MAZ 2-60S	60 Tube Thermomax Collector System (with sloping roof fittings and accessories) 180" x 80", 390 lbs.	$ 5,850.00
Part No.		
MAZ 2-20M	20 Tube Manifold Set	$ 450.00
MAZ 2-30M	30 Tube Manifold Set	$ 650.00
TMA 600	Thermomax Memotron Tube (Box of 10)	$ 750.00
81VR80TC	80 Gallon Rheem Solar Direct Tank without Heat Exchanger	$ 750.00
81V80HE	80 Gallon Rheem Solar Indirect Tank with Heat Exchanger	$ 950.00
81VR120TC	120 Gallon Rheem Solar Direct Tank without Heat Exchanger	$ 950.00
SBB 300 +	80 Gallon Steibel Eltron Solar Tank with two Heat Exchangers	$ 999.00
SBB 400 +	105 Gallon Steibel Eltron Solar Tank with two Heat Exchangers	$ 1,150.00
PCU 20/60	Pump Unit Control for up to 60 Tubes	$ 750.00
USDT 2004	Digital Universal Solar Control Unit (Two Sensors, 3rd optional senor)	$ 149.00
USDT 2005	Analog Universal Solar Control Unit (Two Sensors)	$ 129.00
USDT 3000	Solar Control Unit (Two Tanks, Three Sensors)	$ 239.00
SMT 100T	Solar Control Unit (Two Tanks, Three Sensors)	$ 287.00
SMT 400T	Solar Control Unit (Three Tanks, Three Sensors)	$ 512.00
C0076	Roof Bracket Kit for Flat Roofs	$ 170.00
C0022	Mexican Tile Roof Elevation Kit (set of four)	$ 75.00

Prices Shown Herein are FOB Baltimore, Maryland. Crating: Add $ 150.00 per system for packaging and handling in a wooden crate.

5560 STERRETT PLACE, SUITE 115, COLUMBIA, MD 21044, (410) 997-0778, FAX (410) 997-0779
E-MAIL-> INFO@THERMOTECHS.COM INTERNET -> HTTP://WWW.THERMOTECHS.COM

Figure D.3: Thermomax product price sheet (Thermomax, 2005)

D.4 Solahart Product Specifications for the M-Collector

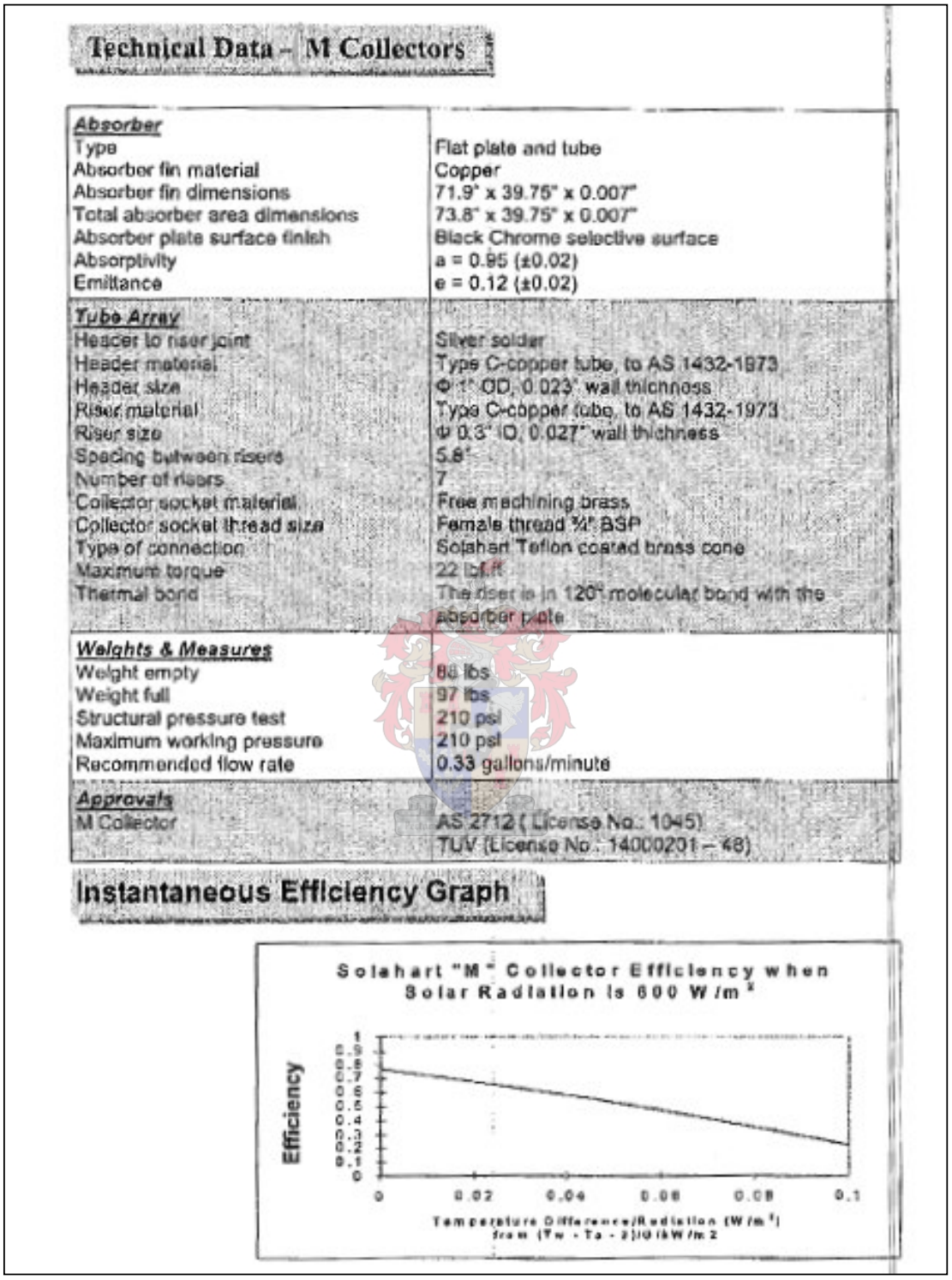

Technical Data – M Collectors

Absorber	
Type	Flat plate and tube
Absorber fin material	Copper
Absorber fin dimensions	71.9" x 39.75" x 0.007"
Total absorber area dimensions	73.8" x 39.75" x 0.007"
Absorber plate surface finish	Black Chrome selective surface
Absorptivity	a = 0.95 (±0.02)
Emittance	e = 0.12 (±0.02)
Tube Array	
Header to riser joint	Silver solder
Header material	Type C-copper tube, to AS 1432-1973
Header size	Φ 1" OD, 0.023" wall thickness
Riser material	Type C-copper tube, to AS 1432-1973
Riser size	Φ 0.3" ID, 0.027" wall thickness
Spacing between risers	5.8"
Number of risers	7
Collector socket material	Free machining brass
Collector socket thread size	Female thread ¾" BSP
Type of connection	Solahart Teflon coated brass cone
Maximum torque	22 lbf.ft
Thermal bond	The riser is in 120° molecular bond with the absorber plate
Weights & Measures	
Weight empty	86 lbs
Weight full	97 lbs
Structural pressure test	210 psi
Maximum working pressure	210 psi
Recommended flow rate	0.33 gallons/minute
Approvals	
M Collector	AS 2712 (License No.: 1045)
	TUV (License No.: 14000201 – 48)

Instantaneous Efficiency Graph

Figure D.4: Solahart M-Collector specifications (Solahart, 2005)

D.5 Solahart Product Specifications for the Bt-Collector

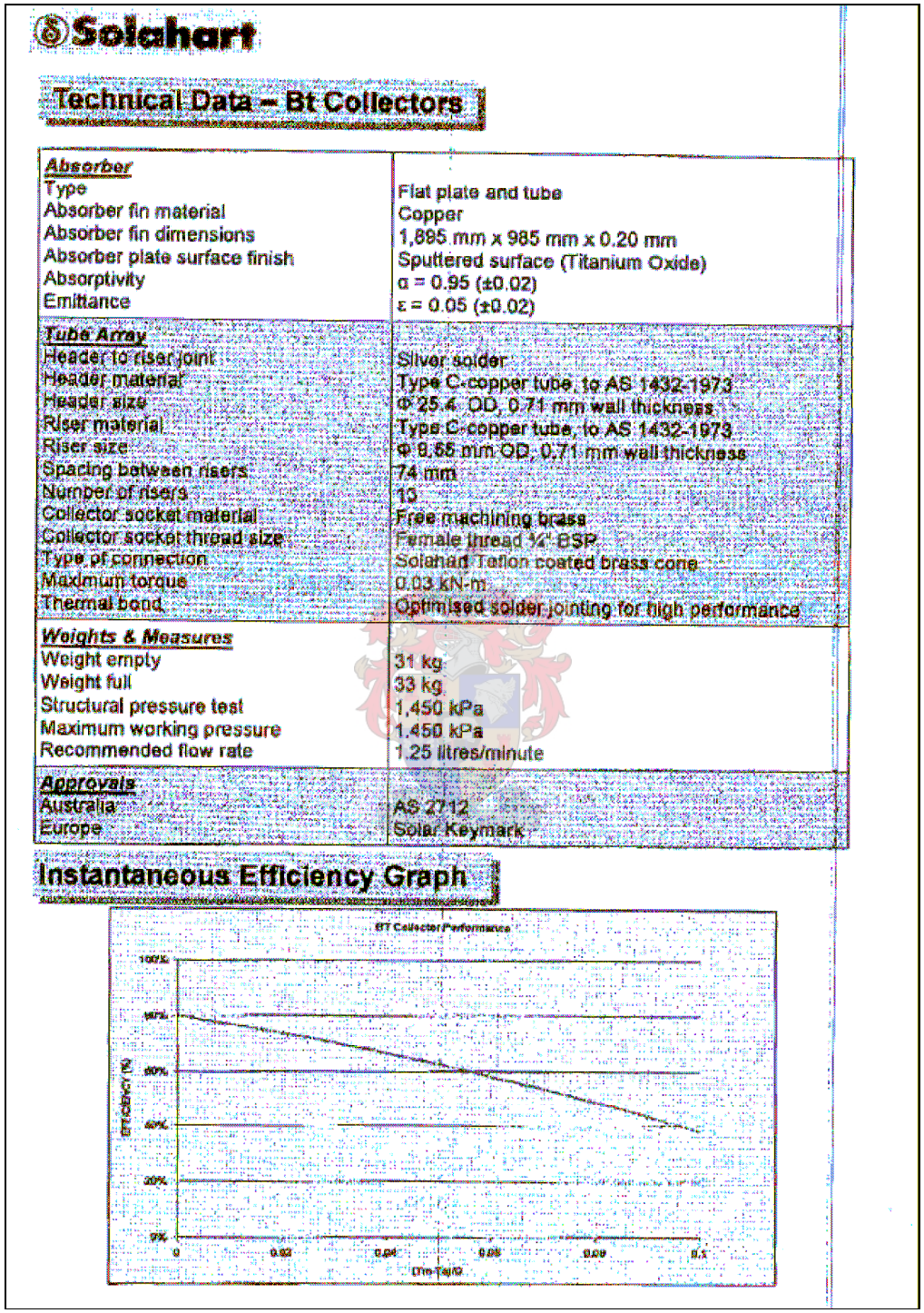

Solahart

Technical Data – Bt Collectors

Absorber	
Type	Flat plate and tube
Absorber fin material	Copper
Absorber fin dimensions	1,895 mm x 985 mm x 0.20 mm
Absorber plate surface finish	Sputtered surface (Titanium Oxide)
Absorptivity	α = 0.95 (±0.02)
Emittance	ε = 0.05 (±0.02)
Tube Array	
Header to riser joint	Silver solder
Header material	Type C-copper tube, to AS 1432-1973
Header size	Φ 25.4, OD, 0.71 mm wall thickness
Riser material	Type C-copper tube, to AS 1432-1973
Riser size	Φ 8.66 mm OD, 0.71 mm wall thickness
Spacing between risers	74 mm
Number of risers	13
Collector socket material	Free machining brass
Collector socket thread size	Female thread ¾" BSP
Type of connection	Solahart Teflon coated brass cone
Maximum torque	0.03 kN-m
Thermal bond	Optimised solder jointing for high performance
Weights & Measures	
Weight empty	31 kg
Weight full	33 kg
Structural pressure test	1,450 kPa
Maximum working pressure	1,450 kPa
Recommended flow rate	1.25 litres/minute
Approvals	
Australia	AS 2712
Europe	Solar Keymark

Instantaneous Efficiency Graph

Figure D.5: Solahart Bt-Collector specifications (Solahart, 2005)

D.6 MATLAB V6.1 Snow Smelter Simulation Programme

```
%%-------------------------------------------------------------------------------------------%%
%%        SNOWSMELTER SIMULATION PROGRAMME SANAE IV -2005   %%
%%-------------------------------------------------------------------------------------------%%
%This programme models the energy transfer characteristics of the snowsmelter at South Africa's
%SANAE IV station in Antarctica. It is used to estimate the reduction in electrical consumption
%of the heating elements when solar thermal collectors are incorperated with the current system.

%%-----------------------------------------------------------%%
%%  Establish some important initial conditions    %%
%%-----------------------------------------------------------%%
close all
clear all
clc
Ta(1)=0;              %The temperature of water in the smelter at which the heating elements are switched off
Ta(2)=50;             %The starting temperature of the solar energy store

while (Ta(1)-Ta(end))<0

   Ta(1)=Ta(1)+3;
   disp(['The starting Temp is: ',num2str(Ta(1))])

for Tmax=20
%The solar collector is currently set as product 1 (see calculation of collector efficiency) with 72 collector panels
NoSolarr=0;                   %Wheather or not the solar contribution must be accounted for in the simulation (1=No contribution)
month=2;                      %The desired month of the year
mm=(0.080*80)*998/3;          %The amount of snow added in one filling of the snowsmleter from: [(L/person.day)*(No. of people at base)*(kg/L)/(No. of smellies per day)]
NoOfPanels=8*3*3;             %The number of panels contributing to the energy demand of the snowsmelter
response2=10;                 %The number of minutes delay between switching heating elements OFF
response1=2;                  %The number of minutes delay between switching heating elements ON
HEMAX=12;                     %The maximum number of heating elements in the snowsmelter that can be turned on
V=6/24*NoOfPanels;            %The volume of the energy solar thermal store (in m^3)
clearsky=0;                   %If the insolation rate is to based on maximum clear-sky conditions (1=YES)

%%-------------------------------------------------%%
%%  Establish the initial conditions        %%
%%-------------------------------------------------%%
p=1;                    %THE MAIN COUNTER
PanelSize=1.98;         %The collector area of a single panel
tend=24*3600;           %The length of time of a simulation (in seconds)
gamma=180;              %The horizontal orientation of the collector (where 180=SOUTH)
mdot=0.0208;            %The flowrate through the collector (kg/s)
Cp=4181;                %The specific heat of water (in J/kg.K)
Cl=335000;              %The latent heat of snow (in J/kg)
U=1500;                 %Overall heat transfer coefficient of the heat exchanger dividing the solar thermal store and the snowsmelter
Aa=((V^(1/3))^2)*0.7;   %Surface area of heat exchanger mentioned in U above
HESIZE=7500;            %The electrical capacity of a single heating element (in W)
massfraction=1/5;       %The fraction of snow added in one filling that remains in the smelter after pumping water to the base
Uu=20;                  %The overall heat transfer coefficient between the smelter and the surroundings (in J/m^2.K)
Aaa=72;                 %The total area of the snowsmelter exposed to heat loss
Tfill1=8.5;             %The time of day at which the first pumping session and snowsmelter filling takes place
Tfill2=13.5;            %The time of day at which the second pumping session and snowsmelter filling takes place
Tfill3=17.5;            %The time of day at which the third pumping session and snowsmelter filling takes place
Tfill4=32.5;            %The time of day at which the third pumping session and snowsmelter filling takes place
Tfill5=37.5;            %The time of day at which the third pumping session and snowsmelter filling takes place
Tfill6=41.5;            %The time of day at which the third pumping session and snowsmelter filling takes place
Tb(1)=Tmax;             %The starting energy of the snowsmelter
HE(1)=0;                %The number of heating elements on at the start of the day
changer=0;              %A tool used in conjunction with the RESPONSE1 & 2 variables
wait=0;                 %A tool used in conjunction with the RESPONSE1 & 2 variables
PumpSessions=0;         %To keep track of how many times water is pumped up the base during the day
PumpSessionsT(1)=0;     %The temperature of the water at the time it is pumped to the base
NoFlow=0;               %If it is necessary to turn the solar thermal collectors off for a short time
Tamb=[-6.60 -10.30 -14.90 -18.20 -19.50 -20.10 -23.10 -22.90 -22.90 -18.20 -12.80 -7.10];
day=[17 16 16 15 15 11 17 16 15 15 14 10];  %Average meteorological days of every month
Beta=[22 63 74 84 86 86 86 88 78 69 52 48]; %Which are the optimum tilt angles of every month

%Some initial calculations
A=PanelSize*NoOfPanels;                 %Total collector area
dt=min([response1,response2])*60;       %ALL CALCULATIONS BASED ON SECONDS (where 300s=5min)
mass=mm+mm*massfraction;                %Total mass in the smelter at any one time
Qtot(1)=mass*Cl+mass*Cp*Tmax;           %Starting amount of energy in the smelter at beginning of day
Aaaa=((V^(1/3))^2)*6;                   %Surface area from which solar energy store can lose heat
```

```
NoSolar=NoSolarr;

%Start the clock
t=0;

while t < tend
   if t>24*3600
      tt=(t/(24*3600)-floor(t/(24*3600)))*24*3600;
   else
      tt=t;
   end
%Start the iterations
hourr=floor(tt/3600);
minn=floor((tt/3600-floor(t/3600))*60);
secc=floor((tt/3600-hourr-minn/60)*3600);
q=datenum([2005,month,day(month),hourr,minn,secc]);

%%-------------------------------------------------------------------------%%
%%  Incident solar radiation                                               %%
%%-------------------------------------------------------------------------%%
if clearsky==1
   [G,Gcb,Gd]=F_ClearSkyInsolation(q);              %Where G is the global horizontal insolation rate, Gd the diffuse insolation, Gcb the beam
radiation and q the datenum
elseif clearsky==0
   [G,Gd,ttt]=F_MonthlyProfiles(month,tt/3600);  %The time input is a number from 0 to 24
end
%And the insolation rate is calculated on a tilted place from the horizontal measurement
[Gt,Gdt,Gbt]=F_TiltISOSKY(q,Beta(month),G,Gd,0.7,gamma);   %Assumes isotropic-sky conditions

%%-----------------------------------------------%%
%%  Calculate the collector efficiency     %%
%%-----------------------------------------------%%
%This needs to be done with iteration since the specifications are in terms of Tm and not Ti to the collector
if Gt>0
   %See F_SolarThermalEfficiency for a description of each product
   [effm1,effm2,effm3]=F_SolarThermalEfficiency(Gt,Ta(p),month,NoOfPanels,PanelSize);
   eff=effm1;
else
   eff=0;
end
sunshine(p)=Gt*eff;   %The useful energy collected in the solar thermal collector

%%-----------------------------------------------------------------------------------------------------------%%
%%%%%  Couple the collector characteristics with the snow smelter electrical heaters      %%%%%
%%-----------------------------------------------------------------------------------------------------------%%

%%-----------------------------------------------------%%
%%  Heating Elements Switched on or off        %%
%%-----------------------------------------------------%%
if Tb(p)<Tmax & wait==0;
   HE(p+1) = HE(p)+1;
   wait=1;
   changer=t+response1*60;
elseif Tb(p)>Tmax & wait==0;
   HE(p+1) = HE(p)-1;
   wait=1;
   changer=t+response2*60;
else
   HE(p+1) = HE(p);
end
%Check to ensure that no more than 12 or less than 0 elements are on
if HE(p+1)>HEMAX
   HE(p+1)=HEMAX;
elseif HE(p+1)<0
   HE(p+1)=0;
end

%%-----------------------------------------------------%%
%%  Timer to enable the switching of elements   %%
%%-----------------------------------------------------%%
if t>=changer
   wait=0;
   changer=tend+60;
end
```

```
%%-------------------------------------------------------------%%
%%  The heat transfer into the tanks is calculated  %%
%%-------------------------------------------------------------%%
Qin=HE(p+1)*HESIZE*dt;          %No. of heating elements x Power per element (in W) x time interval [J]
QinSolar=U*Aa*(Ta(p)-Tb(p))*dt; %The heat exchanged from the solar thermal store to the snowsmelter
if (Ta(p)-Tb(p))<5
   NoSolar=1;
end
if NoSolar==1
   QinSolar=0;
end
NoSolar=0;
contribution(p)=QinSolar;
Qout=-Uu*Aaa*(Tb(p)-0)*dt;      %Heat loss to the surroundings
Qtot(p+1)=Qtot(p)+Qin+Qout+QinSolar;
%Making provision for the latency of snow when calculating the new smelter temperature
if Qtot(p+1)>mass*Cl
   Tb(p+1)=Tb(p)+(QinSolar + Qin + Qout)/(mass*Cp);
elseif Qtot(p+1)<mass*Cl
   Tb(p+1)=0;
end

%%-------------------------------------------------------%%
%%  The water is pumped up to the base         %%
%%-------------------------------------------------------%%
if  (t>(Tfill1*3600-dt)  &  t<(Tfill1*3600+dt))  |  (t>(Tfill2*3600-dt)  &  t<(Tfill2*3600+dt))  |  (t>(Tfill3*3600-dt)  &  t<(Tfill3*3600+dt))  |
(t>(Tfill4*3600-dt) & t<(Tfill4*3600+dt)) | (t>(Tfill5*3600-dt) & t<(Tfill5*3600+dt)) | (t>(Tfill6*3600-dt) & t<(Tfill6*3600+dt))
   if Tb(p+1)>8 %Can only pump water up to the base under these conditions
      PumpSessions=PumpSessions+1;
      PumpSessionsT(PumpSessions)=Tb(p+1);
      Qtot(p+1)=(mm*Cl + mm*Cp*Tb(p+1))*massfraction;     %Remaining energy in the "store" of the snowsmelter
      if Qtot(p+1)>mass*Cl   %If the added snow is immediately melted
         Tb(p+1)=(Qtot(p+1))/(mass*Cp);
      elseif Qtot(p+1)<mass*Cl   %If the added snow still requires heating
         Tb(p+1)=0;
      end
      wait=0;
      changer=tend+60;
   end
end

%%-------------------------------------------------------------------------------------------%%
%%  The end of the snow smelter code                                                         %%
%%-------------------------------------------------------------------------------------------%%

%%-------------------------------------------------%%
%%  Calculate collected energy in store        %%
%%-------------------------------------------------%%
Qsolar=Gt*A*eff*dt;       %The solar energy collected in the collector
Qloss=Uu*Aaaa*(Ta(p)-0);    %Heat lost from the solar thermal store to the surroundings
if (Qsolar-mdot*Cp*Ta(p)*dt)<5
   NoFlow=1;
end
if NoFlow==0
   Qoutt=mdot*Cp*Ta(p)*dt; %The amount of energy leaving the solar store and entering the collector
elseif NoFlow==1
   Qoutt=0;
   Qsolar=0;
end
NoFlow=0;
collected(p)=Qsolar;
Qdiff=(Qsolar+Qoutt)-Qoutt-QinSolar-Qloss;              %The energy effecting a change of temperature in the store
Ta(p+1)=Ta(p)+Qdiff/(V*998*Cp);                         %The new temperature of the energy store

t = t + dt;           %0 to 24*3600
p=p+1;
NoSolar=NoSolarr;
end

end

end
```

```
%%-----------------------------------------------%%
%%  Plot the results                             %%
%%-----------------------------------------------%%
r=length(Tb);
time24=0:dt/3600:(r-1)*dt/3600;
subplot(2,1,1)
plot(time24,Tb,'b-',time24,Ta,'r-.',0:1:tend/3600,Tmax,'r.',0:1:tend/3600,8,'b.'), grid on, ylabel('snow smelter Temperature')
legend('Tb','Ta','Limit temperatures')
if NoSolar==0
   axis([0 tend/3600 0 (Tmax+40)])
end
subplot(2,1,2)
plot(time24,HE*HESIZE/1000,'b-',time24(1:end-1),sunshine/1000*A,'r-.'), xlabel('Time in hours from midnight'), ylabel('Load Profiles [kW]'),
grid on,
axis([0 tend/3600 0 140]), legend('Generator load','Harnessed solar energy')

disp('The energy expended by the heating elements is:')
disp([num2str(sum(HE*HESIZE/1000*dt/3600)),' kWh'])
disp(' ')
disp('The energy passed on to the snowsmelter by the solar collectors is:')
disp([num2str(sum(contribution)/3600000), ' kWh'])
disp('The energy collected by the solar collectors is:')
disp([num2str(sum(collected)/3600000), ' kWh'])
disp(' ')
disp(' ')
```

D.7 Snow Smelter Simulation Programme Results for Thermomax and Mt-Collectors

Table D.2: Estimated daily load for snow smelter with and without Thermomax collector system

ESTIMATED DAILY GENERATOR LOAD FROM SNOW SMELTER (kWh/day)																		
Collector Size	**NONE (0 PANELS)**						**MEDIUM (24 PANELS)**						**LARGE (72 PANELS)**					
Tresponse (min)	*30*	*10*	*30*	*10*	*30*	*10*	*30*	*10*	*30*	*10*	*30*	*10*	*30*	*10*	*30*	*10*	*30*	*10*
Tmax (°C)	*30*	*30*	*20*	*20*	*10*	*10*	*30*	*30*	*20*	*20*	*10*	*10*	*30*	*30*	*20*	*20*	*10*	*10*
January	1715	1578	1485	1313	1318	1069	1618	1440	1369	1140	1168	856	1301	1140	1046	746	885	498
February	1715	1578	1485	1313	1318	1069	1644	1460	1404	1187	1222	907	1464	1310	1192	924	925	630
March	1315	1157	1115	865	663	569	1144	1067	761	688	370	379	887	888	515	491	173	130
April	1315	1157	1115	865	663	569	1211	1092	820	730	485	397	988	963	577	573	241	204
May	1315	1157	1115	865	663	569	1315	1157	1115	865	663	569	1315	1157	1115	865	663	569
June	1315	1157	1115	865	663	569	1315	1157	1115	865	663	569	1315	1157	1115	865	663	569
July	1315	1157	1115	865	663	569	1315	1157	1115	865	663	569	1315	1157	1115	865	663	569
August	1315	1157	1115	865	663	569	1315	1157	1115	865	663	569	1315	1157	1115	865	663	569
September	1315	1157	1115	865	663	569	1211	1092	820	730	485	397	988	963	577	573	241	204
October	1315	1157	1115	865	663	569	1144	1067	761	688	370	379	887	888	515	491	173	130
November	1315	1157	1115	865	663	569	966	935	595	571	295	262	624	617	301	255	28	15
December	1315	1157	1115	865	663	569	919	897	550	528	278	218	488	460	175	145	26	14

Table D.3: Energy savings generated at snow smelter from Thermomax collector system

DAILY SAVINGS (kWh)												
Collector Size	MEDIUM (24 PANELS)						LARGE (72 PANELS)					
Tresponse (min)	*30*	*10*	*30*	*10*	*30*	*10*	*30*	*10*	*30*	*10*	*30*	*10*
Tmax (°C)	*30*	*30*	*20*	*20*	*10*	*10*	*30*	*30*	*20*	*20*	*10*	*10*
January	97	138	116	173	150	213	414	438	439	567	433	571
February	71	118	81	126	96	162	251	268	293	389	393	439
March	171	90	354	177	293	190	428	269	600	374	490	439
April	104	65	295	135	178	172	327	194	538	292	422	365
May	0	0	0	0	0	0	0	0	0	0	0	0
June	0	0	0	0	0	0	0	0	0	0	0	0
July	0	0	0	0	0	0	0	0	0	0	0	0
August	0	0	0	0	0	0	0	0	0	0	0	0
September	104	65	295	135	178	172	327	194	538	292	422	365
October	171	90	354	177	293	190	428	269	600	374	490	439
November	349	222	520	294	368	307	691	540	814	610	635	554
December	396	260	565	337	385	351	827	697	940	720	637	555
Average	*122*	*87*	*215*	*130*	*162*	*146*	*308*	*239*	*397*	*302*	*327*	*311*

Table D.4: Estimated daily load for snow smelter with and without Mt collector system

ESTIMATED DAILY GENERATOR LOAD FROM SNOW SMELTER (kWh/day)																		
Collector Size	NONE (0 PANELS)						MEDIUM (24 PANELS)						LARGE (72 PANELS)					
Tresponse (min)	*30*	*10*	*30*	*10*	*30*	*10*	*30*	*10*	*30*	*10*	*30*	*10*	*30*	*10*	*30*	*10*	*30*	*10*
Tmax (°C)	*30*	*30*	*20*	*20*	*10*	*10*	*30*	*30*	*20*	*20*	*10*	*10*	*30*	*30*	*20*	*20*	*10*	*10*
January	1715	1578	1485	1313	1318	1069	1655	1504	1417	1208	1239	950	1542	1380	1294	1036	1048	689
February	1715	1578	1485	1313	1318	1069	1680	1529	1447	1250	1274	989	1601	1401	1350	1086	1170	809
March	1315	1157	1115	865	663	569	1303	1140	939	781	510	458	1195	1097	853	714	384	267
April	1315	1157	1115	865	663	569	1315	1146	1017	821	445	511	1280	1106	856	749	450	435
May	1315	1157	1115	865	663	569	1315	1157	1115	865	663	569	1315	1157	1115	865	663	569
June	1315	1157	1115	865	663	569	1315	1157	1115	865	663	569	1315	1157	1115	865	663	569
July	1315	1157	1115	865	663	569	1315	1157	1115	865	663	569	1315	1157	1115	865	663	569
August	1315	1157	1115	865	663	569	1315	1157	1115	865	663	569	1315	1157	1115	865	663	569
September	1315	1157	1115	865	663	569	1315	1146	1017	821	445	511	1280	1106	856	749	450	435
October	1315	1157	1115	865	663	569	1303	1140	939	781	510	458	1195	1097	853	714	384	267
November	1315	1157	1115	865	663	569	1167	1075	796	713	467	377	943	945	515	509	178	128
December	1315	1157	1115	865	663	569	1045	1026	688	639	356	309	849	823	460	435	134	79

Table D.5: Energy savings generated at snow smelter from Mt collector system

DAILY SAVINGS (kWh)												
Collector Size	MEDIUM (24 PANELS)						LARGE (72 PANELS)					
Tresponse (min)	*30*	*10*	*30*	*10*	*30*	*10*	*30*	*10*	*30*	*10*	*30*	*10*
Tmax (°C)	*30*	*30*	*20*	*20*	*10*	*10*	*30*	*30*	*20*	*20*	*10*	*10*
January	60	74	68	105	79	119	173	198	191	277	270	380
February	35	49	38	63	44	80	114	177	135	227	148	260
March	12	17	176	84	153	111	120	60	262	151	279	302
April	0	11	98	44	218	58	35	51	259	116	213	134
May	0	0	0	0	0	0	0	0	0	0	0	0
June	0	0	0	0	0	0	0	0	0	0	0	0
July	0	0	0	0	0	0	0	0	0	0	0	0
August	0	0	0	0	0	0	0	0	0	0	0	0
September	0	11	98	44	218	58	35	51	259	116	213	134
October	12	17	176	84	153	111	120	60	262	151	279	302
November	148	82	319	152	196	192	372	212	600	356	485	441
December	270	131	427	226	307	260	466	334	655	430	529	490
Average	60	74	68	105	79	119	173	198	191	277	270	380

Table D.6: System performance comparison

CRITERIA	Bt-COLLECTOR	THERMOMAX	Mt-COLLECTOR
NPV (R)	2 148 811	3 427 161	871 405
IRR (%)	24.47	26.51	15.36
NAW (R)	190 873	304 425	77 404
Breakeven period[∞]	6	5	11

[∞]MARR, 8 % & Fuel escalation rate 5 %

Appendix E: Additional Information to Economic Analysis

E.1 Sample Results for Solar PV System

NET PRESENT VALUE

The NPV of cash flows has been calculated with the help of equations 5.1 and 5.2. For example, the NPV of cash flows for the diesel-only system after the first year equals the total costs at the end of year 1 brought back by the PWF with an interest rate equal to the hurdle rate.

$$NPV = \sum_{n=0}^{N} (C_n + M_n + L_n + F_n) \cdot \left(\frac{1}{(1+i)^n} \right) \qquad E.1$$

$$NPV = -5079770.85 \cdot \left(\frac{1}{(1+0.08)^1} \right)$$

INTERNAL RATE OF RETURN

The IRR can easily be calculated with the help of Microsoft Excel's formulae function, however, by way of example the formula and sample calculation is given here. The IRR is that interest rate which solves the equation given in E.2. Thus for example the IRR in table E.2 at the end of year six is calculated from the column "Yearly Cashflows" in the same table as:

$$\sum_{k=0}^{N} (PWF(IRR,k)) \cdot Income_k = \sum_{k=0}^{N} (PWF(IRR,k)) \cdot Expenses_k \qquad E.2$$

Which is solved by:

$$1653167.13\left[\frac{1}{(1+0.1983)^0}\right] = 92585.66\left[\frac{1}{(1+0.1983)^1}\right] + 100236.95\left[\frac{1}{(1+0.1983)^2}\right] + 108301.02\left[\frac{1}{(1+0.1983)^3}\right] + \ldots$$

$$\ldots 116798.22\left[\frac{1}{(1+0.1983)^4}\right] + 125752.34\left[\frac{1}{(1+0.1983)^5}\right] + 135184.67\left[\frac{1}{(1+0.1983)^6}\right]$$

BENEFIT COST RATIO (BC RATIO)

The BC Ratio is easily calculated as the sum of the total benefits projected to the same point in time (in this instance the NPV) divided by the sum of the total costs. Therefore (excluding externalities):

$$BC = \frac{\sum_{k=0}^{N} (PWF(MARR,k)) \cdot Income_k}{\sum_{k=0}^{N} (PWF(MARR,k)) \cdot Expenses_k} \qquad E.3$$

Which can be calculated from the first 4 columns in table E.1 (viz. Capital, Fuel, Maintenance and Labour) and where "Fuel" is the only column that represents an income as given in equation E.3. Thus the BC-Ratio at the end of year 1 is calculated as:

$$BC = \frac{\left[\frac{1}{(1+0.08)^1}\right] \cdot 168135.79}{\left[\frac{1}{(1+0.08)^0}\right] \cdot 1653167.13 + \left[\frac{1}{(1+0.08)^1}\right] \cdot 74540.13 + \left[\frac{1}{(1+0.08)^1}\right] \cdot 1010}$$

COST OF ENERGY PRODUCED

The cost of energy generation has been calculated by; summing the respective total costs of the system in question (i.e. diesel-only or hybrid) over the 25-year project lifetime, and then dividing by the power generated after that amount of time.

$$Cost = \frac{\sum_{k=0}^{N} (PWF(MARR,k)) \cdot Expenses_k}{\sum_{k=0}^{N} AnnualEnergy\,\mathrm{Pr}oduction_k} \qquad E.4$$

Thus, the normal generation costs of the diesel-only system are calculated as (cost values can be seen at the bottom of table E.1):

$$Cost = \frac{0 + 84903277.43 + 351801.17 + 234534.11}{24 \cdot 1061971}$$

Table E.1: Sample results for the solar PV system (column A is for diesel-only and column B is for the hybrid system)

	A	B	A	B	A	B	A	B	A	B
	CAPITAL INVESTMENT		FUEL COSTS		MAINTENANCE		LABOUR		TOTAL	
0	0.00	-1 653 167.13	0.00	0.00	0.00	0.00	0.00	0.00	0.00	-1 653 167.13
1	0.00	0.00	-5 029 270.85	-4 861 135.06	-30 300.00	-104 840.13	-20 200.00	-21 210.00	-5 079 770.85	-4 987 185.18
2	0.00	0.00	-5 280 734.39	-5 104 191.81	-30 603.00	-105 888.53	-20 402.00	-21 422.10	-5 331 739.39	-5 231 502.44
3	0.00	0.00	-5 544 771.11	-5 359 401.40	-30 909.03	-106 947.41	-20 606.02	-21 636.32	-5 596 286.16	-5 487 985.14
4	0.00	0.00	-5 822 009.67	-5 627 371.47	-31 218.12	-108 016.89	-20 812.08	-21 852.68	-5 874 039.87	-5 757 241.04
5	0.00	0.00	-6 113 110.15	-5 908 740.05	-31 530.30	-109 097.05	-21 020.20	-22 071.21	-6 165 660.65	-6 039 908.31
6	0.00	0.00	-6 418 765.66	-6 204 177.05	-31 845.60	-110 188.03	-21 230.40	-22 291.92	-6 471 841.66	-6 336 657.00
7	0.00	0.00	-6 739 703.94	-6 514 385.90	-32 164.06	-111 289.91	-21 442.71	-22 514.84	-6 793 310.71	-6 648 190.65
8	0.00	0.00	-7 076 689.14	-6 840 105.20	-32 485.70	-112 402.80	-21 657.13	-22 739.99	-7 130 831.97	-6 975 247.99
9	0.00	0.00	-7 430 523.59	-7 182 110.46	-32 810.56	-113 526.83	-21 873.71	-22 967.39	-7 485 207.86	-7 318 604.68
10	0.00	0.00	-7 802 049.77	-7 541 215.98	-33 138.66	-114 662.10	-22 092.44	-23 197.06	-7 857 280.88	-7 679 075.14
11	0.00	0.00	-8 192 152.26	-7 918 276.78	-33 470.05	-115 808.72	-22 313.37	-23 429.04	-8 247 935.68	-8 057 514.54
12	0.00	0.00	-8 601 759.87	-8 314 190.62	-33 804.75	-116 966.81	-22 536.50	-23 663.33	-8 658 101.13	-8 454 820.75
13	0.00	0.00	-9 031 847.87	-8 729 900.15	-34 142.80	-118 136.48	-22 761.87	-23 899.96	-9 088 752.53	-8 871 936.58
14	0.00	0.00	-9 483 440.26	-9 166 395.16	-34 484.23	-119 317.84	-22 989.48	-24 138.96	-9 540 913.97	-9 309 851.96
15	0.00	0.00	-9 957 612.27	-9 624 714.91	-34 829.07	-120 511.02	-23 219.38	-24 380.35	-10 015 660.72	-9 769 606.28
16	0.00	0.00	-10 455 492.89	-10 105 950.66	-35 177.36	-121 716.13	-23 451.57	-24 624.15	-10 514 121.82	-10 252 290.94
17	0.00	0.00	-10 978 267.53	-10 611 248.19	-35 529.13	-122 933.29	-23 686.09	-24 870.39	-11 037 482.75	-10 759 051.88
18	0.00	0.00	-11 527 180.91	-11 141 810.60	-35 884.42	-124 162.62	-23 922.95	-25 119.10	-11 586 988.28	-11 291 092.32
19	0.00	0.00	-12 103 539.95	-11 698 901.13	-36 243.27	-125 404.25	-24 162.18	-25 370.29	-12 163 945.40	-11 849 675.67
20	0.00	0.00	-12 708 716.95	-12 283 846.19	-36 605.70	-126 658.29	-24 403.80	-25 623.99	-12 769 726.45	-12 436 128.47
21	0.00	0.00	-13 344 152.80	-12 898 038.50	-36 971.76	-127 924.88	-24 647.84	-25 880.23	-13 405 772.40	-13 051 843.60
22	0.00	0.00	-14 011 360.44	-13 542 940.42	-37 341.48	-129 204.13	-24 894.32	-26 139.03	-14 073 596.23	-13 698 283.58
23	0.00	0.00	-14 711 928.46	-14 220 087.44	-37 714.89	-130 496.17	-25 143.26	-26 400.42	-14 774 786.61	-14 376 984.03
24	0.00	0.00	-15 447 524.88	-14 931 091.82	-38 092.04	-131 801.13	-25 394.69	-26 664.43	-15 511 011.62	-15 089 557.37
25	0.00	0.00	-16 219 901.13	-15 677 646.41	-38 472.96	-133 119.14	-25 648.64	-26 931.07	-16 284 022.73	-15 837 696.62
PV	R 0.00	R -1 653 167.13	R -84 748 502.27	R -81 915 237.43	R -351 801.17	R -1 217 256.71	R -234 534.11	R -246 260.82	R -85 334 837.55	R -85 031 922.09

Table E.2: Sample results for solar PV system (column A is for diesel-only and column B is for the hybrid system)

		USING A SINGLE CAPITAL INVESTMENT								
A	B	YEARLY CASHFLOWS	DISCOUNTED PAYBACK	SIMPLE PAYBACK	EXTERNALITIES	NPV OF EXTERNALITIES	DSCNTED PAYBACK (WITH EXTERNALITES)	SIMPLE PAYBACK WITH EXTERNALITIES	IRR BASED ON YEARS	BC RATIO BASED ON YEARS
NPV										
0.00	-1 653 167.13	-1 653 167.13	-1 653 167.13	-1 653 167.13	0.00	0.00	-1 653 167.13	-1 653 167.13	#NUM!	0.00
-4 703 491.53	-6 270 931.19	92 585.66	-1 567 439.66	-1 560 581.47	53 554.11	49 587.14	-1 517 852.52	-1 510 994.33	#NUM!	0.09
-9 274 598.69	-10 756 101.32	100 236.95	-1 481 502.63	-1 460 344.51	54 089.65	95 960.30	-1 385 542.33	-1 364 384.21	#NUM!	0.17
-13 717 111.07	-15 112 640.86	108 301.02	-1 395 529.79	-1 352 043.49	54 630.55	139 327.79	-1 256 202.00	-1 212 715.70	#NUM!	0.25
-18 034 705.73	-19 344 384.89	116 798.82	-1 309 679.17	-1 235 244.67	55 176.86	179 884.43	-1 129 794.74	-1 055 360.24	#NUM!	0.31
-22 230 950.76	-23 455 045.00	125 752.34	-1 224 094.24	-1 109 492.33	55 728.62	217 812.39	-1 006 281.85	-891 679.94	#NUM!	0.38
-26 309 308.81	-27 448 213.78	135 184.67	-1 138 904.97	-974 307.66	56 285.91	253 282.06	-885 622.90	-721 025.60	-19.83%	0.43
-30 273 140.36	-31 327 369.17	145 120.06	-1 054 228.81	-829 187.60	56 848.77	286 452.77	-767 776.03	-542 734.83	-14.08%	0.49
-34 125 706.99	-35 095 878.62	155 583.98	-970 171.62	-673 603.63	57 417.26	317 473.53	-652 698.09	-356 130.09	-9.68%	0.54
-37 870 174.49	-38 757 003.05	166 603.18	-886 828.56	-507 000.45	57 991.43	346 483.68	-540 344.87	-160 516.77	-6.23%	0.59
-41 509 615.83	-42 313 900.65	178 205.73	-804 284.82	-328 794.71	58 571.34	373 613.55	-430 671.27	44 818.83	-3.50%	0.63
-45 047 014.07	-45 769 630.53	190 421.14	-722 616.46	-138 373.57	59 157.06	398 985.00	-323 631.46	260 611.42	-1.28%	0.67
-48 485 265.15	-49 127 156.17	203 280.37	-641 891.02	64 906.80	59 748.63	422 712.00	-219 179.03	487 618.80	0.53%	0.71
-51 827 180.59	-52 389 348.84	216 815.95	-562 168.25	281 722.75	60 346.11	444 901.14	-117 267.11	726 623.89	2.03%	0.75
-55 075 490.10	-55 558 990.74	231 062.02	-483 500.64	512 784.77	60 949.57	465 652.09	-17 848.54	978 436.86	3.28%	0.79
-58 232 844.06	-58 638 778.08	246 054.44	-405 934.01	758 839.21	61 559.07	485 058.08	79 124.07	1 243 897.29	4.34%	0.83
-61 301 816.00	-61 631 324.07	261 830.88	-329 508.08	1 020 670.09	62 174.66	503 206.27	173 698.19	1 523 876.36	5.25%	0.86
-64 284 904.89	-64 539 161.74	278 430.88	-254 256.86	1 299 100.96	62 796.41	520 178.19	265 921.34	1 819 279.15	6.02%	0.89
-67 184 537.45	-67 364 746.63	295 895.96	-180 209.18	1 594 996.92	63 424.37	536 050.08	355 840.90	2 131 047.00	6.69%	0.93
-70 003 070.35	-70 110 459.44	314 269.73	-107 389.09	1 909 266.65	64 058.62	550 893.23	443 504.14	2 460 159.89	7.26%	0.96
-72 742 792.27	-72 778 608.51	333 597.98	-35 816.24	2 242 864.63	64 699.20	564 774.33	528 958.09	2 807 638.97	7.77%	0.99
-75 405 926.01	-75 371 432.26	353 928.79	34 493.75	2 596 793.43	65 346.19	577 755.73	612 249.47	3 174 549.15	8.21%	1.01
-77 994 630.43	-77 891 101.49	375 312.65	103 528.95	2 972 106.08	65 999.66	589 895.74	693 424.68	3 562 001.82	8.60%	1.04
-80 511 002.42	-80 339 721.61	397 802.58	171 280.81	3 369 908.66	66 659.65	601 248.90	772 529.70	3 971 157.55	8.94%	1.07
-82 957 078.67	-82 719 334.81	421 454.25	237 743.86	3 791 362.90	67 326.25	611 866.20	849 610.06	4 403 229.10	9.25%	1.09
-85 334 837.55	-85 031 922.09	446 326.11	302 915.46	4 237 689.01	67 999.51	621 795.35	924 710.81	4 859 484.36	9.52%	1.12
R -85 334 837.55	R -85 031 922.09	R 302 915.46	R 302 915.46	R 4 237 689.01	R 621 795.35	R 621 795.35	R 924 710.81	R 4 859 484.36		